12-2019

Study of Internal Strains Developed in Concrete Decks at Early Ages in Steel Continuous Bridges

Fernando R. Benitez Ortiz
University of Arkansas, Fayetteville

Study of Internal Strains Developed in Concrete Decks at Early Ages in Steel Continuous Bridges

A thesis submitted in partial fulfillment
of the requirements for the degree of
Master of Science in Civil Engineering

by

Fernando R. Benitez Ortiz
University of Puerto Rico at Mayagüez
Bachelor of Science in Civil Engineering, 2018

December 2019
University of Arkansas

This thesis is approved for recommendation to the Graduate Council.

_____
Cameron Murray, Ph.D.
Thesis Director

_____
Ernest Heymsfield, Ph.D.
Committee Member

_____
W. Micah Hale, Ph.D.
Committee Member

Abstract

The Arkansas Department of Transportation (**ARDOT**) has identified bridge deck cracking shortly after concrete decks are placed and prior to applying traffic loads. Previous researchers have confirmed improper construction practices and design methods can lead to deck cracking. Currently, many contractors throughout Arkansas are using continuous deck pours. This construction approach may restrict the concrete slab from movement during early age shrinkage, causing tensile stresses to develop. The final stresses at the end of construction must be lower than the concrete tensile strength, if not cracking issues will develop. Eventually, these cracks may enlarge due to service load stresses and environmental damage. A nation-wide Department of Transportation (US DOTs) survey was performed to investigate the early age cracking extensiveness level in other state's bridges and what corrections, if any, they have made to address this problem. Additionally, Arkansas bridges with early age cracking were visited to examine any trends and inform instrumentation for bridge testing. A bridge deck was instrumented with 32 vibrating wire strain gauges prior to concrete placement to investigate strain and temperature changes in the first 14 days. Eurocode and ACI approximations for concrete mechanical properties were compared to field measured data for improving the understanding of an early age concrete deck behavior in a continuous steel bridge. Stress analysis study through the span length of bridge 030428 detected some locations prone to concrete cracking due to the variability of concrete mechanical properties and stress developed in the concrete deck. This thesis describes the results of this monitoring and anything that can be learned about formation of concrete stresses in continuous concrete bridge deck pours.

Keywords: early age cracking, concrete shrinkage, concrete strains, ARDOT

Acknowledgements

I want to thank the Arkansas Department of Transportation for sponsoring my master's project. The knowledge gained through the project has strengthened my interests for horizontal structures. I want to thank William Caster and Patrick (Ross) Phillips for arranging all of the bridge site inspections and helping me with the actual bridge instrumentation as well.

I want to thank Joe Holloway and Rob Clark from the Geokon, Inc. staff for being available and helpful with my questions about advanced technical aspects of the equipment. Also, thanks to David Peachee for assisting me at the concrete laboratory with different tasks I had along the way.

I want to thank the Department of Civil Engineering at the University of Arkansas, especially to my committee, which on multiple occasions, challenged and impacted me positively towards my graduate professional growth. I want to thank my advisor, Dr. Cameron Murray, who supported me unconditionally since the very first day I joined his research team. Dr. Murray's academic commitment and professional skills had a significant contribution to my development as a structural engineering graduate student.

I want to thank Dr. Oscar M. Suarez, for allowing me to be part of his research team in 2015, which was my first research experience. Dr. Suarez taught me the importance of research and how powerful it is for our field. Also, I want to thank Dr. Luis E. Suarez and Dr. Farshad Rajabipour for encouraging me to continue graduate school. All of these outstanding faculty made a positive impact during my undergraduate career.

I want to thank Abdul Aziz Salah for assisting me in setting up the bridge instrumentation. Abdul never said no to help me with any tasks of the project and he is a great colleague to work. I want to thank my family and friends for always supporting all my academic decisions.

Dedication

To my parents

Table of Contents

List of Figures

List of Tables

CHAPTER I

INTRODUCTION

1.1 Overview

The Arkansas Department of Transportation (ARDOT) experiences concrete deck cracking in many continuous steel bridges shortly after construction and before opening to traffic. The University of Arkansas began a research study to investigate potential reasons for cracking in ARDOT's continuous steel bridges. Previous researchers [1, 2, 3] have confirmed improper construction practices and design methods can lead to deck cracking. Currently, many contractors throughout Arkansas counties are using continuous deck pours which may restrict the concrete slab from movement during shrinkage if the concrete does not set uniformly. Eventually, these cracks may enlarge due to service load stresses. Also, temperature differentials can have a direct impact on concrete cracking as the concrete transitions from plastic to harden. The final stresses due to any of these factors must be lower than the concrete tensile strength, if not cracking issues will develop.

1.2 Research Significance

Bridge deck cracking has been a topic of interest in the structural engineering field for a long time. Many states have reduced deck cracking by improving their construction and concrete curing methodologies. However, ARDOT has been struggling with bridge deck cracking in their continuous steel bridges. The present study aims to investigate construction practices in continuous steel bridges to provide recommendations for future construction while improving bridge deck durability. The objective is to review previous research done to improve the understanding of why steel continuous bridges experience early age cracking and provide recommendations to ARDOT for future bridge construction.

CHAPTER II

LITERATURE REVIEW

2.1 Background

Early age cracking in concrete bridge decks has been a consistent issue in the bridge design and construction industry. Early age deck cracking can be the primary cause of deterioration of bridge decks, and it has been known to significantly decrease the durability and service life of bridges [4]. Researchers and engineers have studied the different factors leading to early onset cracking for decades. It has been reported that the predominant form of deck cracking is transverse cracking (cracking perpendicular to the direction of the bridge span) [5, 6, 7, 8] as shown in Figure 1. Previous studies indicated that deck cracks typically: (1) are mostly seen over transverse rebar (in the top of the deck) in regions of negative moment (for continuous spans), (2) are greater in continuous spans; (3) are greater in long spans; (4) are greater in older decks; (5) are somewhat greater on structural steel spans (with greater flexibility and longer spans); and (6) are mostly seen along the edges of girders (in the top of the deck) at girder locations [9, 10]. According to Hopper et al. [4], cracking in concrete bridge decks occurs when the net internal tensile stresses are greater than the tensile strength of the concrete. These tensile stresses are caused by external loads, restrained shrinkage, or differential thermal stresses. Fresh concrete experiences shrinkage due to the cement hydration process, internal chemical reactions, drying, and water evaporation. In addition, the pouring sequence and curing methods have been shown to be another cause of cracking.

To minimize cracking, concrete pouring and curing must be properly designed [11] because these factors play an important role in early age cracking. Field engineers have recommended different curing techniques to minimize the cracking in slabs, however it is still a

problem in many states. Construction practices, such as pouring sequence, design methods, and material selection also need to be taken into consideration in reducing cracking, and these factors are interrelated and interdependent.

Hadidi and colleagues [11] performed an extensive study regarding causes of transverse deck cracking including construction practices, material and mix design. Their recommendations for reducing deck cracking within material and mix design included lowering the cement content to 650-660 lb/yd^3; using fly ash; limit the w/c ratio to 0.40-0.45 and use water reducers; use AASHTO Type II cement for bridge decks; use the largest aggregate size possible; use crushed stone for coarse aggregate, and maximize aggregate content. As for the construction practices, some recommendations presented were: using the evaporation rate chart from ACI, casting concrete in mild temperatures, and curing concrete for a minimum of 7 days after finishing. Manafpour et al. [12] investigated 203 bridge decks in Pennsylvania and concluded: limit maximum concrete compressive strength at 28 days to 4,000 psi – 5,000 psi; limit maximum cementitious material content to 620 lb/yd^3; and use epoxy coated rebar to increase the critical chloride content required to corrosion propagation.

Hale et al. [13] concluded that one of the possible causes of deck cracking was compressive strength variations at early ages. They confirmed that cracking tends to increase with compressive strengths as a result of the larger amount of cement in the mixtures. The Minnesota Department of Transportation (MnDOT) [3] recommended limiting the cement content to 470 lb/yd^3; using Type II cement; limiting water cement ratio between 0.40 and 0.45; limiting compressive strength to less than 6,000 psi; use a 1.5 in. maximum aggregate size; replace 20% of cement with fly ash; deck placement within the optimum temperature range

between 45˚F and 80˚F (daily temperature fluctuation less than 50˚F) while maintaining a girder/deck differential temperature under 22˚F for at least one day after pouring.

2.2 Concrete Shrinkage

Cracks in concrete occur when the concrete mass is restricted from free volume movement in any direction during the hardening process. This restriction can be attributed to shear studs, formwork, steel reinforcement and any material in the deck that tries to prevent concrete volume change. After concrete is poured, differential volume changes known as shrinkage occur. The level of restraint of the concrete can induce tensile stresses in response to this volume change and when these exceed the concrete tensile strength, cracks start to develop [14]. Shrinkage can be split into several categories, as follows: plastic shrinkage, thermal shrinkage, autogenous shrinkage and drying shrinkage [11]. Each term is briefly explained in the following sections.

2.2.1 Plastic Shrinkage

Plastic shrinkage (example shown in figure 1) refers to volume changes which occurs while the concrete is still fresh (or plastic), before hardening [15]. The resulting cracking occurs when the evaporation of water from the surface of the fresh concrete, exceeds the rate at which the bleed water within the concrete can reach the surface [4]. It is directly proportional to the rate at which water evaporates from fresh concrete meaning ambient temperature conditions will have an impact in plastic shrinkage extensiveness. Cracks will look like tears in the surface (not too deep) [15] possibly random and shallow but they are generally not a structural issue and can be minimized by minimizing evaporation from the concrete surface. Construction procedures can be implemented to reduce surface evaporation such as: fogging during placement, night

placements, and early application of curing compounds or evaporation retarders, and protection from direct sunlight [16].

Figure 1. Plastic shrinkage in concrete *[15]*.

2.2.2 Thermal Shrinkage

Thermal shrinkage can be defined as the expansion or contraction of concrete after being placed due to rapid changes in temperature or temperature differentials within the concrete. During the concrete curing stage, the cement hydration reaction process takes place inside the slab and is accompanied by a temperature increase. This reaction is the biggest concern in thermal shrinkage because generates a high internal heat early on, which gradually cools down. Tensile stresses will start developing in the solid volume as a function of the internal differential temperature and the degree of restraint. Because these differentials occur while concrete still low strength material, they can easily lead to cracking. In massive structures (mass concrete), the combination of heat produced by cement hydration and relatively poor heat dissipation conditions results in a large rise in concrete temperature within a few days [17]. Controlling the rise in concrete temperature will reduce thermal shrinkage. Retarders can be used in the concrete mixture to slow the hydration process, and therefore, reduce the temperature differential. Casting

a deck monolithically is not a good practice since cracking can occur due to non-uniform temperature distribution throughout the slab and resulting in non-uniform contraction. However, retarders can be used at varying doses to ensure that all parts of a bridge deck set at the same time. Thermal shrinkage can also be caused by external temperatures, for example a bridge deck exposed to high ambient temperatures and solar radiation may expand on the top surface.

2.2.3 Autogenous and Chemical Shrinkage

Autogenous shrinkage is the reduction in concrete volume due to the change in water content during the cement reaction [11]. It occurs during the cement hydration process when tension stresses develop due to inadequate moisture and is mostly seen in low water/cement ratio mixtures. Chemical shrinkage occurs simultaneously with autogenous shrinkage [15]. Figure 2 shows the early age behavior of a volume of cement paste after being cast and the autogenous and chemical shrinkage over time. Autogenous shrinkage can be mitigated in the design phase by proper selection of cementitious materials, mixture proportioning [16] and wet curing during construction phase. It is typically only of concern in low w/c mixtures.

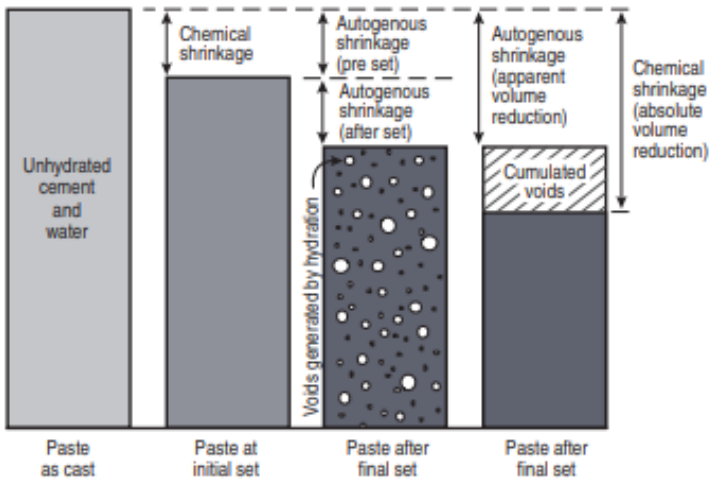

Figure 2. Chemical and autogenous shrinkage volume changes in early age stages of paste *[15]*.

2.2.4 Drying Shrinkage

Drying shrinkage (shown in figure 3) is usually associated with transverse cracking and is considered one of the main causes of concrete bridge deck cracking [9]. As concrete hardens the internal moisture is used up in the cement reaction and is lost to the environment. This loss of moisture causes capillary pressures which result in a volume reduction known as drying shrinkage. This volume change may cause cracking if the stresses in the restrained concrete exceed the strength of the concrete. Drying shrinkage is therefore especially important at early ages. Curing techniques can be applied to the concrete after it has reached final set to mitigate drying and delay the shrinkage strains from forming before the concrete acquires enough strength to resist these stresses. Exposure conditions are a factor which influence drying. Extreme cold weather can delay concrete strength gain, whereas warm weather can accelerate the rate of moisture loss. Since these factors are uncontrollable, contractors must use efficient and effective construction methods in order to delay drying shrinkage until the concrete is mature. Examples of these curing methods include using wet burlap to maintain hydration for 7-14 days, using night pours for cooler temperatures during curing and using lower strength concrete (which tend to shrink less due to lower water demand) with proper placement and consolidation, among other techniques.

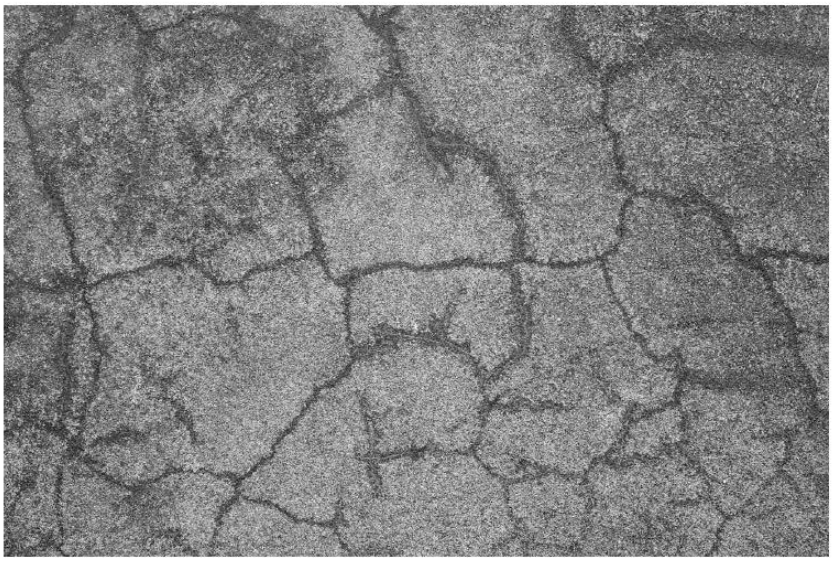

Figure 3. Drying shrinkage in concrete *[18]*.

2.3 Deck Pouring Sequence

Construction methodology is highly related to the durability of a concrete superstructure, including early age cracking. The procedures that can affect the cracking potential of bridge decks during construction include the sequence and length of placement, consolidation, finishing, and curing [4]. In a bridge deck pour, contractors must be aware that the slab sections that will gain strength first are those which are placed first (if no set retarding admixtures are used). If no admixtures are added, the last concrete sections poured will be relatively weak compared to the first sections which affects the amount of stress they can resist. Carper [19] conducted a review regarding structural failures during construction and identified that improper sequencing is one cause that can lead to structural failure. The Minnesota Department of Transportation (MnDOT) [20] researched the best construction practices and gave the following recommendations: (1) pour the complete deck at one time for each simple span whenever feasible; (2) if a single placement cannot be poured over the full span length for a simple span, place the center of span segment first; and (3) if the bridge is continuous span and multiple placements are needed, pour the positive moment region first. This last mentioned is a favorable practice since the selected

sequence protocol increases the negative moment within the pier sections due to the concrete load in the positive regions, however does not induce new tensile stresses in the bridge deck slab within the negative moment region near the bridge piers [21]. Therefore, a staged or sequential pouring sequence would reduce early age cracking severity compared to continuous pouring, but staged pours take more work and time for the contractors to complete. Some agencies require in their plans a staged pour but the contractor ends up doing a continuous pour with the proper engineers' approval.

2.3.1 Continuous and Sequential Concrete Deck Pouring

Improper concrete casting practices can affect the initial tensile stresses developed in a slab, especially in continuous bridges. The reason behind this is concrete slab sections harden at different times based on when they are placed. Initially placed concrete will harden before the following sections placed after, if no retarding admixture is added. Another explanation would be that the slab moment diagram will change through the casting sequence and negative moments could be induced due to slab dead loads and shrinkage effects. There are two common practices contractors perform during a bridge deck pour: continuous and sequential. A continuous pour consists of casting the concrete slab from one end to another. This method will benefit the contractor in saving working time and make the process easier. However, it will have a potential negative impact on the concrete internal stresses specifically within the pier regions. As mentioned above, early placed concrete sections harden first, creating a restraint for later placed adjacent sections. The created restraint prevents the solid volume change due to shrinkage leading to induce tensile stress in the slab and which probably are not considered in the design phase. Researchers and scientists have studied and encouraged sequential pours for multi-span bridge deck construction [20], [1]. A sequential pour consists of casting the concrete deck by

sections within a specific location throughout the spans. Issa [2] confirmed the prominence of initiating the sequence of pour in the positive moment regions prior to the negative moment regions (at piers). Ramey et al. [10] recommended: 1) place complete deck at one time whenever possible but having limits on maximum placement length based on drying shrinkage; 2) if span is too long for one placement divide the deck longitudinally and place each strip at one time. If this cannot be done too, then place the center of span first and then place other portions; 3) if multiple placements should be made on continuous beams, place middle spans first and observe a 72 hour delay between placements. Ramey et al. also recommend use of a bonding agent to enhance bond at joints. They support the fact that for continuous spans, placement in positive moment regions first will minimize the negative moment cracking at the top of the deck at bridge pier locations and for simple span, placement at the center first will cause most of the deflections due to deck dead load to occur while concrete is wet. Fabrizio et al. [1] stated that minimizing the stresses in steel-concrete composite decks as result of the self-weight and thermal shrinkage can be reduced by casting slab sections at sagging regions before casting hogging regions such that maximum negative moments as a result of the new slab sections only act on the steel component.

CHAPTER III

SURVEYS

3.1 US Department of Transportation Surveys (US DOT)

As part of the research objectives, a nation-wide survey study was launched into the US DOT agencies. The purpose was to collect information from DOTs regarding early age cracking and getting an overall idea of what is the current extensiveness of this problem through the different states. After getting the DOTs staff's answers, a trend study was done to see if there was any links between bridge type, curing methods, pouring sequence, geographical locations and the reported crack extensiveness for each surveyed state. Also, results were compared to previous surveys where researchers investigated the primary contributors to early age cracking and actions taken to address this problem among DOT agencies.

3.1.1 Previous US DOTs Surveys

In 1996, a similar survey was conducted by the National Cooperative Highway Research Program (NCHRP) of North American DOT agencies regarding causes of early transverse cracks. Fifty-two agencies participated in the survey (including Canada) and 62% of responders reported to have a problem with early age transverse cracks, while 24% did not consider it a problem, and 14% had no opinion [21]. The survey also determined the bridge types most used at the time which included steel girders; precast, pre-stressed concrete girders; and cast-in-place, post-tensioned girders. Some transportation agencies perceived deck cracking to be worse with steel girders than concrete girders and some agencies perceived cracking to be worse in continuous than in simply supported structures [21]. Moreover, curing methods allowed by the agencies included monomolecular film, clear curing compound, pigmented curing compound, fogging, wet burlap or fabric and plastic sheeting. In general findings from a comprehensive

literature review, this report concluded some concerns regarding design parameters including: 1) cracking is more common on steel girder structures; 2) continuous-span structures are more susceptible to cracking than simple-span structures; 3) longer span decks are more susceptible to cracking; and 4) dead load deflections during construction should be considered during design.

In 2003, the Michigan Department of Transportation (MDOT) also performed a nationwide survey through the United States DOTs studying the problem of early age reinforced concrete bridge deck cracking. Thirty-one state DOTs responded to the survey in which 30 of 31 (97%) of the states reported having early age cracking problems [22]. The report determined the most commonly used curing procedure among the surveyed states was continuous wet curing (maintaining new cast concrete wet continuously and thoroughly for at least 7 days), but other methods were used such as curing with wet burlap covers, air curing, and commercial curing compounds. Furthermore, they identified 3 main causes which state agencies considered to be the major contributor to premature cracking such as substandard curing, construction practices, and mix design. This survey did not take in consideration the types of bridges in the responding states.

3.1.2 DOT Survey 2018

Following the previous studies mentioned in the literature review, DOTs were surveyed in this work to obtain an overview with the perception of early age cracking in concrete bridge decks was in the different states and to find some trends, if any, between the responses and what is known about the practices in each state. The DOTs were first contacted by phone and then the questions were sent via email (some states responded to the questions by phone). Seventeen out of the fifty states (34%) responded to the survey. The response rate was considered satisfactory

considering an average response rate of 20% is reported for most surveys [22]. A geographic illustration of the responding states is shown in figure 4.

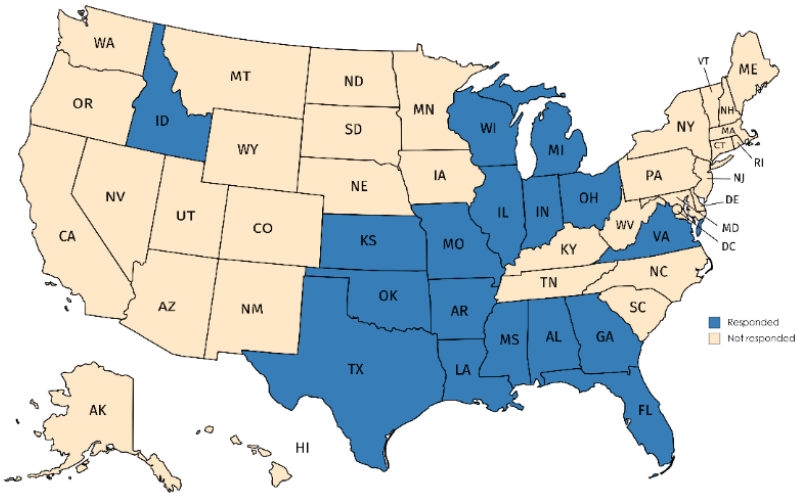

Figure 4. DOTs agencies who responded to the research survey *[23]*.

3.1.3 Results and Analysis

Seventeen states participated in the survey administered by the research team. Below, questions from the survey are shown in different figures with the responses. All seventeen responding states stated that there is a specified or standardized concrete deck pouring sequence. This first question was aimed to see how many DOTs are conscious in the fact that pouring sequence influences early age stresses. Every state has a pouring sequence standardized in their specifications manual and all of them require the pouring sequence be described in the design plans. Some of them reported to let the contractors choose how the pouring sequence would be subjected to the engineer evaluation approval. However, this action of letting the contractor decide to do either a sequential or continuous pouring can be a step to increase potential cracking. Also, it was asked if the sequence is available on their online DOT website or if it is shown only in the plans which most of them do both.

The second question was made to see if early age cracking is a current issue in each state. As shown in figure 5, 70% of the responding states consider early age cracking a current issue;

18% do not consider it an issue; and 12% consider it to be somewhat an issue. Moreover, the fact that it is a current issue in some states, does not mean it has been addressed in the past with specification changes. More than 50% have addressed it with some success but some of them are still working on further improvements. The Indiana DOT indicated that early age cracking is not a severe issue in their state. Indiana previously addressed the problem of bridge deck cracking by updating their specifications regarding curing requirements. The Indiana DOT 2018 Standard Specifications [24] require curing the concrete continuously for at least 7 days commencing immediately after the surface can support the protective covering without deformation. This curing shall continue until a flexural strength of 550 psi has been attained. They cover the surfaces with pre-wetted burlap underneath a layer of white plastic sheeting with a network of soaker hoses to protect and keep the concrete continuously and thoroughly wet during the curing period. Then, a membrane forming curing compound is applied to provide a uniform, solid, white opaque coverage on all surfaces. The Louisiana DOT 2016 Standards and Specifications for Roads and Bridges [25] requires maintaining the deck surface in saturated conditions using foggers until a curing compound is applied. Immediately after concrete is finished and exposed it is covered with wet burlap or an approved equivalent.

Virginia DOT started using low shrinkage Class A4 modified concrete. According to their 2016 Road and Bridge Specifications [26] this low shrinkage concrete shall have less than 600 pounds per cubic yard of cementitious materials. Also, the 28-day drying shrinkage shall be less than 0.035% based on three specimens following ASTM C157 [27]. Lightweight concrete can be used with lightweight aggregates in conformance with ASTM C330 [28] and the maximum cementitious materials shall be 650 pounds per cubic yard. All other requirements shall conform to their low shrinkage Class A4 modified concrete section (table II-17 [26]).

However, for other DOTs, early age cracking has been a challenge to overcome. Figure 6 shows percentages of agencies that have been able to control or mitigate this problem effectively.

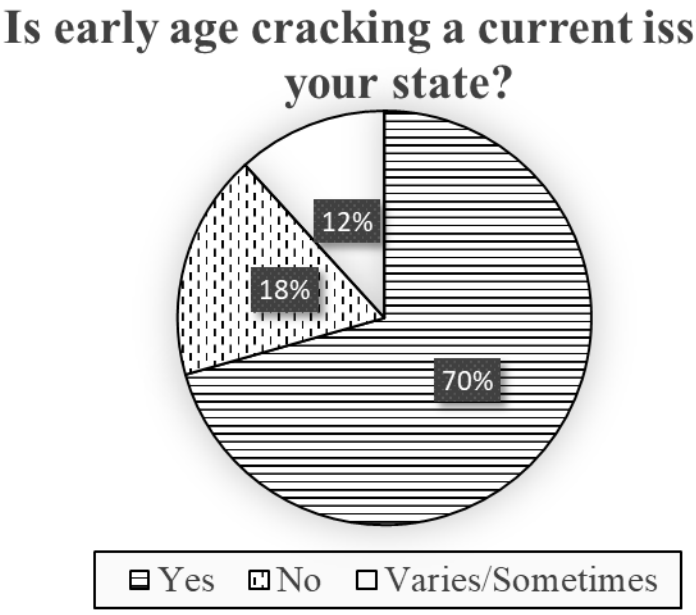

Figure 5. Second question from the survey.

The next survey question asked how extensive the contacts considered early age cracking to be in their state's bridges on a personal judgement scale. Figure 7 summarizes the responses in which 6% do not consider it as a problem, 47% consider it to be low, 23% medium, and 18% high. The final question was how many of the DOTs have conducted research regarding the change in design method from ASD to LFD to LRFD. None of the surveyed states have done any research on this topic. It is clear that this survey is not an accurate representation because of the low participation of DOTs but it gives us an overview of what is currently going on in some state bridges and how is it been addressed.

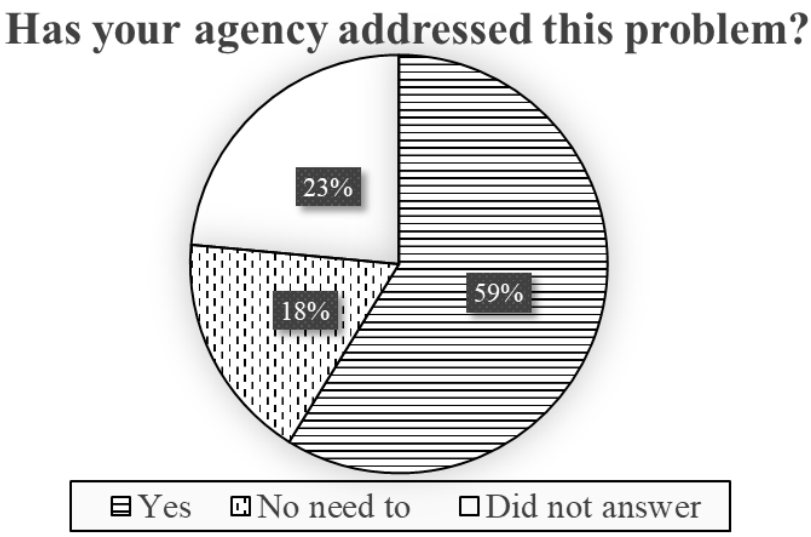

Figure 6. Third question from the survey.

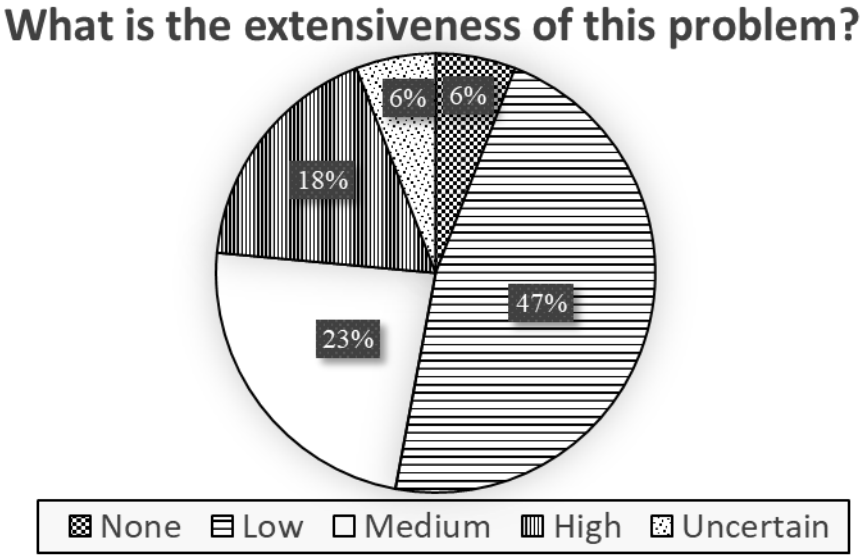

Figure 7. Third question from the survey.

3.2 Continuous DOT Bridges in US

According to the Federal Highway Administration [29], there are a total of 77,012 continuous concrete bridges; 50,585 continuous steel; and 26,339 pre-stressed continuous among the seventeen surveyed states. The focus in this study is towards continuous steel bridges given the fact that these are more commonly constructed in Arkansas currently. Table 1 [29] shows the

total number of bridges including concrete, masonry, wood and others per state and the corresponding percentages of the continuous type bridges. Ohio and Illinois DOTs use the most continuous steel bridges of the states surveyed. The Ohio DOT confirmed early age cracking is an issue, but they have reduced the extensiveness of the problem by implementing internal curing and adding fibers to the mixtures. Illinois DOT reported early age cracking to be very common in their bridges prior to opening to traffic and steel bridges are the most used/constructed. The states with the fewest continuous steel bridges are Mississippi and Louisiana. Both agencies said they have low or no problem with this type of cracking. Looking at the Louisiana continuous bridge percentages it could be inferred that most bridges are simply supported. One hypothesis is that continuous steel girders bridges are expected to experience more premature cracking due to the higher stresses developed in the concrete deck [4, 21].

Table 1: Continuous bridges in the surveyed states *[29]*.

	Total per state	**Concrete Continuous (%)**	**Steel Continuous (%)**	**Prestressed Concrete Continuous (%)**	**Continuous bridges (%)**
ALABAMA	16098	7.40%	5.97%	2.84%	16.21%
ARKANSAS	12871	1.65%	11.56%	0.42%	13.64%
FLORIDA	12313	6.02%	4.52%	1.70%	12.23%
GEORGIA	14835	0.73%	6.98%	0.71%	8.43%
IDAHO	4445	2.74%	3.67%	1.73%	8.14%
ILLINOIS	26704	8.31%	16.56%	1.89%	26.77%
INDIANA	19245	13.56%	10.78%	10.30%	34.65%
KANSAS	25013	23.14%	11.78%	3.66%	38.58%
LOUISIANA	12915	1.06%	1.73%	3.13%	5.92%
MISSISSIPPI	17068	2.64%	1.69%	6.81%	11.15%
MISSOURI	24468	21.83%	12.06%	9.51%	43.41%
OHIO	28284	9.23%	20.85%	2.66%	32.74%
OKLAHOMA	23053	4.05%	4.23%	0.35%	8.63%
TEXAS	53488	3.36%	6.16%	0.53%	10.05%
UTAH	3039	10.17%	10.04%	6.09%	26.29%
VIRGINIA	13892	2.23%	10.11%	1.11%	13.45%
WISCONSIN	14230	19.61%	9.16%	12.19%	40.96%

3.3 Survey trends

The principal objective of the survey was finding some similarities between states and trying to relate them with the problem of early age concrete deck cracking. In figure 8, the percentage of continuous bridges (steel, concrete, pre-stressed and pre-stressed concrete) recorded by the FHWA [29] in the 17 surveyed DOTs is plotted against the self-reported early age cracking extent in each state. Since not all agencies answered in the same words, the research team's judgement was used to categorize each states response into four categories (None, Low, Medium, and High). Only 3 (Oklahoma, Arkansas and Illinois) out of the 17 states reported to have early age cracking to be a very common problem. Georgia and Kansas reported only minor problems with early cracking. The rest of the states have medium or low issues with cracking. Based on figure 8, there does not appear to be a clear trend between the percentage of continuous bridges used and the self-reported incidence of early age cracking.

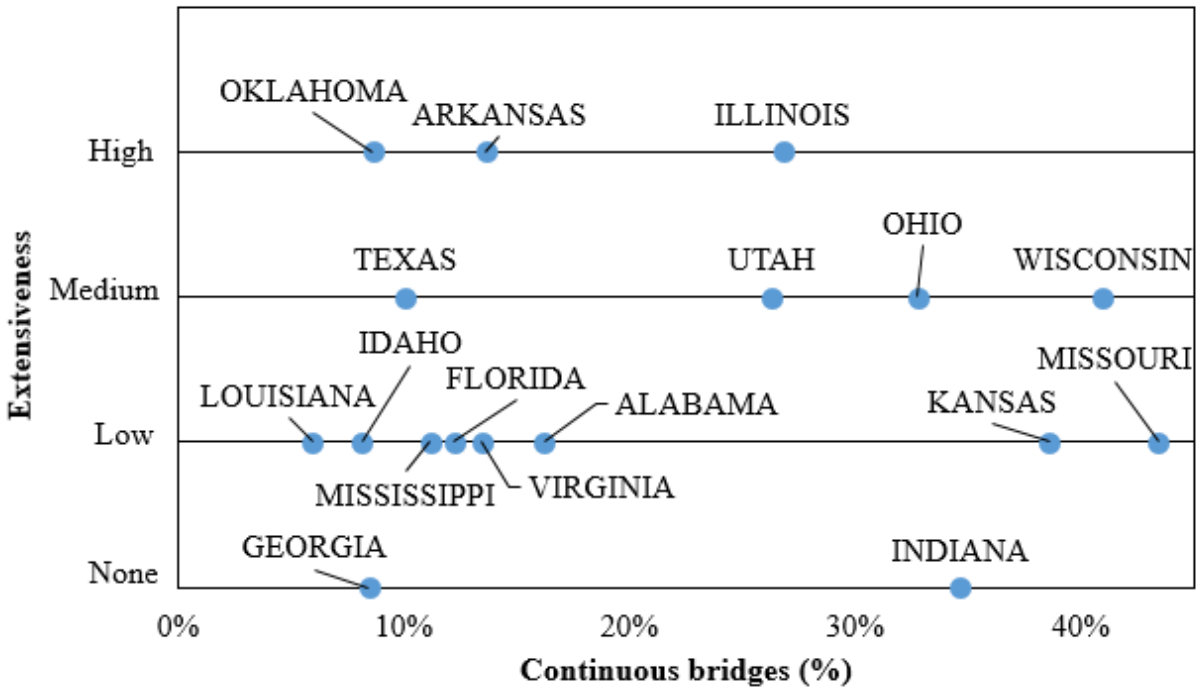

Figure 8. Percentage of continuous bridges (steel, concrete, pre-stressed and pre-stressed concrete) by state versus extensiveness of Early-age cracking issue.

In Figure 9, the same states are shown, but with their current percentage of continuous steel bridges. According to the FHWA [29], Kansas, Missouri, Ohio and Illinois are the states with a higher percentage of continuous steel bridges. Similar to Figure 9, the early age cracking extensiveness varies from low to high with no correlation to percentage of continuous steel bridges. However, based on this survey it is seen little to no correlation between bridge superstructure type and the extensiveness of early age deck cracking. Kansas and Missouri have similar percentages of continuous steel bridges while reported low issues with early age cracking.

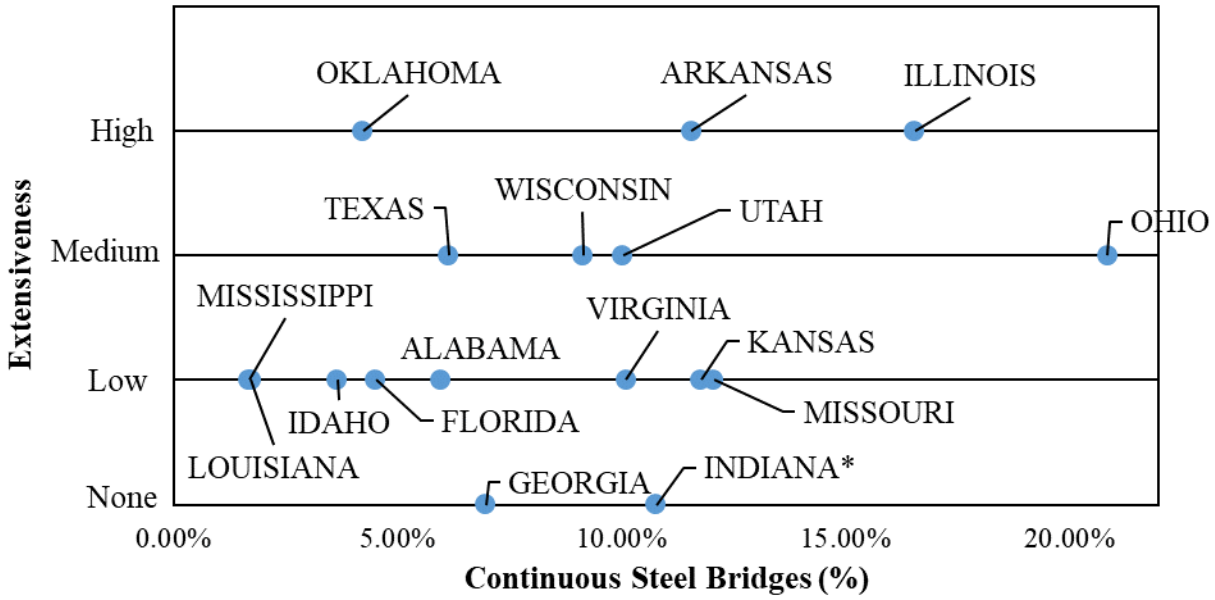

Figure 9. Continuous steel bridges in surveyed states and their reported extensiveness cracking level. (*Indiana DOT reported an uncertain extensiveness cracking level)

3.4 Review of State Construction Practices

3.4.1 Cement Content

The factors regarding deck deterioration can be numerous including aggregate type, aggregate size, water content in mixture, water/cement ratio among many others. Kansas DOT reported improvement in their deck cracking as a result of specification changes. Deck concrete strength and curing methodologies were cited as important factors in phone discussions with Kansas DOT engineers. Kansas DOT implemented a maximum concrete strength of 4,000 psi for bridge decks. Their best practices for concrete deck construction include: making proper and uniform placement and consolidation; curing with wet burlap on the very recently placed concrete within 15 minutes after being cast (quick cover up); keeping the wet burlap on the deck for at least 14 days plus a curing membrane for 7 days and let it cool down very slowly until concrete fully hydrates. They are conscious that concrete drying rate can contribute directly to crack formation at early ages, therefore their specifications emphasize wet curing and delaying concrete drying. The Kansas DOT engineer interviewed for this study was confident that these specifications were effective in reducing cracking. Previous research funded by Kansas DOT on high-performance concrete found out some helpful information regarding cracks including [30]: reducing cementitious content; improving early-age and long-term curing methods; reducing maximum compressive strength limits; limitation on maximum slump; controlling concrete's temperature; and minimizing finishing operations. Ohio DOT self-identified a medium level of early age cracking in their bridge decks and reported success in addressing the problem by promoting internal curing and adding fibers to the mixtures. The ODOT Construction and Material Specifications [31] require a minimum cement content of 520 lb/yd^3 and a design strength of 4,500 psi. As shown in tables 2 and 3, the required cement content varies between

different DOT agencies. Reducing cement content is known to be effective in reducing early age cracking [30].

Table 2: Curing methods, cement content and design strength of surveyed DOTs.

DOT Agency	Curing methods	Minimum Cement Content [lb/yd^3]	Minimum Design Strength [psi]
ALABAMA	1) Fog spraying or sprinkling with nozzles or sprinklers 2)saturated burlap, saturated plastic-coated burlap, or cotton mats	550	min 4,000psi
ARKANSAS	Burlap-polyethylene sheeting with minimum thickness of 0.10mm Copolymer/synthetic blanket; membrane curing compound	611	min 4,000psi
FLORIDA	1) continuous moisture; 2) membrane curing compound; 3) curing blankets; 4) accelerated cure	611	min 4,500
GEORGIA	White poly covers, white poly burlap sheet	611 or 635	
IDAHO	Water cure method	660	min 4,500
ILLINOIS	1) Waterproof paper method; 2) poly sheeting method; 3) wetted burlap method; 4) membrane curing method; 5) wetted cotton mat method	580	min 4,000psi
INDIANA	Water Curing Method and Membrane Forming Curing Compound	658	-
KANSAS	Saturated burlap covered with white polyethylene sheeting during the 14-day period plus additional 7 day membrane cure	-	-

Table 2 Cont.: Curing methods, cement content and design strength of surveyed DOTs.

DOT Agency	Curing Methods	Minimum Cement Content [lb/yd^3]	Minimum Design Strength [psi]
LOUISIANA	1) Foggers to maintain surface saturated; membrane cure; curing compound. 2) Use wet curing methods when concrete has set sufficiently to support blanketing materials without marring the surface.	-	min 4,000psi
MISSISSIPPI	Burlap, liquid membrane compound, poly sheeting	550	4,000psi
MISSOURI	Continuously wet Burlap or jute mats	517	min 4,000psi
OHIO	Water and membrane curing	520	4,500psi
OKLAHOMA	1) General method; 2) Forms-in-place method; 3) water method; 4) liquid membrane method; 5) waterproof cover method; 6) steam or radiant heat method	564	min 4,000psi
TEXAS	water curing, blankets, water spray (overlaps); ponding; membrane curing	-	min 4,000 psi
UTAH	1) Liquid membrane-curing compound method; 2) water method	-	min 4,000psi
VIRGINIA	Cured with white PE sheeting with or without the use of wet burlap. Later white pigmented curing compound shall be applied	<600 (Low shrinkage concrete)	min 4,000psi
WISCONSIN	Continuous wet cure method	-	-

CHAPTER IV
EXPERIMENTAL PROCEDURE

4.1 Overview

The field experiment detailed herein included visiting Arkansas bridges with early age cracking and structural monitoring of bridge 030428 by placing Vibrating Wire Strain Gages (VWSGs) in top rebar. Bridge 030428 is located in Sevier County on Highway 71, east of DeQueen, AR. The principal objective of monitoring the deck was looking into temperature and strain data developed in the concrete as it hardened after being continuously poured and later cured with a lithium based spray curing compound. The recorded data was analyzed as a function of time and location for improving the understating of early concrete behavior on bridge 030428.

Before the visit to bridge 030428, laboratory testing was performed on 4” x 8” concrete cylinders made with ARDOT class S(AE) concrete. This lab testing consisted of compressive strength, modulus of elasticity (MOE), and tensile strength tests. The purpose of this work was to create a relationship showing how mechanical properties change during early ages for ARDOT mixtures and compare it to the European Standard Code (Eurocode) [32] and the American Concrete Institute (ACI) [33] approximation models. Field and laboratory experimental work validation was performed to assist finite element work done by another student on the project. Both laboratory and experimental investigations are explained below in this section.

4.2 Laboratory Tests

4.2.1 Concrete Mechanical Properties

A common challenge structural engineers have faced in computer modeling is approximating values of the concrete's mechanical properties at an early age. It is crucial to know how concrete behaves after being cast because tensile stresses develop and they must be lower than the concrete tensile strength capacity (which evolves over time), if not cracks appear. Therefore, the concrete's durability and performance depend not only on how strains develop internally at early ages, but also on the strength development. Three compressive strength, tensile strength and modulus of elasticity (MOE) tests were completed at 1, 2, 3, 4, 7, 14, and 28 days. These tests were performed following ASTM C [34], ASTM C496 [35] and ASTM C469 [36], respectively. A comparison between the laboratory results and the Eurocode 2 [32] equations approximations are shown in Chapter V.

According to the Eurocode 2 [32] the compressive strength of concrete at a given age t depends on the type of cement, temperature and curing conditions. For a mean temperature of 20°C and curing in accordance with EN 12390 the compressive strength of concrete at various ages $f_{cm}(t)$ may be estimated from equations (1) and (2):

$$\boldsymbol{f_{cm}(t)} = \beta_{cc} * f_{cm} \qquad \textbf{(1)}$$

with

$$\boldsymbol{\beta_{cc}(t)} = e^{\{s[1-\sqrt{(\frac{28}{t})}]\}} \qquad \textbf{(2)}$$

where:

$f_{cm}(t)$ is the mean concrete compressive strength at an age of t days, psi

f_{cm} is the mean compressive strength at 28 days; see Appendix A (f_{cm} = 4000 psi)

$\beta_{cc}(t)$ is a coefficient which depends on the age of the concrete

t is the age of the concrete in days

s is a coefficient which depends on the type of cement:

= 0.20 for cement of strength Classes CEM 42.5 MPa and 52.5 MPa;

= 0.25 for cement of strength Classes CEM 32.5 MPa and 42.5 MPa;

= 0.38 for cement of strength Classes CEM 32.5 MPa;

The elastic modulus of ARDOT class S(AE) concrete was also measured. The American Concrete Institute (ACI) [33] MOE estimate for normal weight concrete is given by equation (3):

$$\textbf{MOE} = 57{,}000\sqrt{f'c} \qquad \textbf{(3)}$$

where:

MOE = modulus of elasticity, psi

f'_c = concrete minimum compressive strength at 28 days, psi

However, Eurocode 2 does accounts for the early variation and with equation (4) estimates early elastic modulus behavior:

$$\mathbf{E_{cm}} = (f_{cm}(t)/f_{cm})^{0.3} * E_{cm} \qquad \textbf{(4)}$$

where:

$E_{cm}(t)$ is the Elastic modulus at an age of t days

$f_{cm}(t)$ is the mean concrete compressive strength at an age of t days

E_{cm} is the Elastic modulus at an age of 28 days

$\mathbf{f_{cm}}$ is the mean concrete compressive strength at an age of 28 days, psi

The last laboratory test performed was the split tensile strength. ACI [33] recommends estimate the split tensile strength of concrete with equation (5):

$$\textbf{ACI Tensile Strength} = 6.7\sqrt{f'c} \quad \textbf{(5)}$$

Eurocode 2 estimates the behavior of concrete's tensile strength capacity using equation (6):

$$\boldsymbol{f_{ctm}(t)} = (\beta_{cc}(\mathrm{t}))^{\alpha} * f_{ctm} \quad \textbf{(6)}$$

where:

$\boldsymbol{\beta_{cc}(t)}$ is a coefficient which depends on the age of the concrete

$\boldsymbol{\alpha}$ = 1 for t < 28; α = 2/3 for t ≥ 28

$\mathbf{f_{ctm}}$ is a value from table 3.1 of the Eurocode which is based on the concrete strength class (see appendix A)

4.3 Field Tests

4.3.1 Bridge Visits

The bridge visits were performed to study crack patterns (transverse, diagonal or longitudinal) and locations (near support or mid-span) formed in the decks. This information would help the team identify possible causes of bridge deck cracking. Also, the crack mapping would provide an informed rationale of where to locate the strain sensors through bridge 030428. Field observations were performed on three ARDOT composite continuous steel bridges. These bridges were selected in consultation with ARDOT research staff. A 50 ft. horizontal grid was drawn on the deck plans to help locate the cracks. The first bridge (bridge 07315) was located in

Lowell, Arkansas. Bridge 07315 is an onramp from I49 south onto 612 west. ARDOT staff mentioned it was a “new” bridge (2-3 years old) that had experienced some cracking prior to opening to traffic. Figure 10a shows the bridge from the northeast abutment looking towards the southwest. The overall bridge dimensions were roughly 42 ft wide and 230 ft long, and the bridge was skewed. Figure 10b shows a digitalized version of the observed cracks from the visit. There was a minimal degree of cracking near the northeast pier, most cracks appeared to be due to plastic shrinkage. Overall, it was in reasonably good condition so little information could be garnered from this visit to inform bridge instrumentation.

Figure 10. (a) Bridge 07315 site (photo by author) and (b) map cracking.

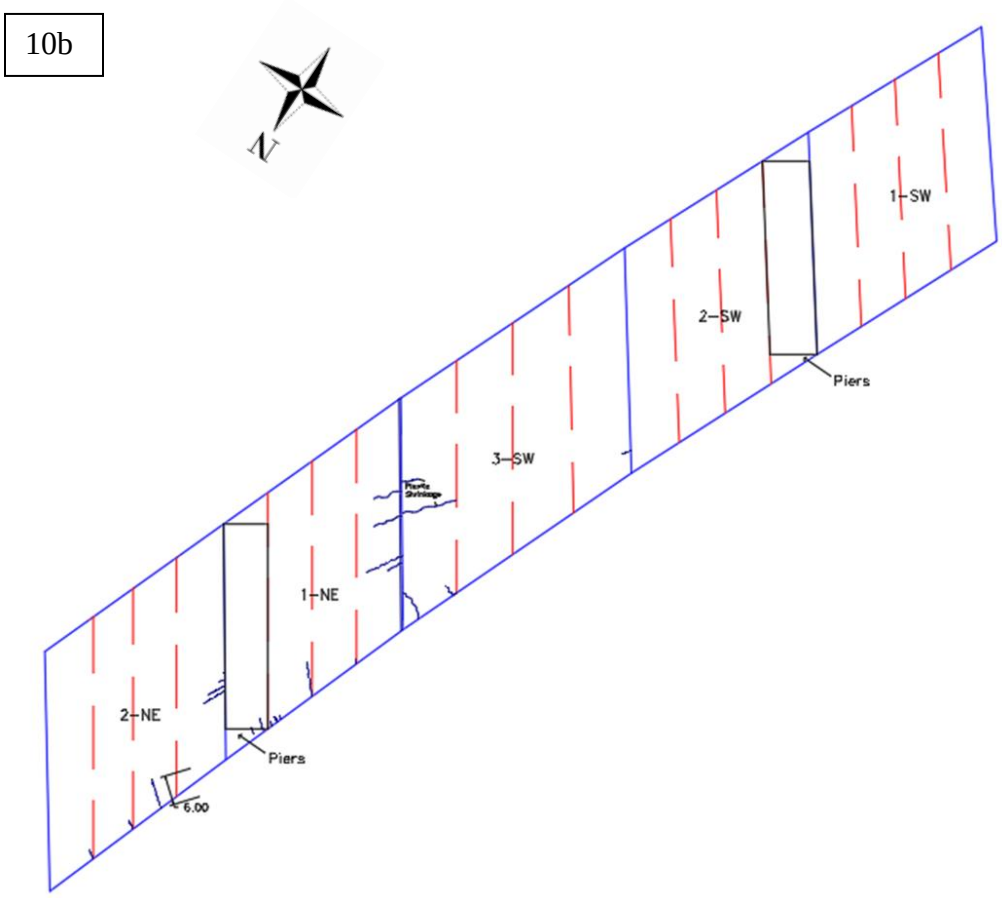

Figure 11. (a) Bridge 07315 site (photo by author) and (b) map cracking.

The second bridge visit was in Springdale, Arkansas (BB0413) shown in figure 11a. Bridge BB0413 carries Elm Springs Road over I49. The 3-span bridge with a skew angle of 13º54’30” consisted of 7 existing beam lines reused from 1982 on the bridge deck, and 7 new ones placed during construction. The bridge deck was recommended to the research team by ARDOT engineers due to bad conditions observed on the bridge deck consisting of extensive surface cracks, as shown in figure 11b. Oddly, the positive moment regions were more severely cracked rather than the negative moment regions. The old girders were located in the central part of the deck (#6-12), the new girders were located on the outside sections of the bridge deck. Girders 1-6 were placed 6 ft between each one; girders 6-12 had 7 ft spacing. ARDOT had

treated the bridge with crack sealer when early age cracking was observed. Regular curing compound was used during the deck pour for the initial set, and the sealer was a class 2 protective surface treatment (this is different than using boiled linseed oil or lithium curing compound). The crack inspection was made on half of the bridge due to traffic.

The final bridge visit was in Bella Vista, Arkansas. Bridge 07273 was a two-span continuous bridge with steel girders with a skew angle of 28º containing four steel plate girders. The bridge deck appeared to be severely cracked mostly in the negative moment region. The majority were transverse cracks, longitudinal cracks were also observed. Figure 12a-12c shows the shape and extent of cracking in this bridge. ARDOT treated the cracks on surface with epoxy filling material. Information compiled from the three bridge visits, especially bridges 2 and 3 provided the research team with a path forward for instrumentation of a new bridge. Since mostly transverse cracking was observed in the field visits, most VWSGs would be oriented to measure longitudinal strains, with emphasis in negative moment regions. All three bridges had the pouring sequence in the plans but the final method was done continuously.

Figure 12. (a) Bridge BB0413 (photo by author) site and (b) map cracking.

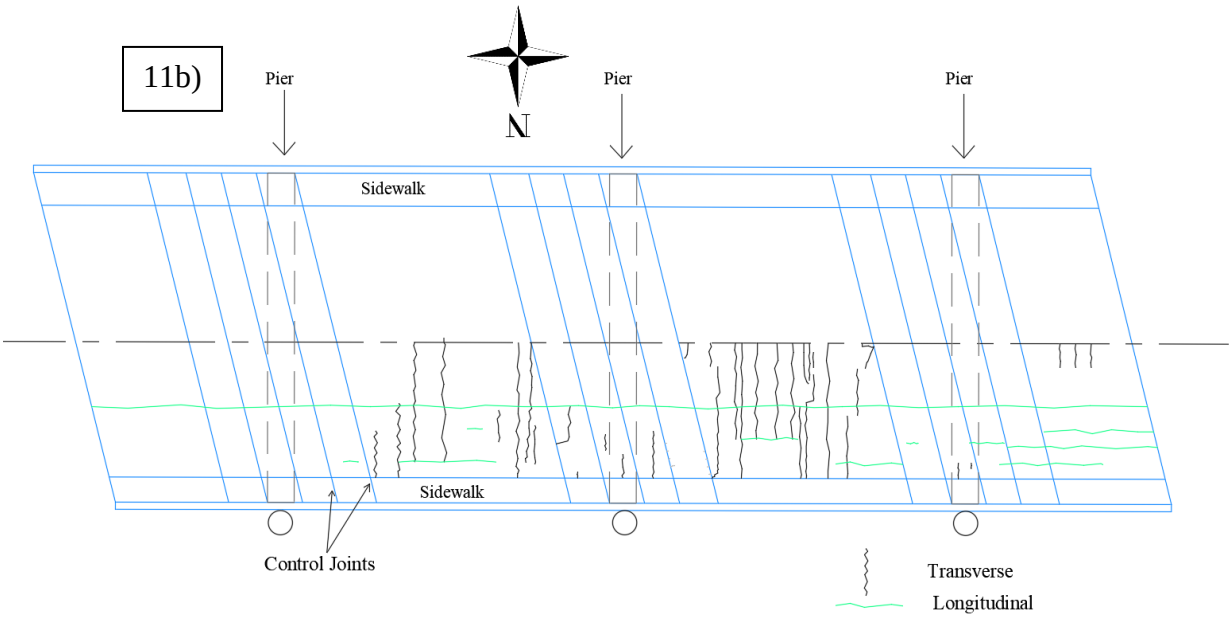

Figure 13. (a) Bridge BB0413 (photo by author) site and (b) map cracking.

Figure 14. (a) Bridge 07273 site, (b) in-situ crack shapes and (c) map cracking.

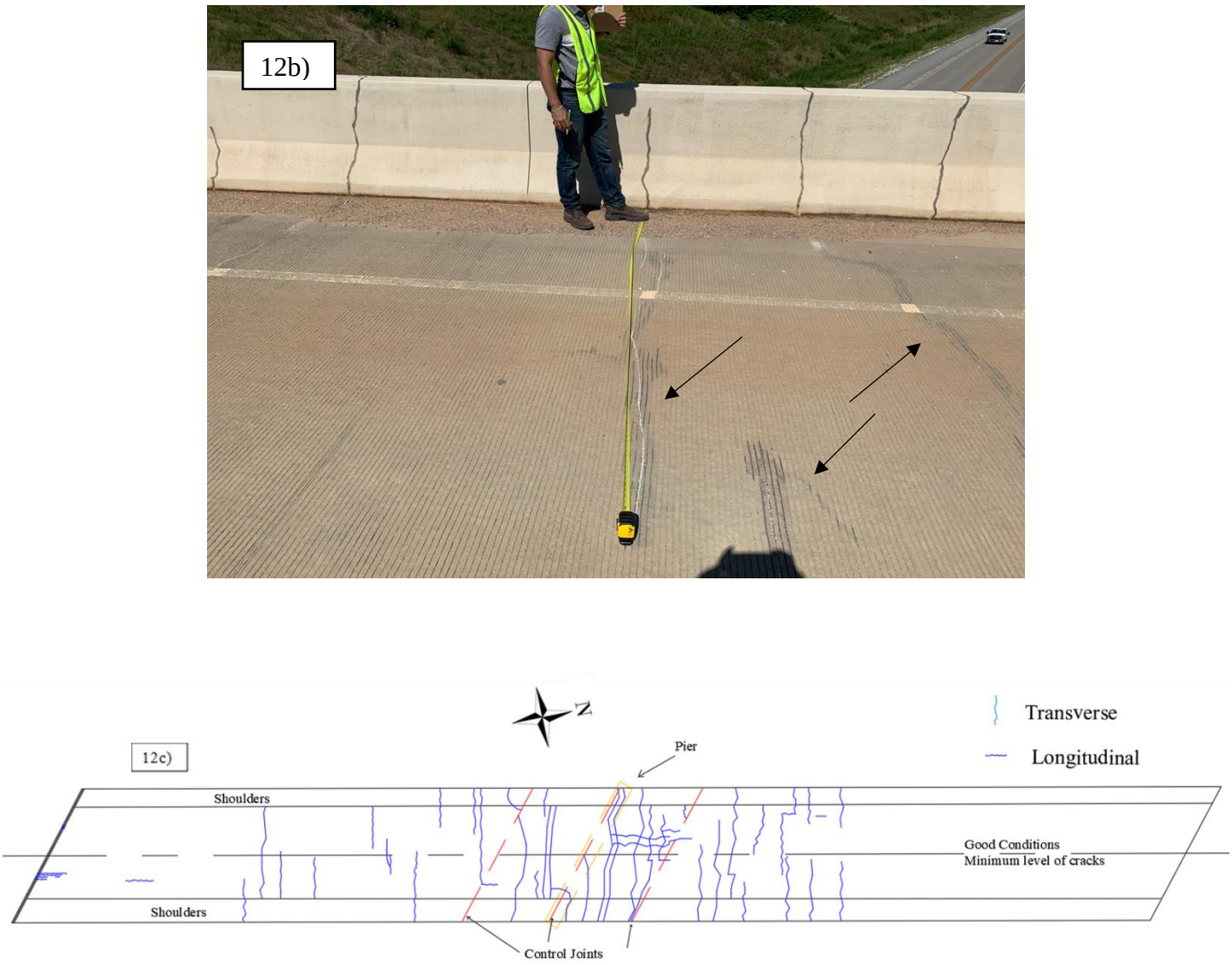

Figure 15. (a) Bridge 07273 site, (b) in-situ crack shapes and (c) map cracking.

4.3.2 Curved Bridge 030428

Curved girder bridge 030428 was targeted for instrumentation by the Transportation Research Committee for project 1903 (TRC 1903) for studying early age strains developed in the concrete deck with internal strain instrumentation. The bridge was located in Sevier County on Highway 71, east of DeQueen, AR. The bridge consisted of an existing bridge (removed) which was 27.6 ft wide and 104 ft long composed of three 34 ft steel beams spans with a concrete deck and supported on concrete pile bents. The new bridge (bridge 030428) consisted of 3 span steel girders with a skew angle of 15˚ supported by two piers and two abutments. The structure's construction was divided in two stages due to heavy daily traffic flow. Stage one and two consisted of an array of four and six steel girders (W36X135) placed below an 8.75 in. concrete deck (see figure 13). All deck reinforcement was epoxy coated as shown in figure 14. The bridge width was 78 ft and its total length was approximately 191 ft with a center line curvature radius of 1910 ft. and a cross slope of 7.70%.

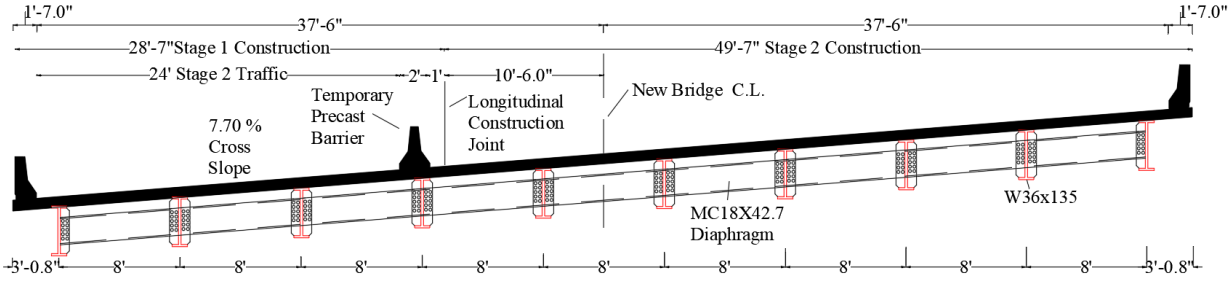

Figure 16. Bridge 030428 cross-section.

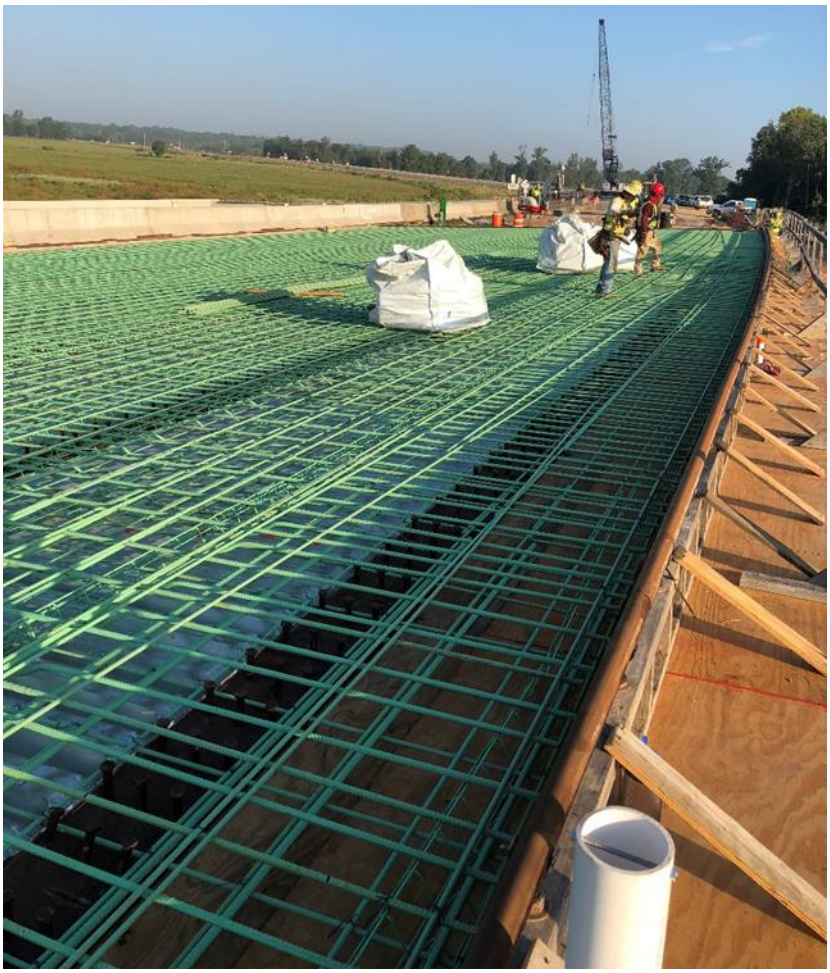

Figure 17. Site view from bent 1 looking to bent 2.

Cylindrical specimens were collected from 3 trucks arriving to the site at 3:50 a.m., 6:00 a.m., and 7:45 a. m. approximately (taken with lots typically sampled by ARDOT). These were stored in a foam cooler for one day and then taken to the laboratory to a 72 °F environmental chamber at 50% relative humidity. Afterwards, these were tested for compressive strength and MOE at 1, 3, 7, 14 and 28 days. Appendix C shows weather conditions reported by ARDOT engineers during the deck pour. The pour was carried out in the early morning during the summer time (August 2019). Bridge 030428 mix design is show in table 4 and the ARDOT reported results for slump, air content and temperature in table 5. The hydration stabilizer was reduced as pour went along the bridge length.

Table 3. Bridge 030428 concrete deck mix design.

Mix Design – Bridge 030428		
Specified Strength	>4000	psi
Slump range	1"-4"	in
w/c ratio	0.42	-
Portland/Fly Ash	6.5	bags/yd^3
AER	0.5	oz/cwt
WRA	4	oz/cwt
Hydration Stabilizer	14*	oz/cwt
% Fly ash	0	%
% Fine Agg.	36.4	%
% Course Agg.	63.6	%
% Air	4-8%	%
Gal/bag	4.8	Gal/bag

Table 4. ARDOT on-site testing reported results.

ARDOT Reported Results			
	Slump (in)	**Air Content**	**Temperature (ºF)**
Truck 1/30	4	5.90%	86
Truck 12/30	5.75	5.30%	79
Truck 16/30	4.5	7%	82
Truck 23/30	3.75	6.60%	80

4.3.3 Strain and Stress Analysis

The internal tensile strains developed in the concrete at early ages are expected to be the highest due to the material's low strength gain. This is why there is a concern about what loads are acting on the bridge deck at initial stages so it does not surpass the capacity. The main strain study analysis was concentrated at the very first hours after concrete pouring (0-36 hours). The strain data collected from bridge 030428 was calibrated according to Geokon [37] calibration procedures for 4200 model sensors. Furthermore, principal strains [38] were calculated to be multiplied by the expected MOE at a specified time, approximated by the Eurocode and

therefore, obtain the principal stresses. These principal stresses were compared with the approximate concrete strength at the time when these principal stresses occured. The modulus of elasticity was approximated with the Eurocode equation (see section 4.2.1) to obtain the behavior as a function of time.

4.4 Vibrating Wire Strain Gages (VWSG)

The bridge selected was instrumented to measure deck behavior (strains and temperature) during construction and for the following 25 days. This was achieved by using Vibrating Wire Strain Gauges (VWSGs) manufactured by Geokon, Inc. These sensors are designed to be directly embedded in concrete. The 4200 Model has a 6 in. (153 mm) gage length and consists of a vibrating wire and a thermistor. The thermistor collects temperature data and the vibrating wire is calibrated to capture strain. The sensors are capable of measuring concrete curing strains as well as structural and temperature related strains. Strains were continually recorded for approximately 25 days using battery powered data loggers. Figure 15a-15b show an example of the 16-channel data logger box and 4200 VWSG model.

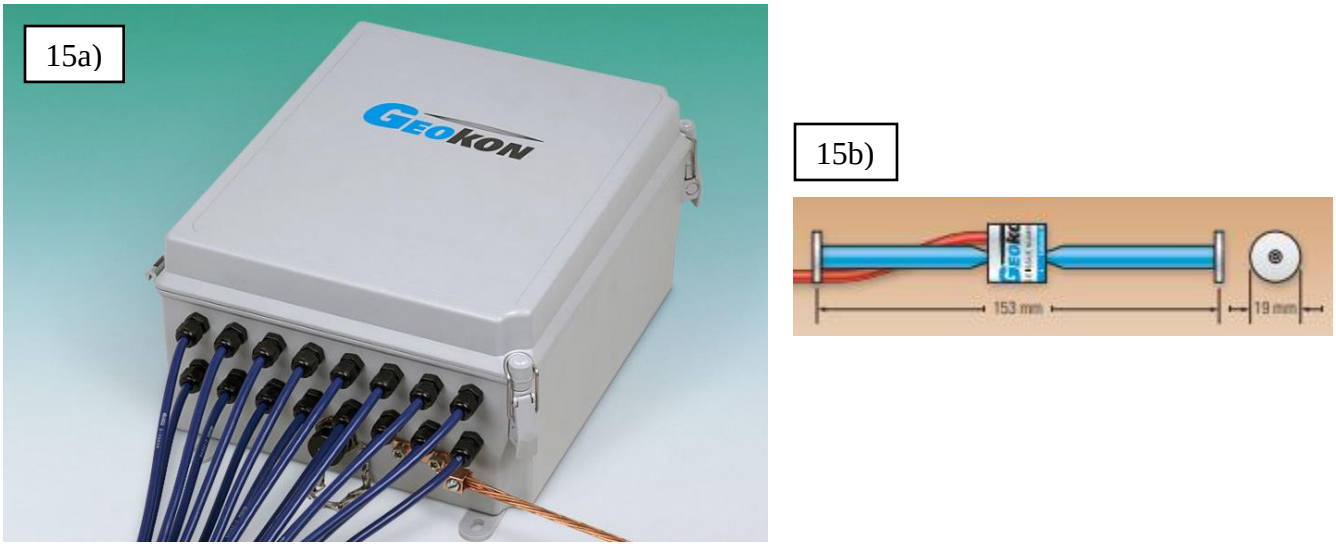

Figure 18. (a) 16-channel DAQ Geokon box and (b) VWSGs 4200 Geokon Model *[37]*.

4.5 Sensors Location Plan and Instrumentation

The sensor locations were defined based on the bridge visits mentioned in section 3 and engineering judgement. 32 gages were installed and therefore, they were strategically located. Negative moment regions (at piers) were a major focus because there should be higher tensile stresses in the deck at these locations and because during the research team's bridge visits transverse cracking appeared to be more extensive in these regions. The objective was capturing the strains and stresses developed in concrete during early days after casting. Initially, the proposed idea was to distribute the sensors throughout one quarter of the bridge and by symmetry approximate the internal behavior of the whole deck could be known. Bridge 030428 is a curved horizontal structure and that principle could not be applied. Therefore, 32 sensors where located strategically through the whole bridge covering both piers at the negative and positive moment regions mostly attached to the underside of the top rebar (approximately 3 inches from surface) mat parallel to the steel girders. Figure 16 shows the final VWSG sensors location plan for the specific bridge to be instrumented. Each number and symbol represent a VWSG sensor attached to the deck top rebar.

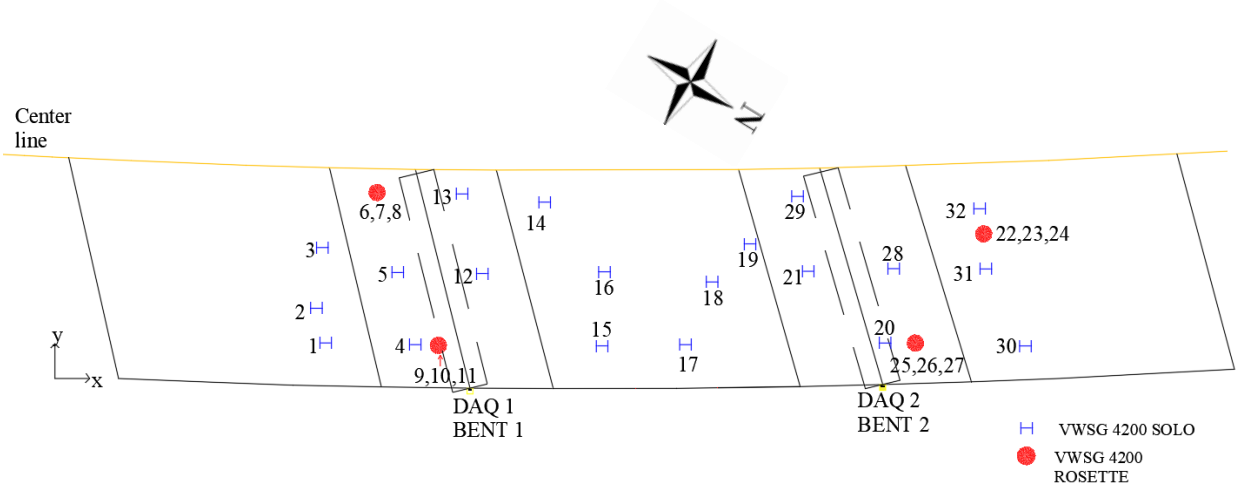

Figure 19. VWSGs sensors layout on Bridge 030428.

Also, we were interested in strain and stresses developed at a certain point in 3 directions: longitudinal, transverse and at angle. Figure 17 shows the “strain rosette” technique which was achieved by attaching 3 VWSG sensors together in the top rebar at a certain location in the previous mentioned directions. The VWSGs were attached to the reinforcing steel using foam pieces and plastic ties to prevent amplification of the emitted frequency by the sensor (errors could be induced if ends are touching metal material). Two 16-channel data acquisition boxes (DAQ) were installed at bent 1 and 2. Figure 18a-18b shows the actual installation in site.

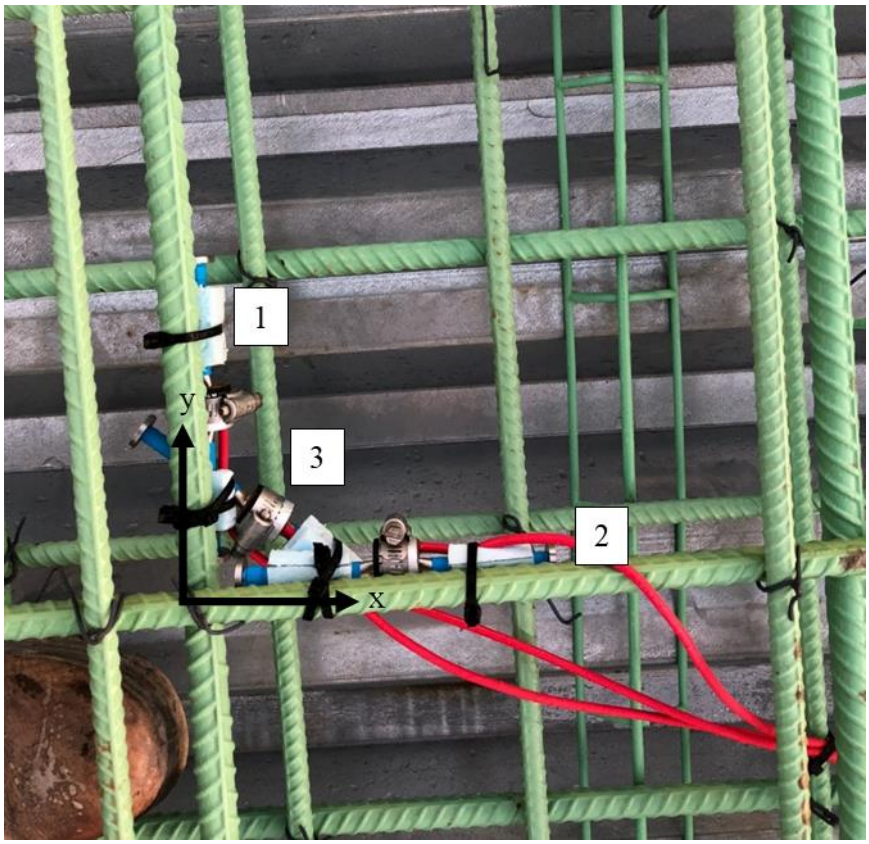

Figure 20. Strain rosette display.

Figure 21. (a) DAQ installation before and (b) after concrete pour.

CHAPTER V

RESULTS AND DISCUSSION

5.1 Results and Discussion

5.1.1 Laboratory results

Concrete cylindrical specimens with dimensions 4 in. x 8 in. were tested at 1, 2, 3, 4, 7, 14, and 28 days (3 specimens per age). The tests performed were compressive strength, split tensile strength, and elastic modulus. Specimens were cured in a 50% saturation environment at 73 °F approximately. Specimens were tested at different ages to have a control case for each mechanical property previously mentioned and use the Eurocode equations to approximate the concrete bridge deck's initial behavior for future finite element modeling.

Results for average compressive strength for specific ages are showed in table 6. Also, these values were compared to the Eurocode approximation using equation (1) shown in Chapter 4. This formula approximates the concrete's compressive gain behavior and converges to the 28 days compressive value used as input. Therefore, $\mathbf{f_{cm}}$ was taken as the 28-days laboratory results and as the Eurocode standard suggested value (28 MPa = 4,061 psi). These cases are plotted in figure 19 to see how close the agreement between laboratory values and the estimate were. Eurocode approximations with $\mathbf{f_{cm}}$ as the 28-day lab value were close to the actual behavior. However, using $\mathbf{f_{cm}}$ as 4,061 psi (Eurocode suggested value for 28-days compressive strength) the first 4 days values are close to the actual results; after day 5 approximately, the percent difference starts increasing and ends with a difference of approximately 500 psi (13%) at 28-days. The compressive behavior changes at early days due to curing and aging of the concrete.

Table 5: Compressive strength results.

Age (days)	Measured (psi)	Eurocode (psi)	Difference Percentage	Eurocode (psi)	Difference Percentage
1	1480	1390	6%	1200	21%
2	2100	2050	3%	1770	17%
3	2360	2430	3%	2100	11%
4	2530	2690	6%	2330	8%
7	2690	3160	16%	2730	2%
14	3100	3660	17%	3170	2%
28	3510	4060	15%	3510	0%

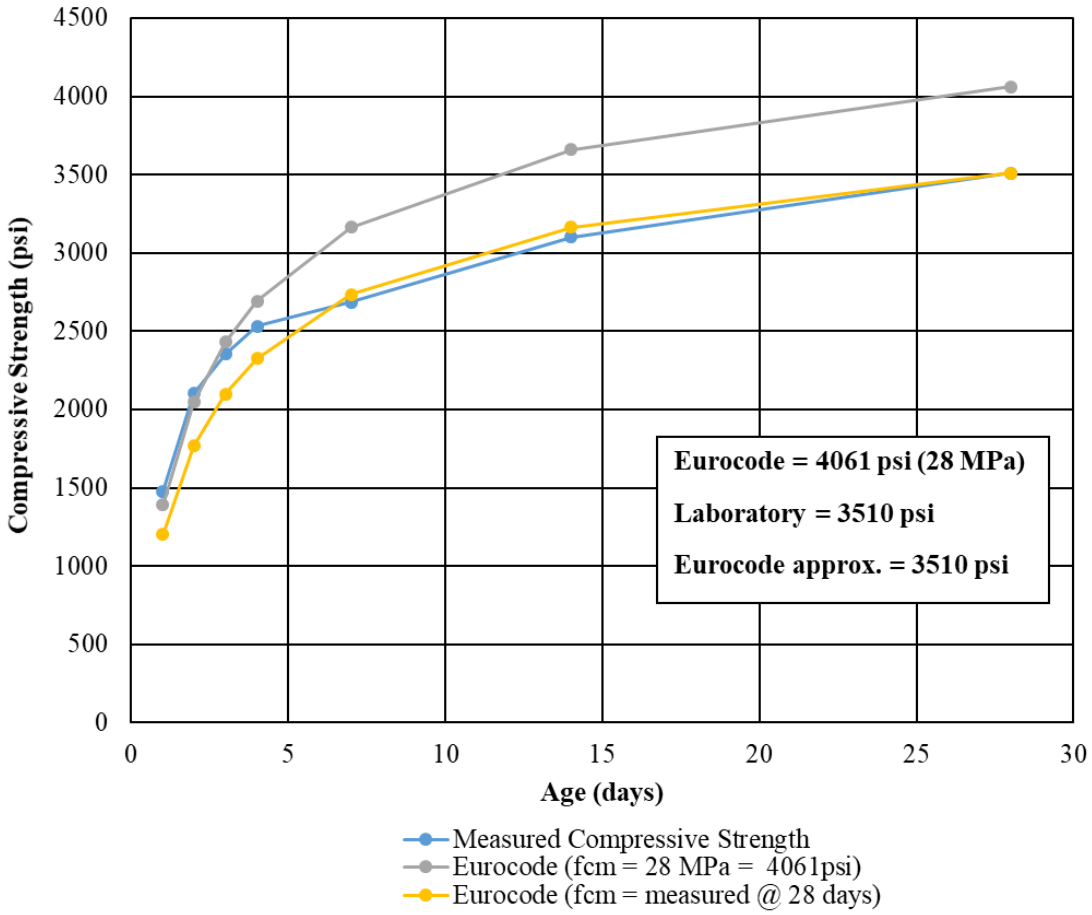

Figure 22. Compressive strength comparison between measured laboratory results and Eurocode 2 results.

The analysis process was repeated for the modulus of elasticity with the corresponding equations (refer to equations 3 and 4 on Chapter 4). Figure 20 shows the MOE values for the tested (control) specimens along with the ACI and Eurocode approximations. There are two cases presented using the Eurocode: one consists of using the suggested value by the Eurocode [32] for MOE at 28-days and the second case is using the actual laboratory values at 28-days. Table 7 illustrates the difference percentage between these methods and compares it with the average measured values. ACI results had a higher percent difference compared to the measured values than the Eurocode estimations. Also, the Poissons's ratio was measured and values fluctuated between 0.15 to 0.30 (see table 8). Eurocode 2 takes Poisson's ratio equal to 0.2 for uncracked concrete and 0 for cracked concrete. It can be noticed that this value changes over time at early days after concrete is being cast.

Table 6: Modulus of Elasticity averaged laboratory results, ACI, and Eurocode 2 numerical approximations and percent difference compared to measured results.

Age (days)	Measured (psi)	ACI (psi)	Difference Percentage	Eurocode (psi)	Difference Percentage	Eurocode (psi)	Difference Percentage
1	2892487	2190116	28%	3153023	9%	3127077	8%
2	3351768	2612690	25%	3541676	6%	3512531	5%
3	3464978	2765920	22%	3728834	7%	3698149	7%
4	3589429	2867427	22%	3845075	7%	3813433	6%
7	3782396	2953568	25%	4035880	6%	4002669	6%
14	3839137	3174820	19%	4217145	9%	4182442	9%
28	4314413	3376979	24%	4350211	1%	4314413	0%

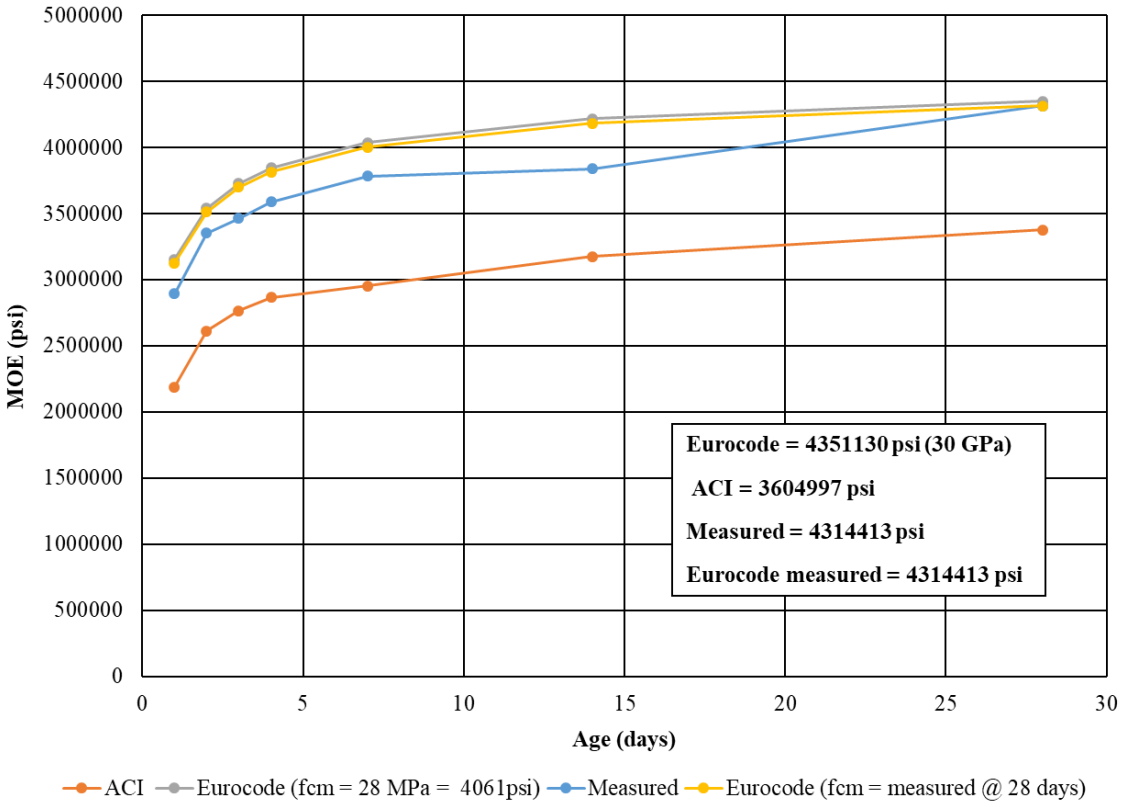

Figure 23. Modulus of Elasticity comparison between averaged measured laboratory results, ACI and Eurocode 2 values.

Table 7: Poisson's ratio averaged laboratory results compared to Eurocode assumption.

Age (Days)	Measured	Eurocode 2	Difference Percentage
1	-0.19	-0.20	5%
2	-0.22	-0.20	11%
3	-0.25	-0.20	22%
4	-0.24	-0.20	20%
7	-0.25	-0.20	22%
14	-0.24	-0.20	20%
28	-0.29	-0.20	36%

As popularly known, concrete's tensile capacity is extremely low compared to the compressive capacity. Similar to the previously mentioned mechanical properties, tensile strength changes over time, specifically at early ages which are the most notable increments. This is a concern especially when considering the likelihood of cracks forming at early ages in response to volume changes. Cracks in concrete develop due to insufficient tensile strength capacity. Therefore, results from the laboratory were compared to the ACI and Eurocode prediction methods. Average results from laboratory tests are shown in table 9 along with the percent differences. Eurocode predicted the same behavior of the measured values but at a higher capacity. ACI values are closer to the measured but Eurocode values were low compared to the measured. Figure 21 shows the plotted tensile strength values for measured, ACI, and Eurocode results.

Table 8: Tensile strength results and percent difference comparison.

Age (days)	Measured (psi)	ACI (psi)	Percent Difference	Eurocode (psi)	Percent Difference	Eurocode (psi)	Percent Difference
1	200	260	24%	110	60%	110	58%
2	310	300	2%	160	64%	160	63%
3	300	330	8%	190	44%	190	43%
4	320	340	4%	210	42%	210	40%
7	290	350	19%	250	14%	250	13%
14	420	370	13%	290	38%	290	37%
28	320	400	20%	320	1%	320	0%

From these laboratory results, it could be advised to use Eurocode approximations for early age predictions for compressive strength and modulus of elasticity. Good results can be achieved if an accurate 28-days compressive strength value is used. However, tensile strength is more difficult to estimate. The 28-days sample testing was low to what was expected. This had an effect on the Eurocode approximation since the tensile strength will depend on the compressive strength at 28 days. ACI showed to be a better approximation for this case.

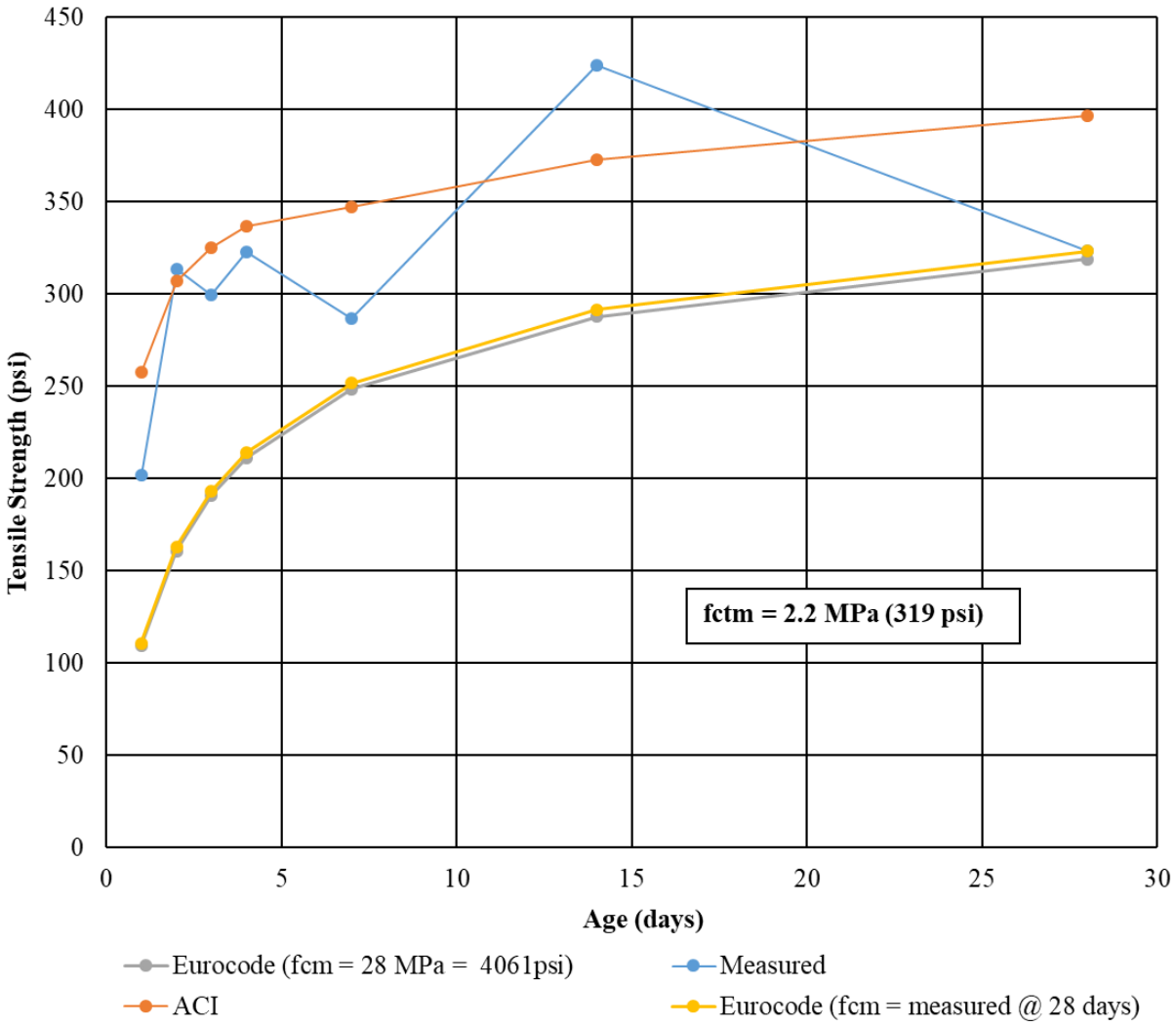

Figure 24. Tensile strength results.

5.1.2 Field results

5.1.2.1 Concrete Mechanical Properties from Bridge 030428 Samples

In order to study the early age concrete mechanical properties of bridge 030428, 4 in. x 8 in. cylinder samples were taken from different ready mix concrete trucks. The target was looking into the variation of concrete mechanical properties through the bridge. Figures 22-24 show the 1, 3, 7, 14 and 28 day compressive strengths from the field specimens tested at the University of

Arkansas concrete laboratory. Numerical values can be seen in Appendix C. Final 28 day results using the Eurocode 2 equation converge to a selected value of $\mathbf{f_{cm}}$ (equation 1 in section 5.1.1) which is the compressive strength of the concrete at 28 days. For these calculations, $\mathbf{f_{cm}}$ was taken as the field measured value at 28 days.

The field results at 28 days were notably higher than the minimum deck strength specified in ARDOT standards (4,000 psi). The laboratory values for compressive strength at 28 days from the 3 trucks were 6,170 psi, 5,420 psi and 4,640 psi. ARDOT's reported averaged compressive strength values at 7 and 28 days were 5,500 psi and 6,400 psi, respectively. At 3 days old, the deck already reached the 4,000 psi minimum 28 day strength through the entire length. The Eurocode 2 equation was included in the graph to estimate the early behavior and compare final results. Figure 25 shows all the behaviors and their Eurocode 2 approximations. Additional markers are shown in the early ages (prior to one day) so these strengths could be used to assist accurate modeling of the bridge deck.

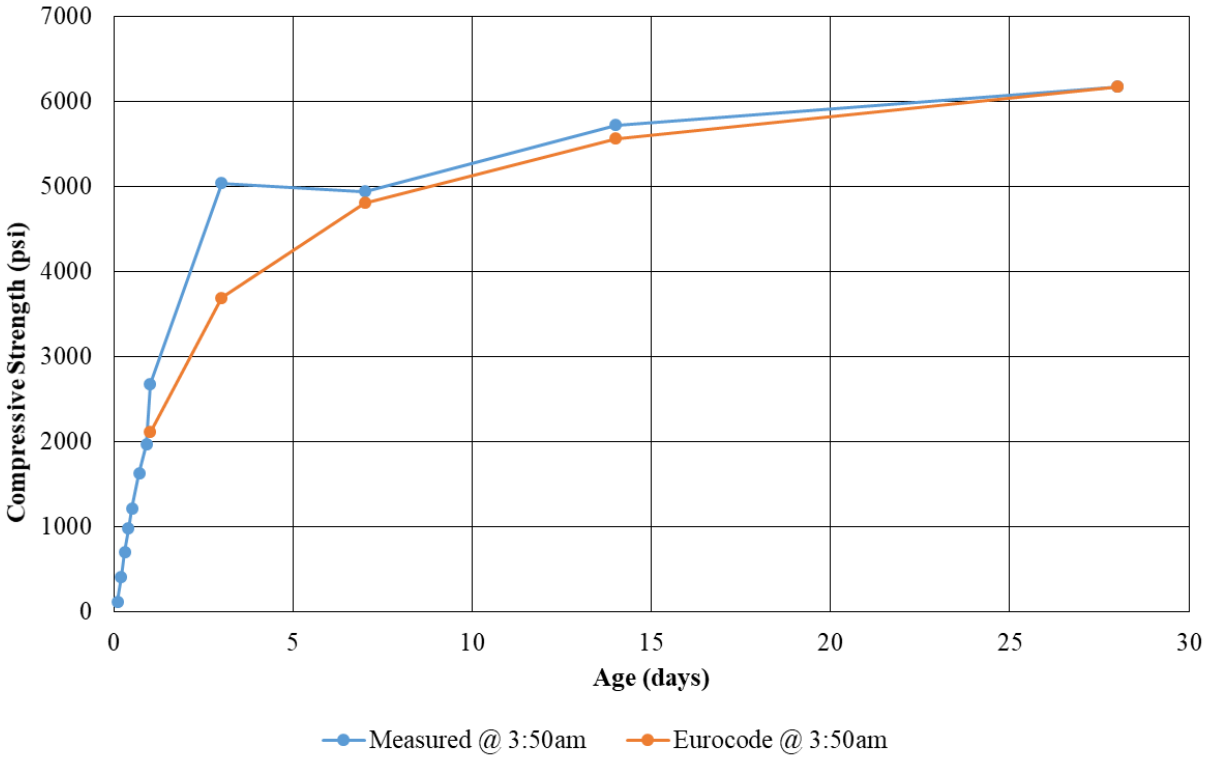

Figure 25. Compressive strength results for 3:50 a.m. samples.

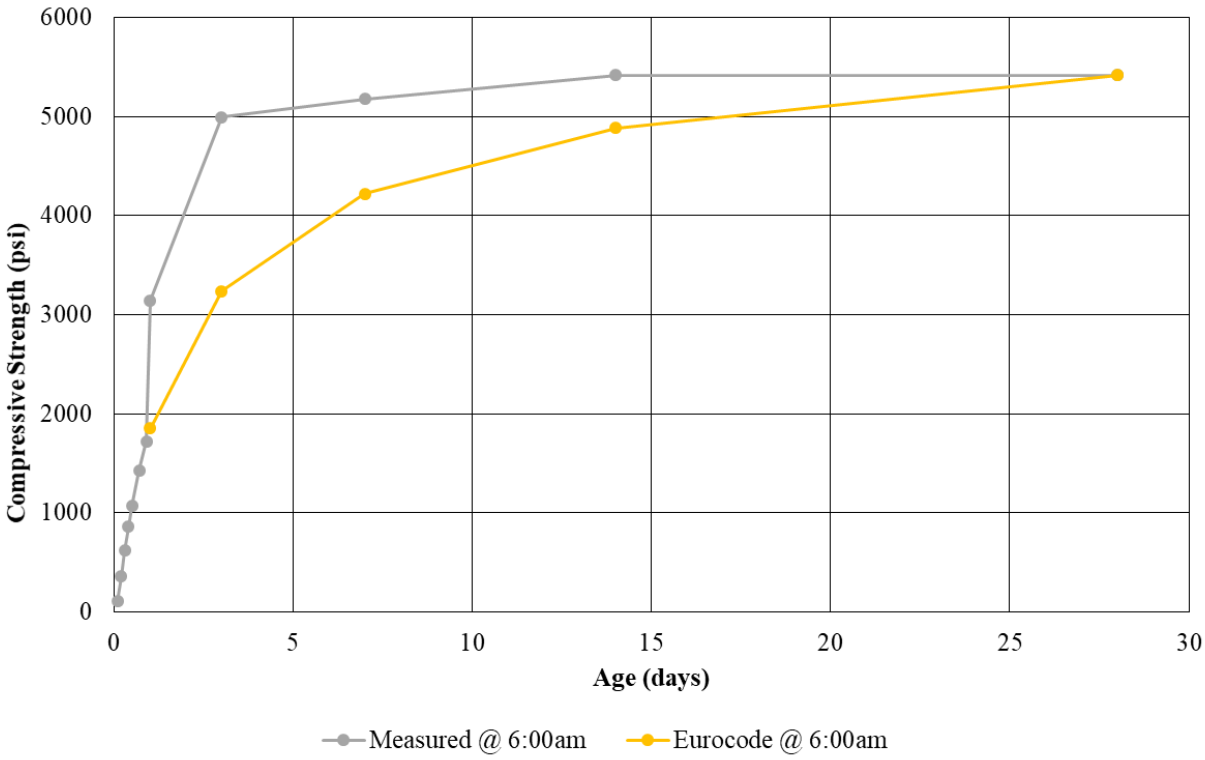

Figure 26. Compressive strength results for 6:00 a.m. samples.

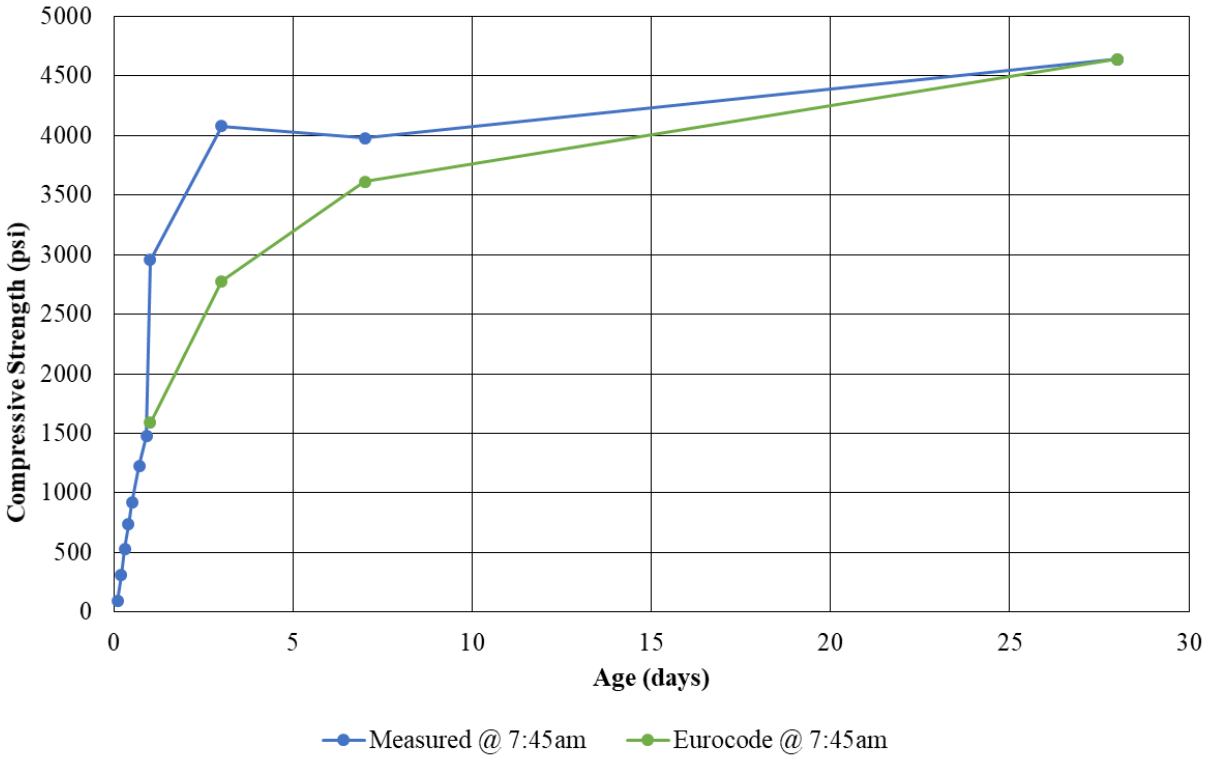

Figure 27. Compressive strength results for 7:45 samples.

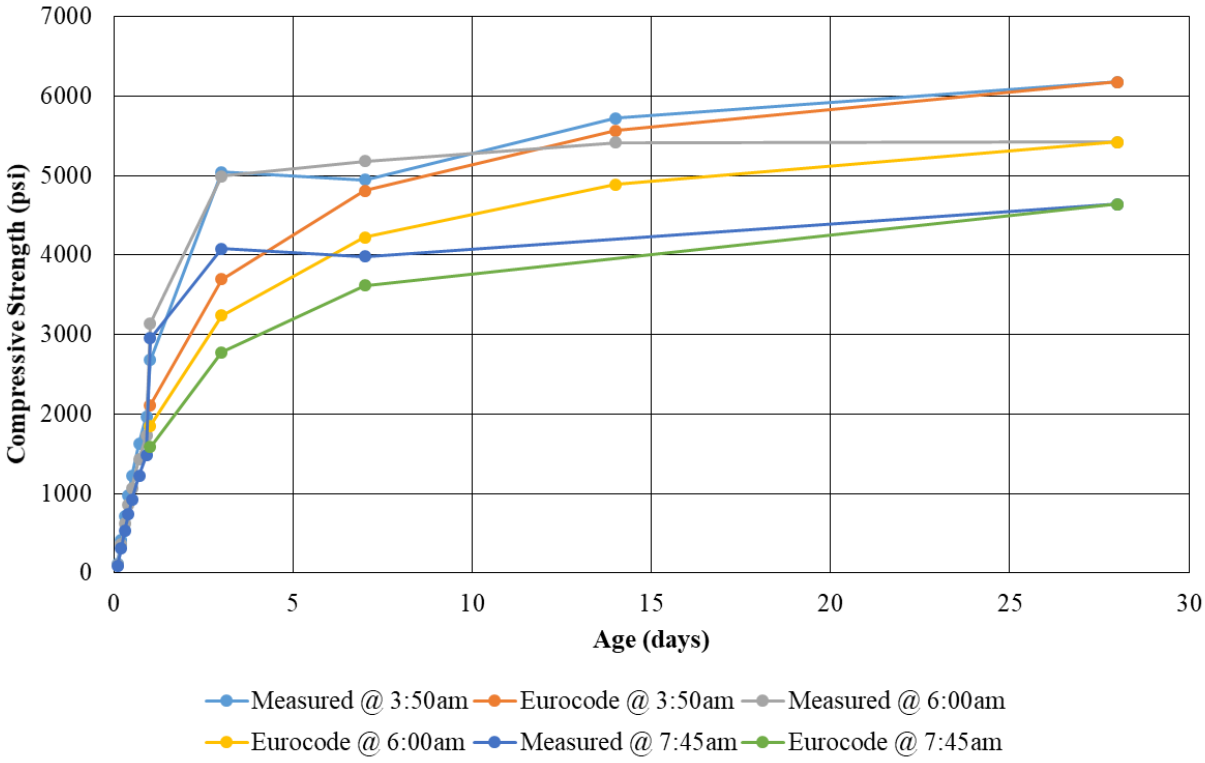

Figure 28. Compressive strength results for all collected samples.

Modulus of elasticity results are illustrated in figures 26-28. At 28 days, the results of the 3:50 am, 6:00 and 7:45am specimens were $3.21x10^6$ psi, $3.14x10^6$ psi, $3.00x10^6$, respectively. Final 28 days results using the Eurocode 2 equation will converge to $\mathbf{E_{cm}}$ (equation 4 in section 5.1.1) which is the MOE value of the concrete at 28 days. For these calculations, $\mathbf{E_{cm}}$ was taken as the field measured value at 28 days. Figure 29 shows all the MOE measured behaviors and Eurocode 2 approximations.

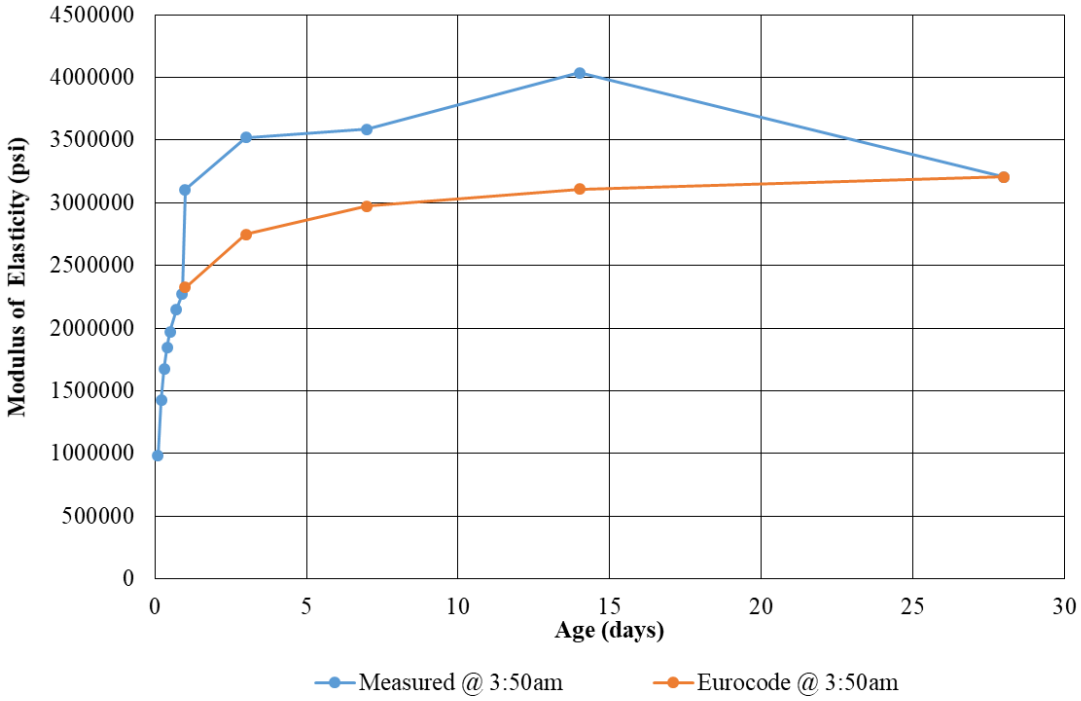

Figure 29. Modulus of elasticity results for 3:50am.

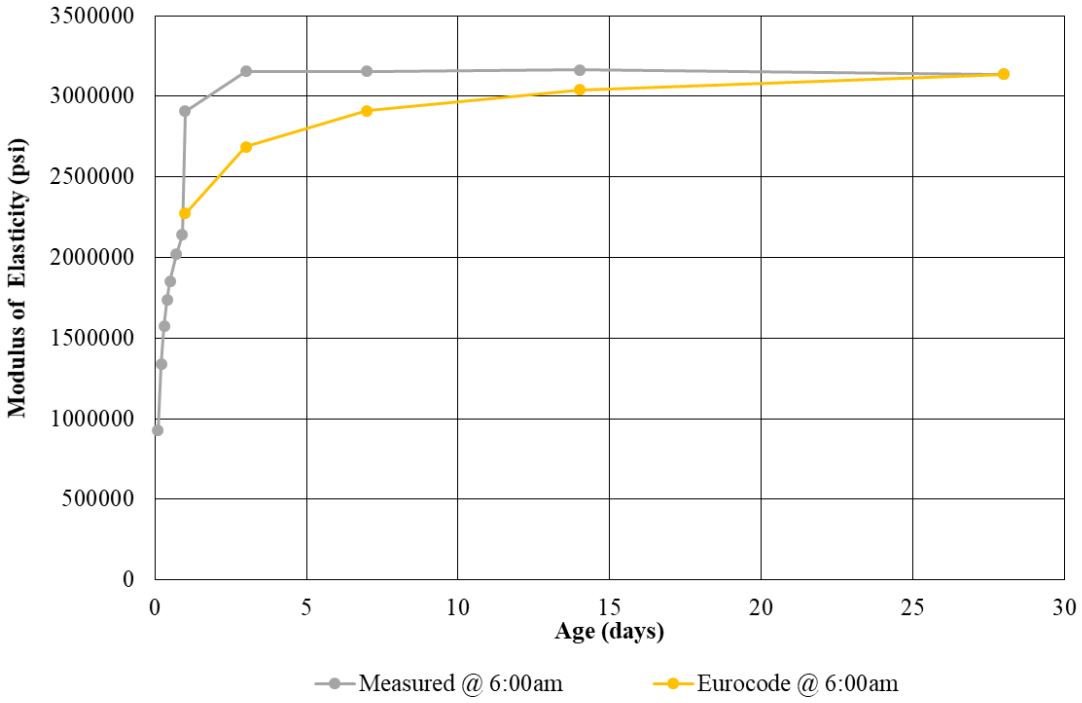

Figure 30. Modulus of elasticity results for 6:00am.

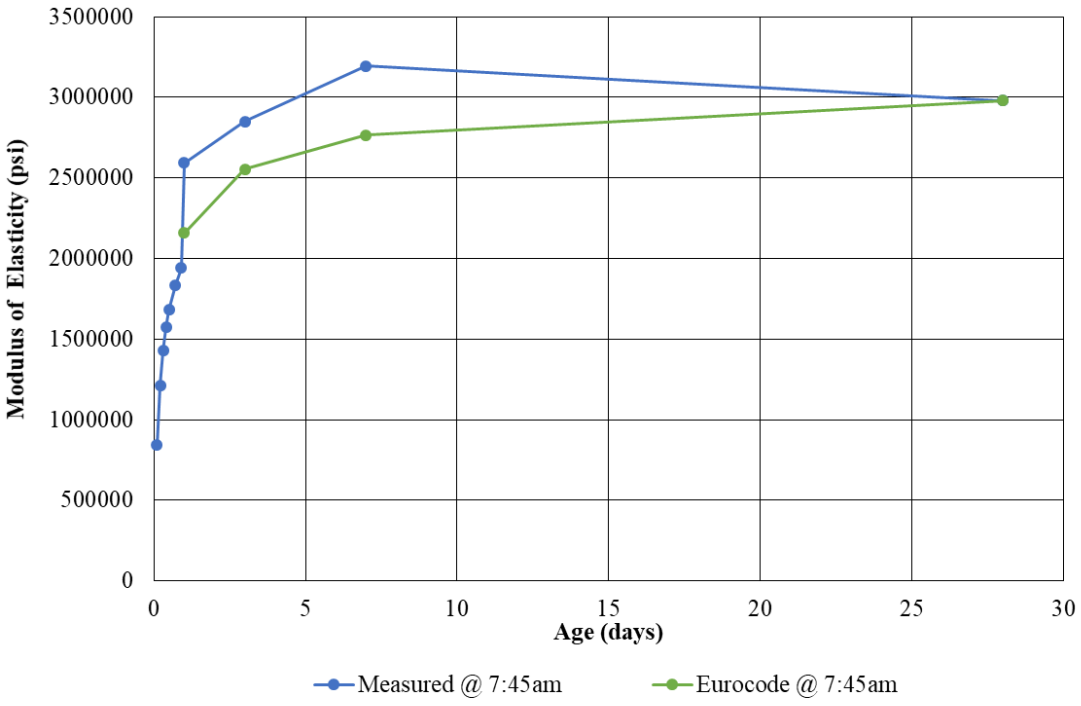

Figure 31. Modulus of elasticity results for 7:45am.

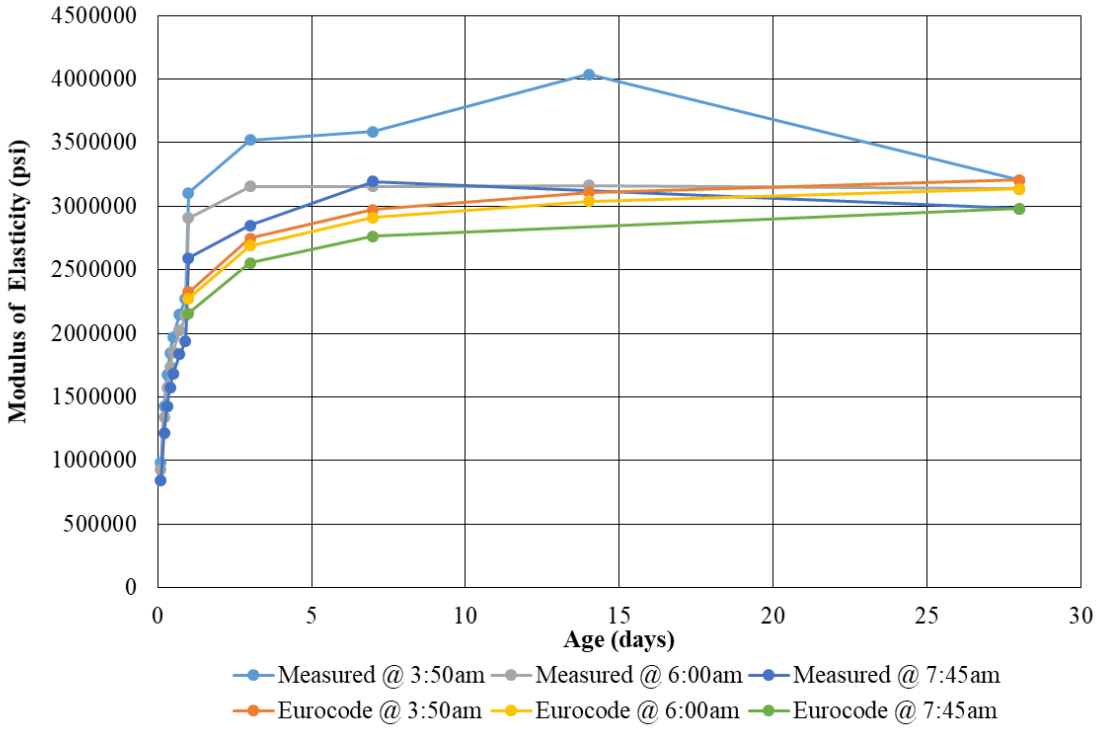

Figure 32. Modulus of elasticity for all collected data.

Eurocode 2 value approximations have been estimated with $\mathbf{f_{cm}}$ equal to the measured compressive strength at 28 days for each hour data set (3:50am, 6:00 and 7:45am). If $\mathbf{f_{cm}}$ is taken as 4,000 psi (minimum specified strength) the percent difference increased drastically since the equation will converge to 4,000 psi but the real 28 day compressive strength was higher, in this case approximately 6,000 psi. This presents a challenge for modeling a bridge prior to placement, since the in place strength is not known. Figure 30 shows the measured compressive strength values of the field samples and the Eurocode 2 approximation with $\mathbf{f_{cm}}$ equal to 4,000 psi. The Eurocode 2 equation proved inaccurate if the specified $\mathbf{f_{cm}}$ was used. On the other hand, if $\mathbf{f_{cm}}$ is taken as 5,000 or 6,000 psi the approximations showed to be better. Figure 31 shows the improved estimations compared to the measured values. Therefore, the $\mathbf{f_{cm}}$ value to be used is an important determinant on the estimated compressive strength behavior if the Eurocode 2 equation is going to be used as a prediction of mechanical property development over time.

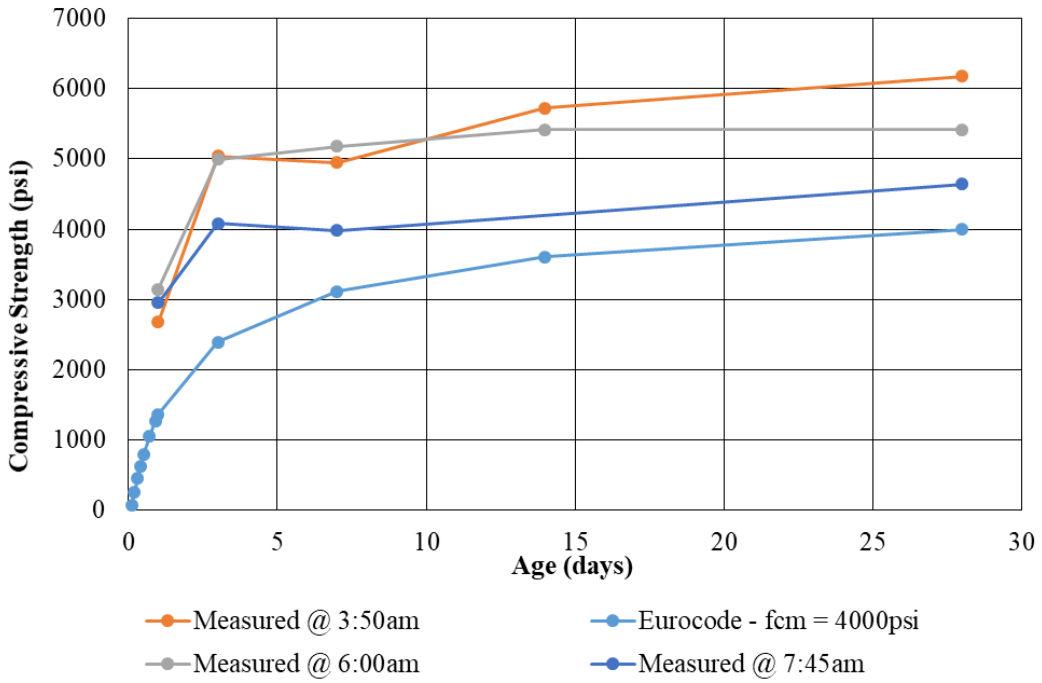

Figure 33. Measured compressive strength values of the field samples and the Eurocode approximation with $\mathbf{f_{cm}}$ equal to 4,000 psi.

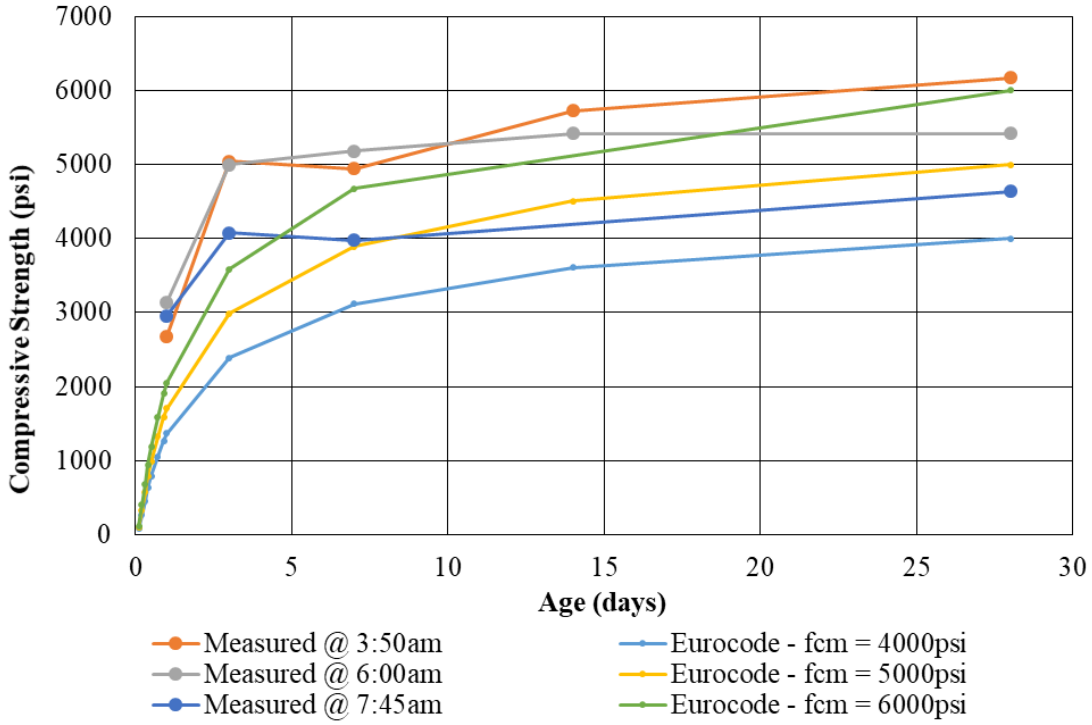

Figure 34. Compressive strength results comparison between measured values and Eurocode 2 approximations using $\mathbf{f_{cm}}$ = 4000 psi, 5000 psi and 6000 psi.

However, for the MOE results, using an $\mathbf{f_{cm}}$ equal to 4,000 psi provided an accurate estimate of the MOE development over time. Figure 32 illustrates the comparison between field samples and the Eurocode 2 approximation using $\mathbf{f_{cm}}$ equal to 4,000 psi. The final value at 28 days was higher than measured, but at early ages the behavior could be considered representative of the measured data. Figure 33 shows how the MOE is overestimated if $\mathbf{f_{cm}}$ is taken as 5,000 or 6,000 psi. No split tensile strength testing was performed for the bridge 030428 samples due to the limited number of specimens.

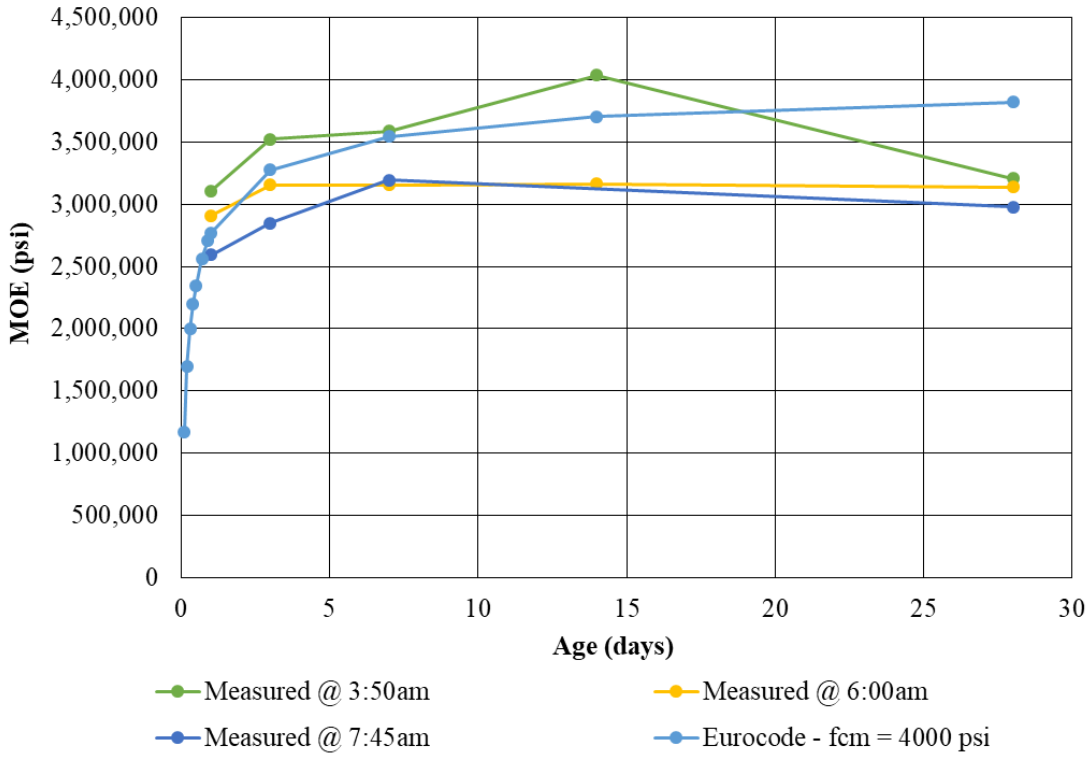

Figure 35. Elastic modulus results comparison between measured values and Eurocode 2 approximations using $\mathbf{f_{cm}}$ = 4,000 psi.

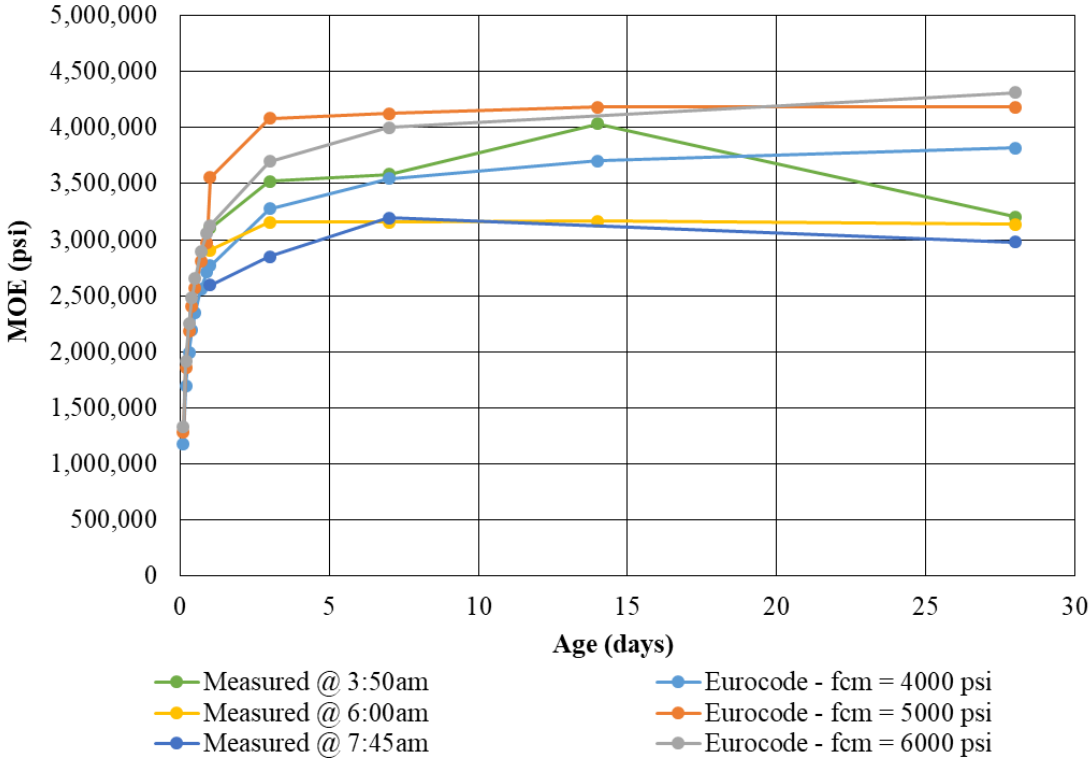

Figure 36. Elastic modulus results comparison between measured values and Eurocode approximations using $\mathbf{f_{cm}}$ = 4000, 5000 and 6000 psi.

5.1.2.2 Internal Temperature measurements of Bridge 030428

After 25 days of constant monitoring, the VWSG sensor cables were cut and the DAQ removed from the bridge due to the contractor's concern about pouring the parapet wall. The temperature data helped to determine at what time approximately the concrete reached final set and how the heat of hydration developed inside the concrete. Temperature versus time were graphed for all the sensors to see when the fresh concrete reached each sensor and when the peak hydration temperature was reached. Values before fresh concrete was placed on a specific sensor were averaged and subtracted from subsequent measurements to zero the strains. Sensors started recording 1 hour prior to the arrival of the first concrete truck. Therefore, whenever the concrete reached a sensor, a clear jump in temperature of approximately 10°C could be seen in the sensor

readings. Figure 34 shows an example of concrete reaching sensor 1, 16, 21 and 32 and the peak heat of hydration. The total temperature data for the previously mentioned sensors are shown in figure 35. Set retarding admixtures were added to the mixtures in varying quantities to ensure that the entire bridge deck reached final set at approximately the same time. As the peak temperatures indicate in figure 34, the retarder successfully delayed concrete setting along the bridge deck so that the heat development and setting behavior was the same throughout the continuous pour. The peak heat of hydration was approximately 14 hours after the initial concrete arrived on site. All 25-days recorded temperatures are graphed in figures 36 and 37 for sensors 1, 5, 12 and 16 (bent 1) and sensors 18, 21, 28 and 31 (bent 2). It should be mentioned that some sensors recorded very high temperatures for a single reading after day 3 (see figure 35). These are erroneous readings which are not uncommon for these VWSGs but are also not representative of the actual temperature. It is unknown why sensors recorded these peak values for temperature as well for strains. Geokon staff suggested it was a malfunction of the DAQ boxes which at that time could have been physically moved or hit by on site workers or equipment. However, all the recorded sensors showed approximately the same behavior in terms of the heat of hydration and peak temperature regardless of the location in the bridge (and thus what time the concrete initially reached the sensor). Concrete temperature differentials while the deck cooled down ranged from 17℃ to 20℃. In the following days the concrete deck experienced an internal temperature change of 10℃-12℃.

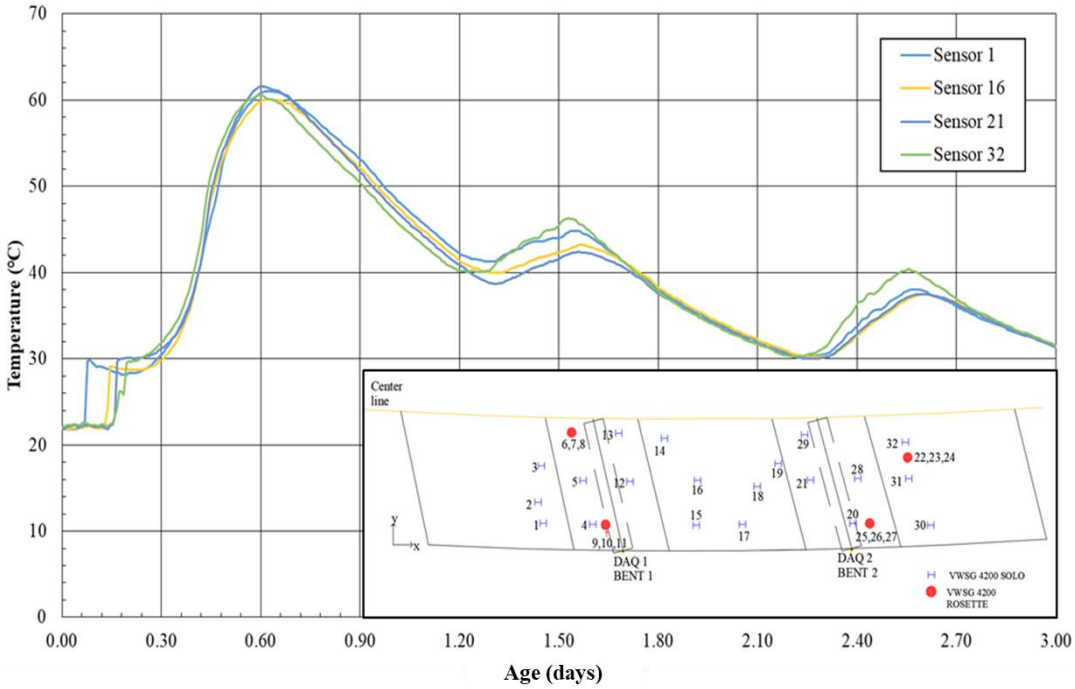

Figure 37. Temperature data for sensors 1, 16, 21 and 32 during the first 24 hours after casting.

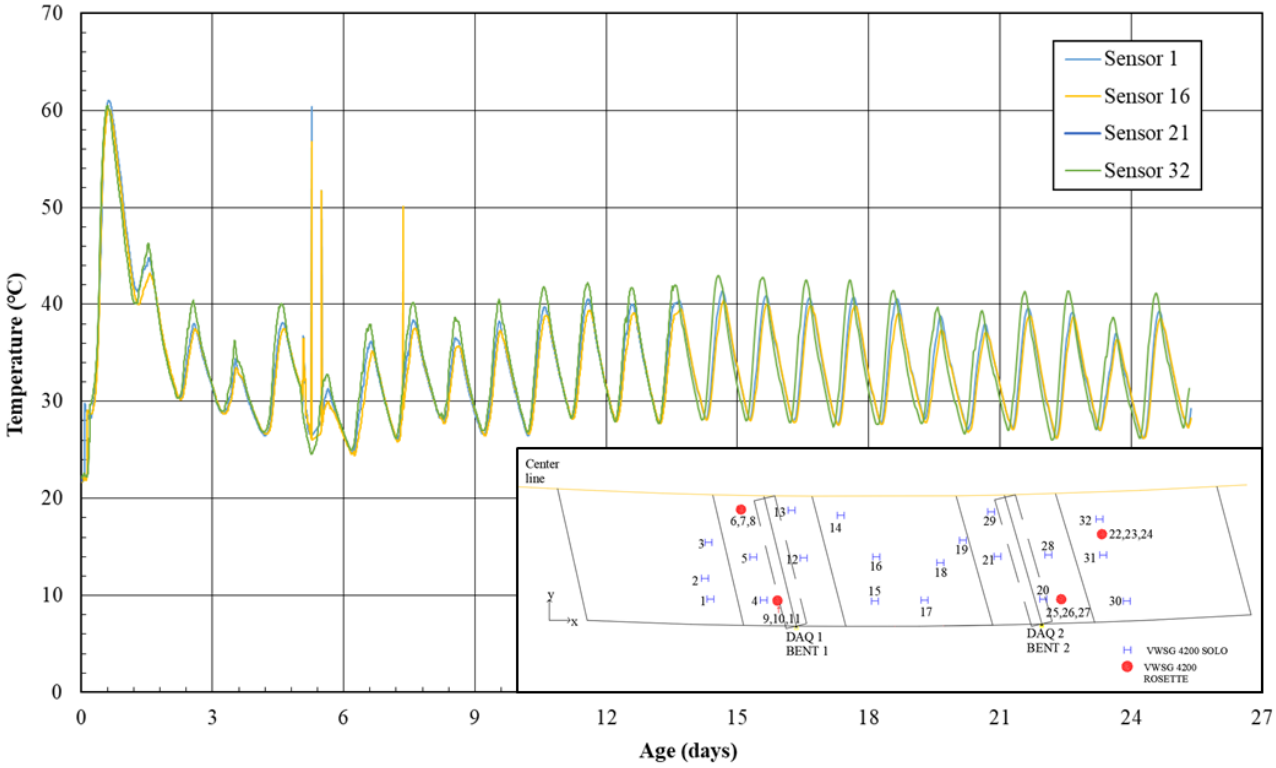

Figure 38. Total temperature data for sensors 1, 16, 21 and 32.

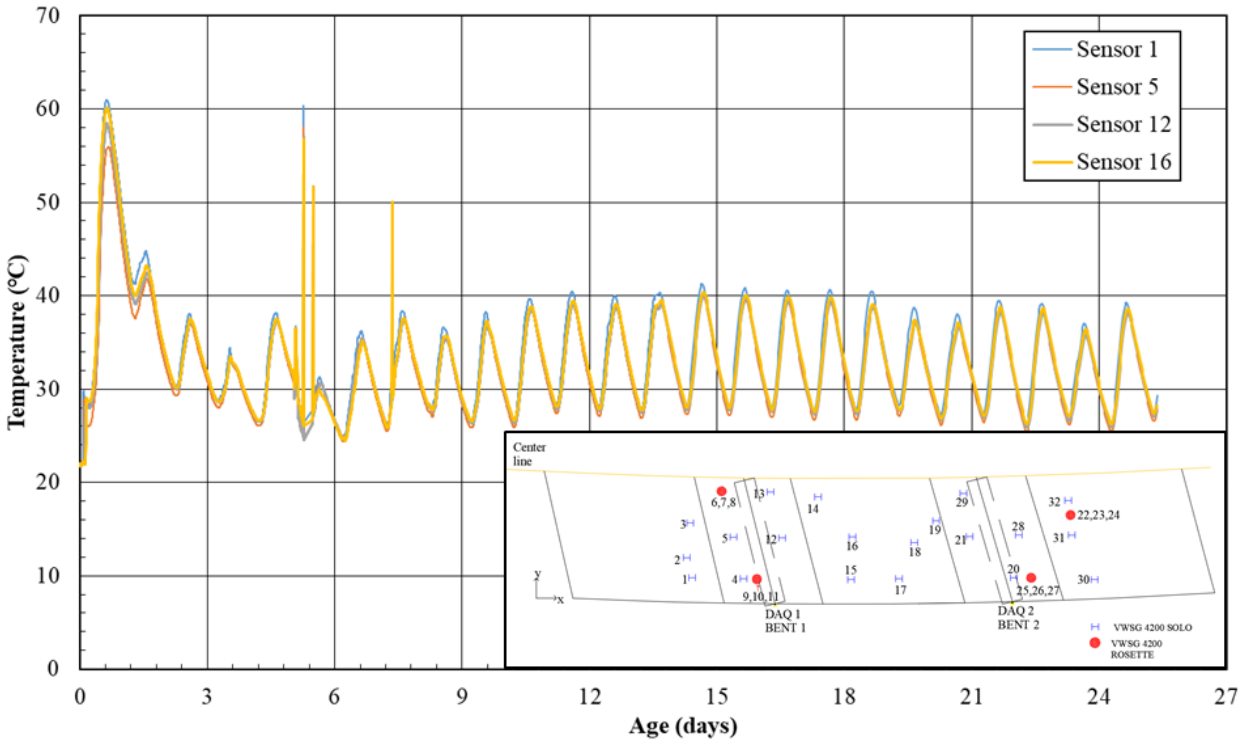

Figure 39. Total 25-day temperature data for sensors 1, 5, 12 and 16 (bent 1).

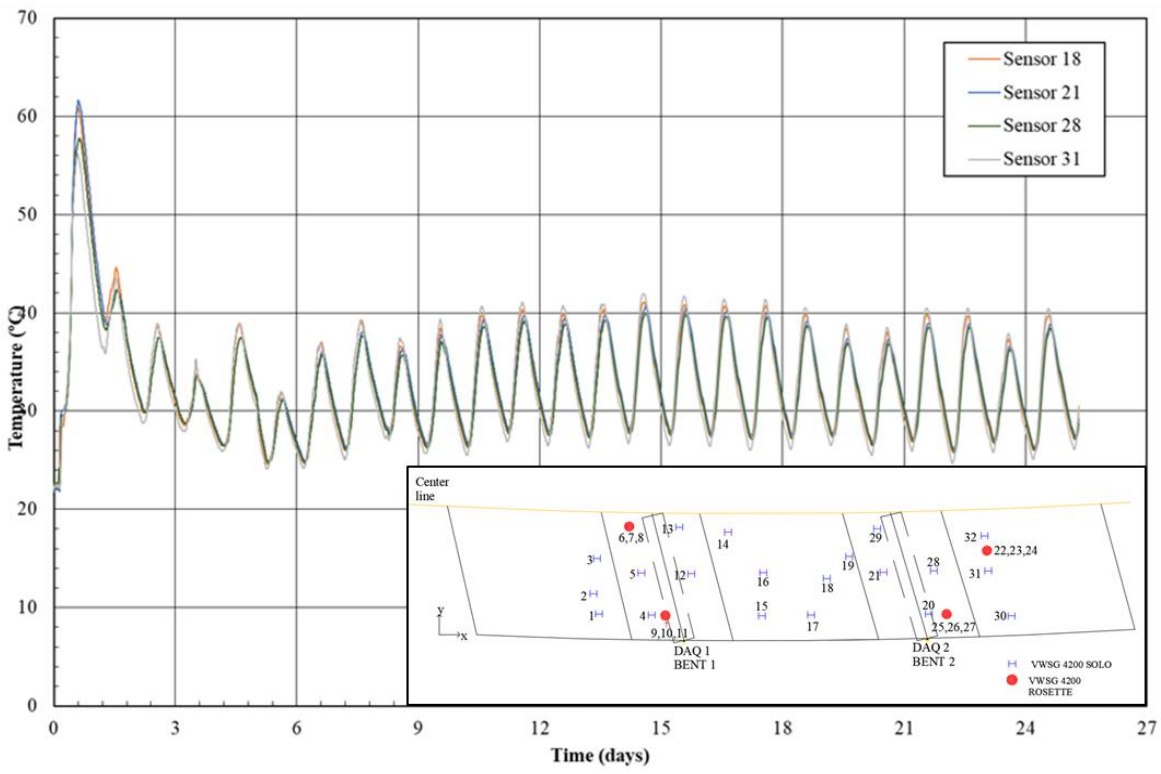

Figure 40. Total 25-day temperature history for sensors 18, 21, 28 and 31 (bent 2).

5.1.2.3 Strain Measurements of Bridge 030428

The concrete initially behaves as a liquid or plastic material until it reaches initial set, then mechanical properties start changing as and mechanical strength is gained. This phenomenon can be called viscoelastic behavior. The challenge behind this effect is to estimate and approximate the mechanical properties of the material at initial stages. In this study, there was an interest in relating measured strains to the stresses in the concrete. Additionally, the variation in material properties in the first day is important in modeling early age cracking in bridge decks. Usually, concrete has an approximate tensile strength capacity of 10% of its compressive strength capacity. This means, at early age, it has an even lower tensile strength. Therefore, if during the construction process principal stresses developed in the concrete deck surpass its early age tensile strength, cracks will form before opening to traffic. The goal of the rest of this thesis was to calculate the principal tensile stresses at specified locations and compare it to the stresses estimated by the results of a finite element model being worked by another graduate student. In the following graphs, a negative value of strain or stress indicates compression, while a positive value indicates tension.

The concrete deck was poured from bent 1 to bent 2 and from the edge towards the centerline direction. Therefore, the team installed the sensors accordingly to the pour direction. As mentioned in the previous section, the temperature rise was an indication that the concrete reached each particular VWSG. Therefore, each sensor has a different time of initial or zero strain and different sets of data points for temperature and strain. Also, the VWSGs used in this project have a particularity of recording outlier data whenever the concrete is still in the liquid state. The initial data (after casting) was therefore processed prior to analysis to remove

inaccurate spikes in strain and to zero the sensors. Time zero is when the sensors were turned on (approximately 1 hour previous to the concrete pour).

The sensors' locations (see figure 38) were established to encompass regions prone to cracking from the bridge surveys earlier in this thesis. Expectations were to see the higher tensile stresses near piers where the largest negative moments can be expected. The analysis also focused on the bridge mid-span region through the bridge length to compare with the negative moment regions. Fewer sensors were used near the abutments since stresses were expected to be low there. Curved bridges tend to have a different stress-strain distribution than straight bridges. Analyzing bent 1 first (see figure 38), strains results from sensors 3, 5, 12 and 16 at 1 day old are shown in figure 39 (negative for compression; positive for tension). Peaks occurred at different times and the highest tensile strain recorded was by sensor 16 with 178 με 6 hours after the concrete was placed. Figure 40 illustrates the strain behavior of these sensors in the first 7 days. For the following results sections, negative values represent compression stresses and positive values, tension stresses in the concrete.

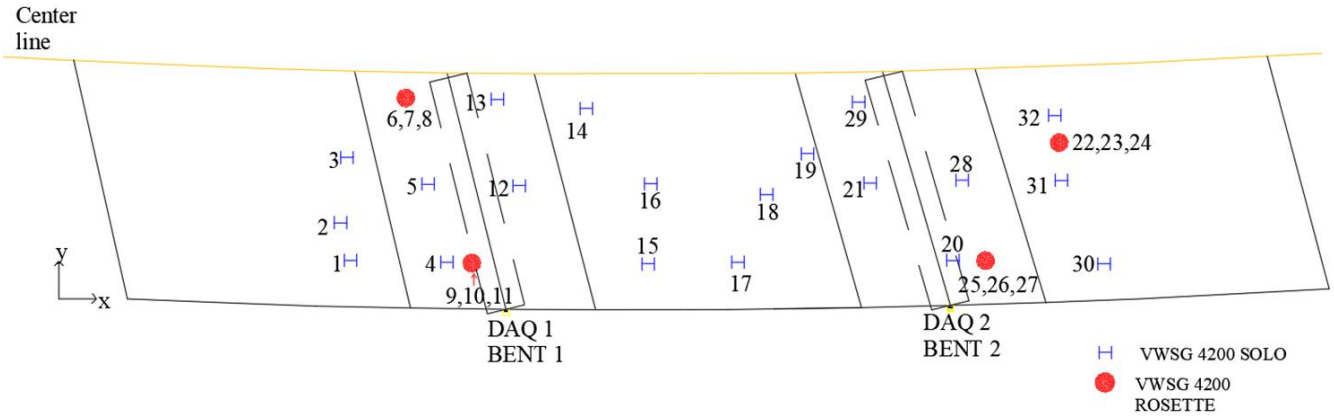

Figure 41. Bridge sensors locations configuration.

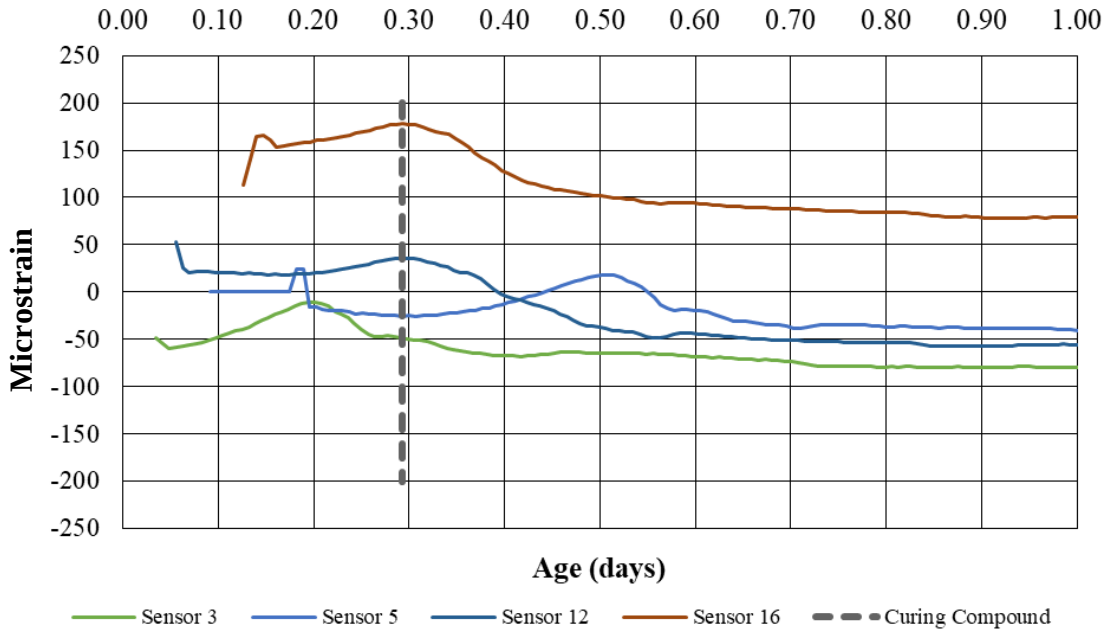

Figure 42. Recorded strains from sensors 3, 5, 12 and 16 in the first 24 hours after casting.

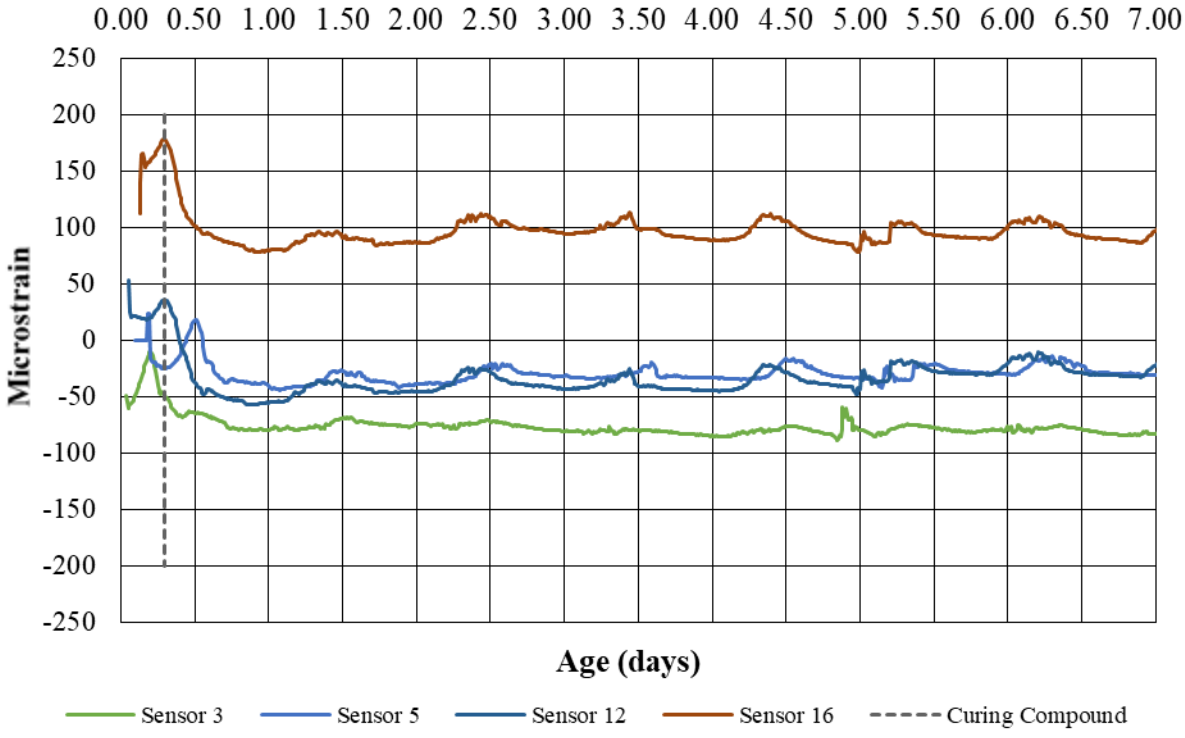

Figure 43. Recorded strains from sensors 3, 5, 12 and 16 in the first 7 days after casting.

Sensors 18, 21, 28 and 31 were selected for bent 2 analysis. Figure 41 shows the strains measured at these locations. Sensor 21 recorded the highest tensile strain (81 microstrain) after approximately 6.5 hours of curing. Peaks strains occurred at different times. However, sensors 18, 21, and 31 reached their maxima fairly close in time. Now combining all these strain measurements between bent 1 and 2 (see figure 44), it can be seen which strains took place through the bridge length as a function of time. Peak tensile strains occurred between the first 3.5-12 hours after casting.

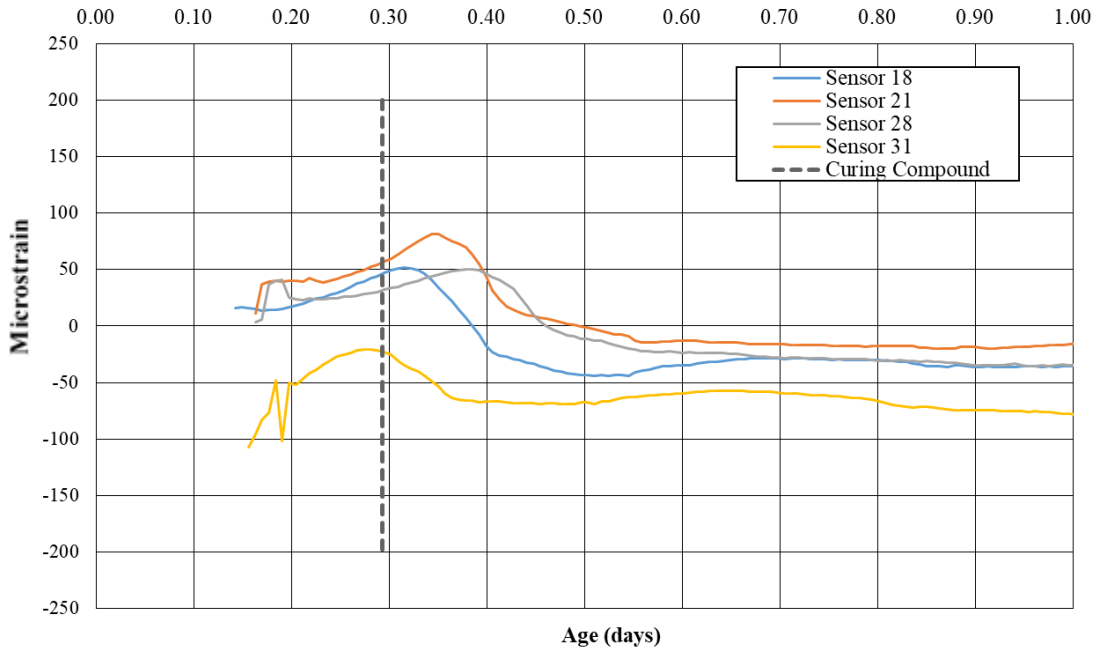

Figure 44. Recorded strains from sensors 18, 21, 28 and 31 in the first 24 hours after casting.

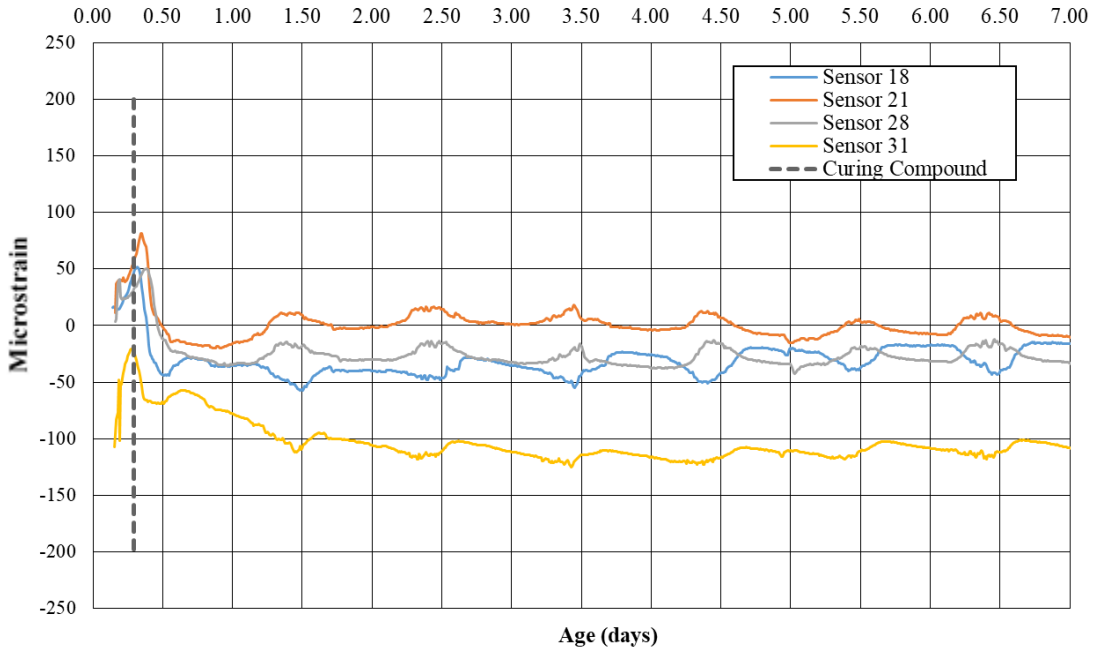

Figure 45. Recorded strains from sensors 18, 21, 28 and 31 in the first 7 days after cast.

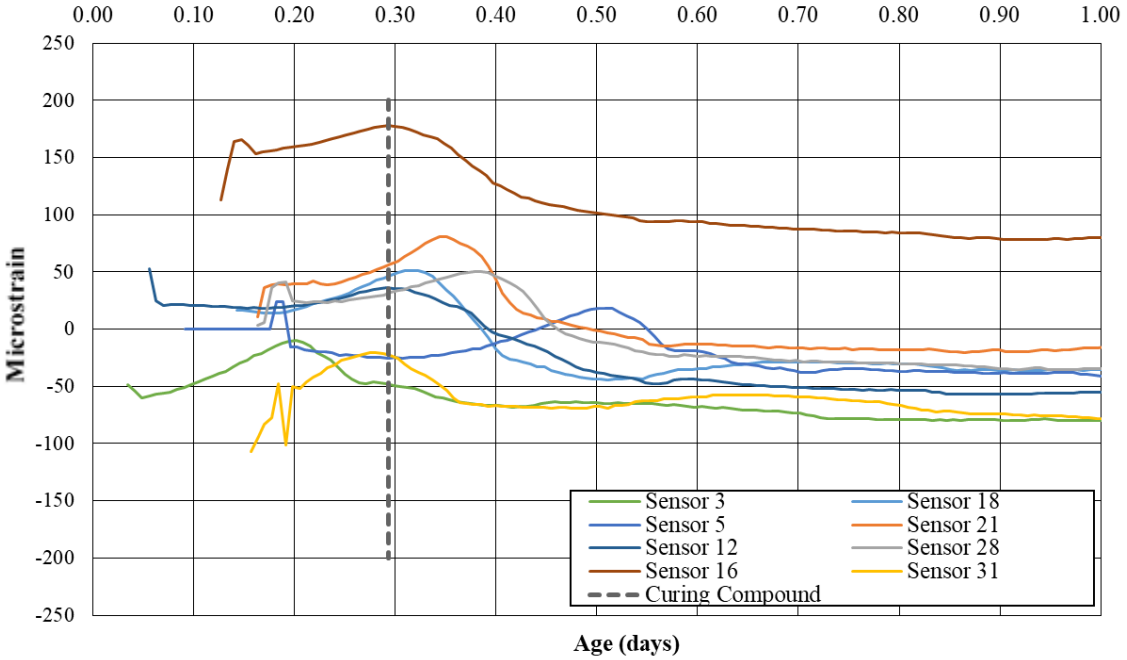

Figure 46. Recorded strains from sensors at bent 1 and 2 in the first 24 hours after cast.

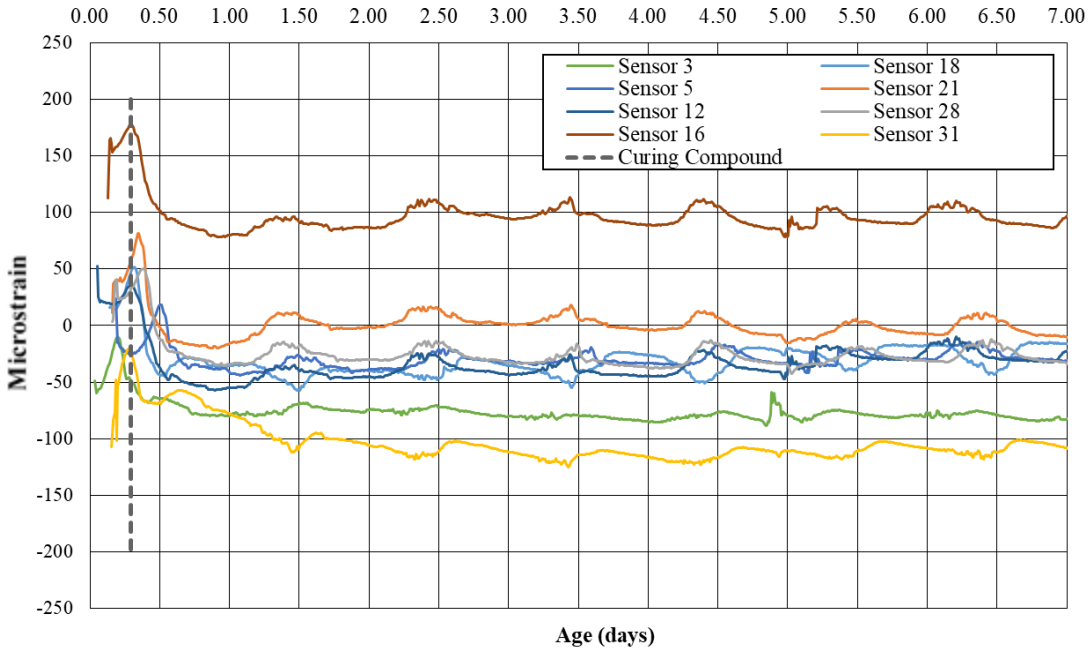

Figure 47. Recorded strains from sensors at bent 1 and 2 in the first 7 hours after cast.

5.1.2.4 Bridge 030428 stress analysis

The main interests of these strain recordings were to see the magnitude of the peak strains and when these occurred. This would help improve the understanding of where in the bridge deck concrete is under tension or compression at the top surface. As seen in section 5.1.2.3, the highest tensile strains recorded by the sensors occurred within the first 12 hours after concrete was cast. Time zero was the time when sensors started to record, which was approximately 1-1.5 hours before concrete reached the first sensor. It has to be noted that sensor data were filtered because whenever the concrete was plastic and transitioning to solid, sensors gave an error or inaccurate recording. Random peaks were seen in the initial data set, these were filtered and taken out for the final results. Therefore, each sensor had a different amount of time and strain data, even though they were started and stopped at the same time. DAQ boxes were started relatively at the same time. At bent 1 and bent 2, peak tensile strains occurred approximately

between 0.2-0.4 days (4.8-9.6 hours) and 0.25-0.50 days (6-12 hours). The time when different locations in the deck developed the highest strains varied through the span length. The addition of retardant agents to the mixture reduced the setting time difference, which was convenient and helped the material harden relatively at the same time.

The principal stresses were calculated only for the locations with strain rosettes for bridge 030428. The measured strains were transformed to principal strains, and then principal stresses were calculated by multiplying the principal strains by the Eurocode behavior approximation for MOE (see section 4.2). For the unidirectional sensors, strains were calculated [38] and converted to stresses multiplying by the approximated MOE value at a specific time using the Eurocode equations. Figure 45 shows the approximated calculated stresses developed in the concrete at bent 1 in the first 36 hours. VWSG parallel to girders orientation are demonstrated in the layout map (see figure 38 for clear view) as an "I" symbol rotated 90 degrees. Figure 46 shows the total stress behavior recorded at bent 1 by sensors 3, 5, 12 and 16. Sensors 3, 5 and 12 were initially experiencing tensile stresses but then as concrete started hardening compressive stresses took place at those locations. On the other hand, sensor 16 recorded stresses tensile stresses at the beginning of the recorded strain history and remained like that until reducing in magnitude at 9 days. Figures 47 and 48 show the stresses recorded at bent 2 with sensors 18, 21, 28 and 31 within the first 36 hours and the total stress behavior at these locations, respectively. Also, the day-night temperature cycle can be clearly seen in both bents.

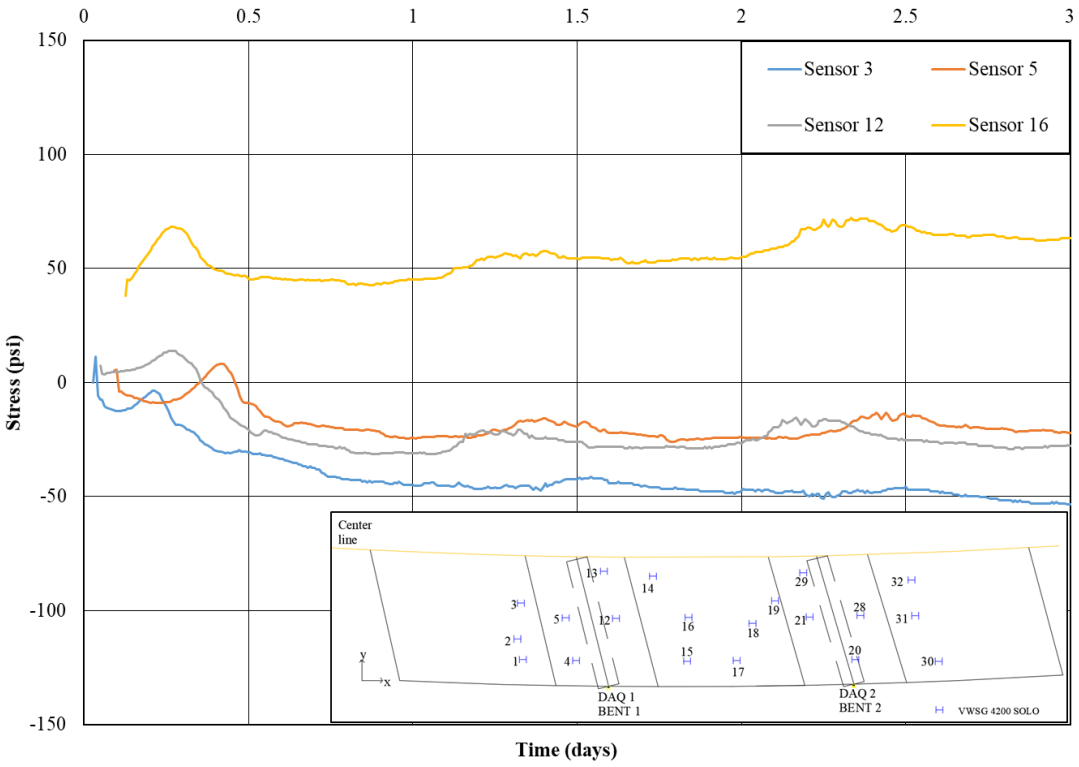

Figure 48. Stresses developed in concrete deck at bent 1 the first 36 hours.

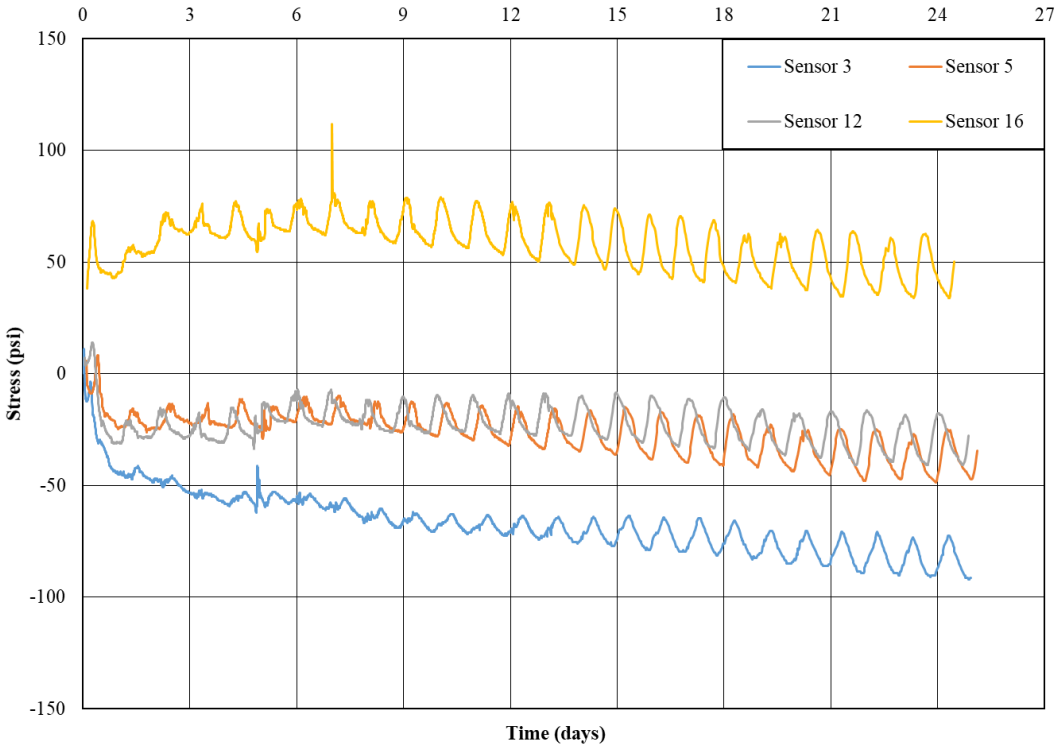

Figure 49. Total stresses behavior developed in concrete deck at bent 1.

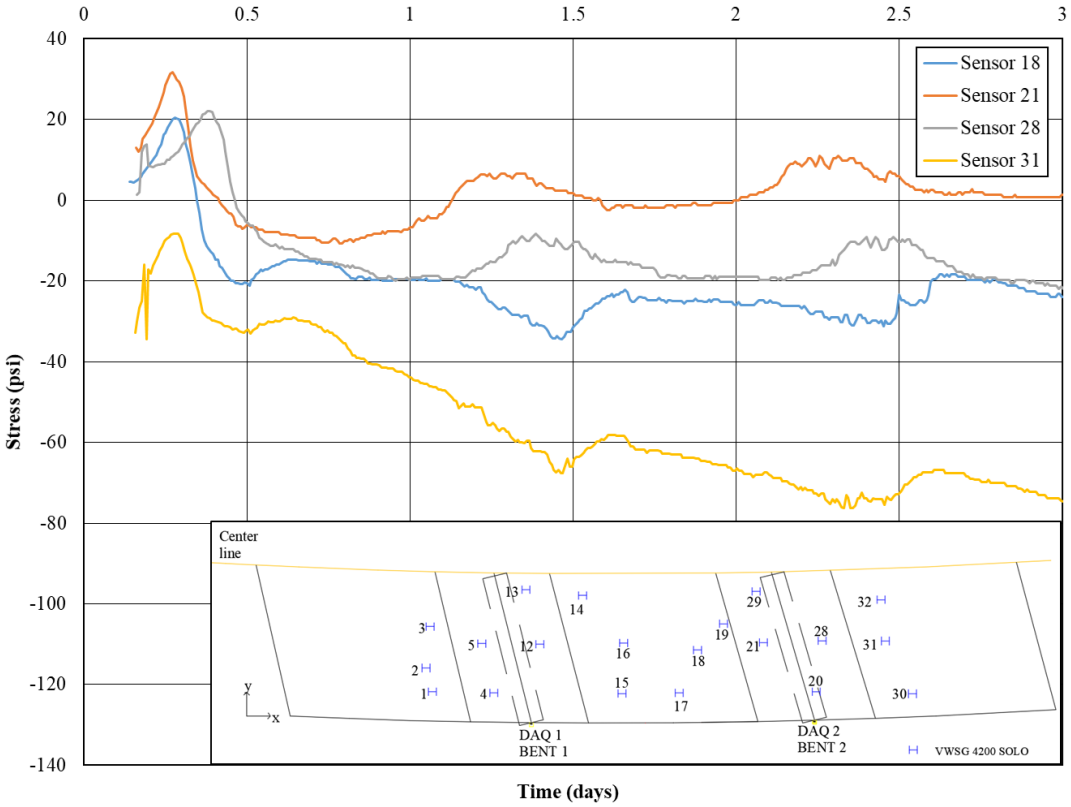

Figure 50. Stresses developed in concrete deck at bent 2.

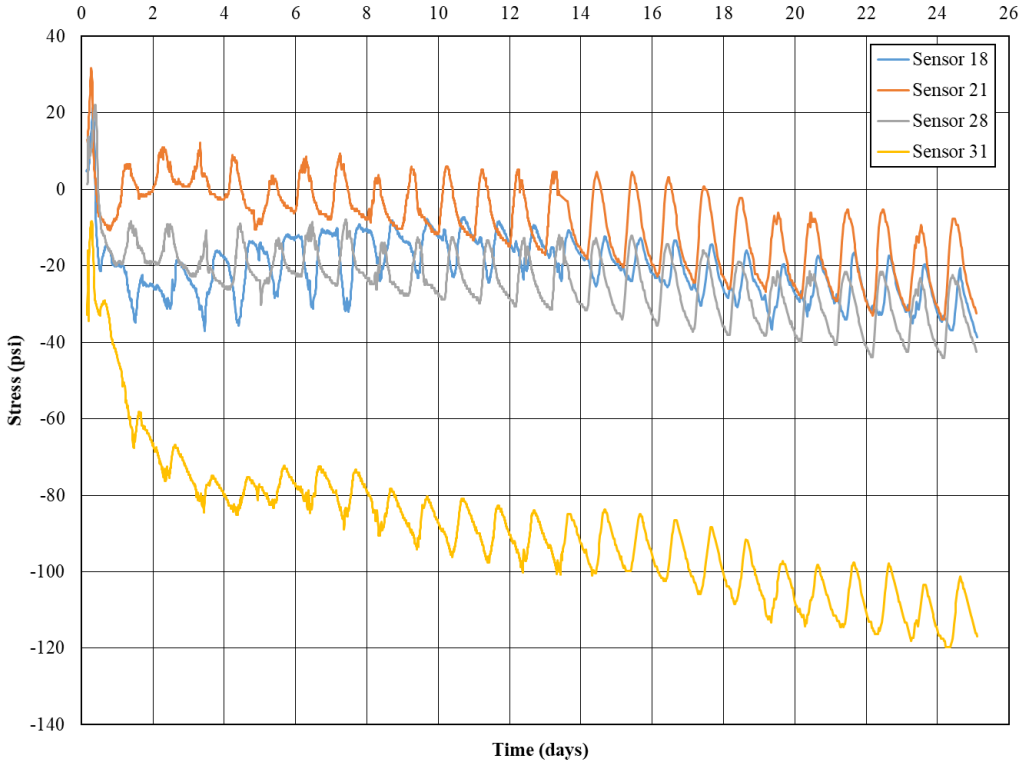

Figure 51. Total stresses behavior developed in concrete deck at bent 2.

After analyzing the uni-directional stresses, the principal stresses for the strain rosette data were calculated following the same procedure previously described using Eurocode approximations and field data. Since strains at 0°, 45° and 90° are known, these were transformed [38], and multiplied by the varying MOE to obtain approximate principal stresses. Figures 50-53 show the different stress behaviors at 0° (parallel to the girders), 45° (diagonal to the girders) and 90° (transverse to the girders) directions in the respective rosette locations (see figure 49). Figures 54-57 show the calculated principal stresses for the four rosettes at the respective locations. Also, these were compared to the Eurocode's approach for tensile strength gain of concrete and ACI's split tensile strength at the maximum recorded stress on each rosette location.

The 3 of the 4 strain rosettes recorded the highest tensile stresses in the sensor at a 45° angle. Rosette 6, 7, 8 recorded the highest tensile stress values in the longitudinal direction of the bridge deck. Also, it would be expected to see higher stresses at the edges of the bridge but rosette 22, 23, 24 recorded the lowest between the four rosettes.

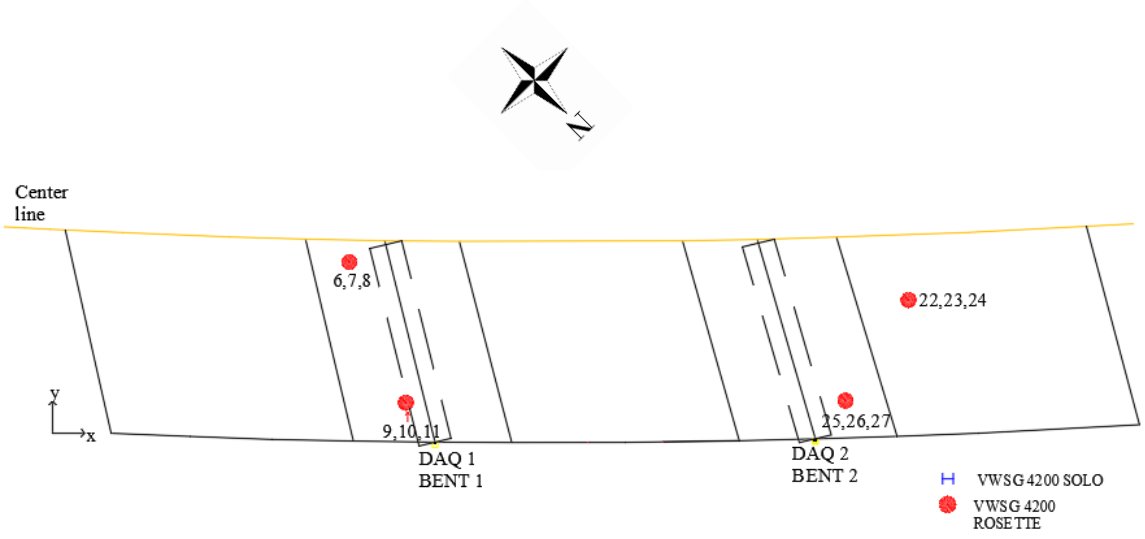

Figure 52. Strain rosettes layout.

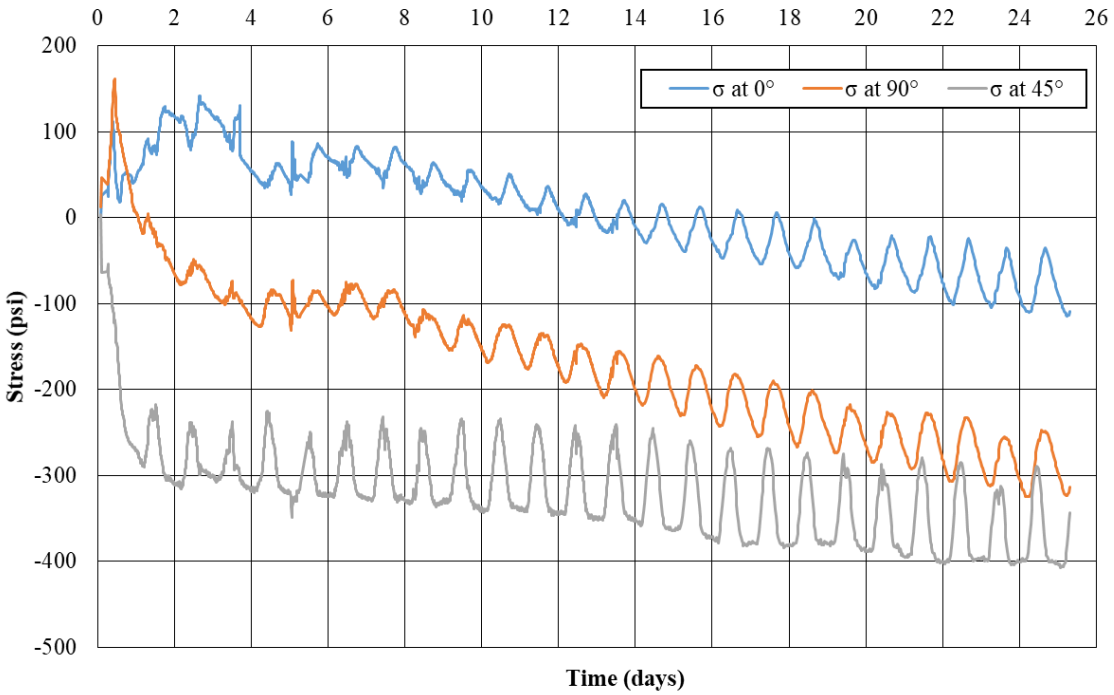

Figure 53. Stresses in rosette sensors 6, 7 and 8.

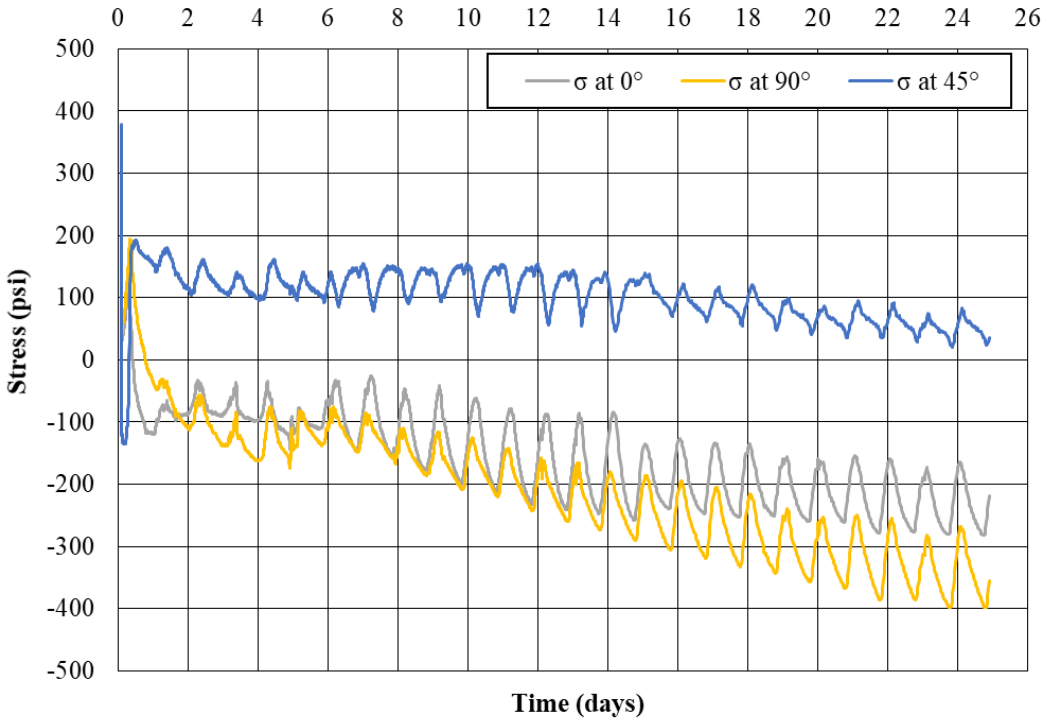

Figure 54. Stresses in rosette sensors 9, 10 and 11.

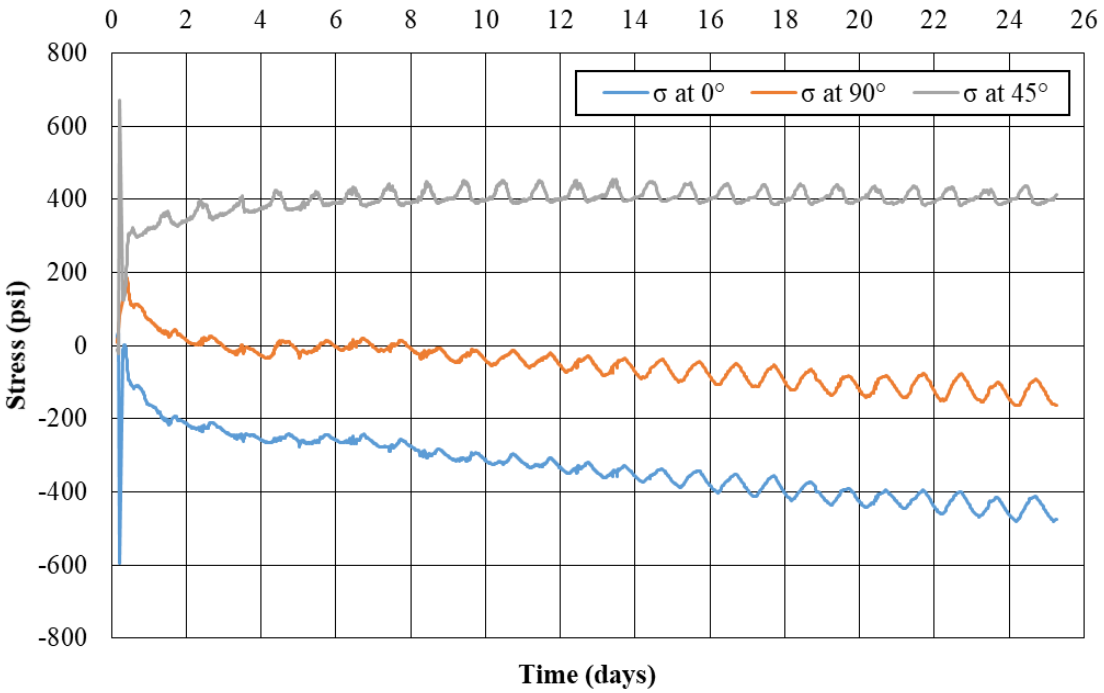

Figure 55. Stresses in rosette sensors 22, 23 and 24.

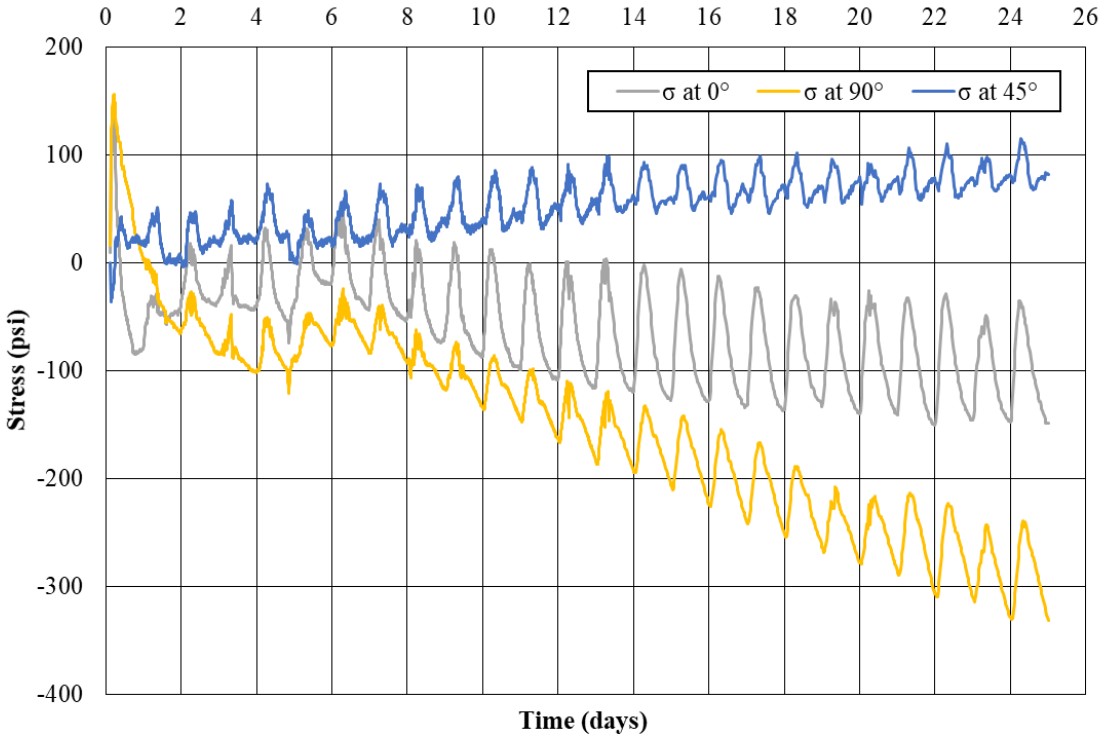

Figure 56. Stresses in rosette sensors 25, 26 and 27.

The major concern about this stress analysis was determining if the concrete tensile strength was sufficiently developed at the time where maximum stresses took place internally in the concrete deck. From these previous principal strains presented, all rosettes recorded higher tensile stresses than the tensile strength of concrete at a specific time according to Eurocode tensile strength approximations. For the ACI equation Rosette 6, 7, 8 recorded a maximum positive stress of 358 psi at 1.76 days (42 hours) after cast. At this time, the Eurocode and ACI approximation estimated a tensile strength capacity of 254 psi and 369 psi, respectively. This means stresses could have surpassed the concrete strength gain at that time. The same analysis was made for the other rosettes and results are summarized in table 10. Figure 58 shows the maximum stresses recorded by sensors at mid span through the bridge length. These were not exactly aligned on a straight line and did not occur at the same time.

Table 9. Maximum tensile stresses compared with approximate concrete tensile strength at the time when the maximum stress took place in concrete.

Rosette	σ_1 Max (psi)	Eurocode (psi)	ACI (psi)	Time (days)
6, 7, 8	358	254	369	1.76
9, 10, 11	413	44	153	0.23
22, 23, 24	494	44	153	0.23
25, 26, 27	168	72	188	0.37

As previously mentioned, principal tensile stresses were higher at early ages after the concrete was poured for all rosettes. The day-night temperature change cycle also caused stress changes over time. These changes caused expansion and contraction of the slab. If a straight line was drawn from day 2 through day 25 connecting the first and last point, it could observed that the slope of the stress data varies among the rosettes. This slope could represent the rate of increase of the daily average stress for compression or tension. For example, tensile stresses recorded at 3 of the 4 rosettes seemed to stabilize after 14 days, meaning the slope was low (see

figures 54, 56 and 57). Tensile stresses at rosette 9, 10, 11 kept decreasing after 14 days until the location was in compression. All four rosettes showed a change in compressive stress as well after 14 days. Section 5.1.2.3 showed how strains behaved through time. After 1 day, the strains fluctuated but did not increase with time (no slope). The increment we see in these stress graphs could be influenced by the changing modulus of elasticity of the concrete. A steady value of strain coupled with a changing modulus results in a changing stress.

Stress recordings in the longitudinal direction were taken from the nearest VWSG sensors to the bridge centerline. These were sensors 3, 5, 12, 16, 18, 21, 28 and 31. Figure 58 demonstrates the maximum and minimum values recorded and shows that these stresses tended to be low in the longitudinal direction. Even though these occurred at different times, this graph gives an indication of the maximum and minimum strains recorded along the length of the bridge. Table 11 shows the sensor and the respective compression and tension values as well as when they occurred.

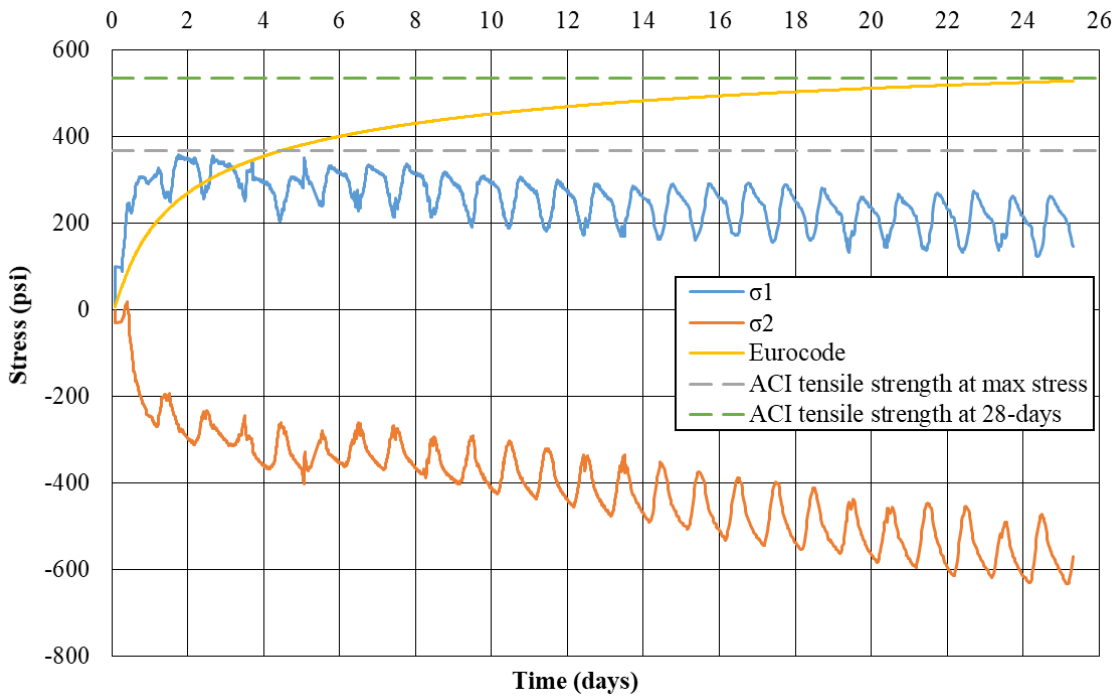

Figure 57. Principal stresses recorded in rosette 6, 7, 8 at bent 1.

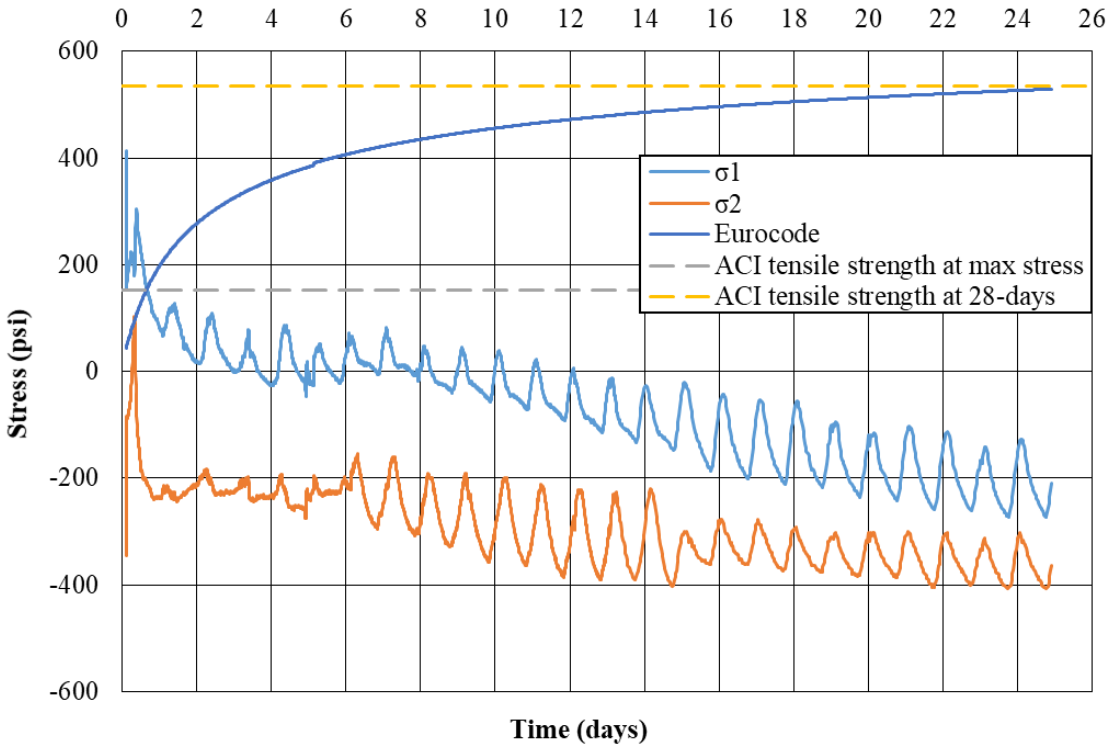

Figure 58. Principal stresses recorded in rosette 9, 10, 11 at bent 1.

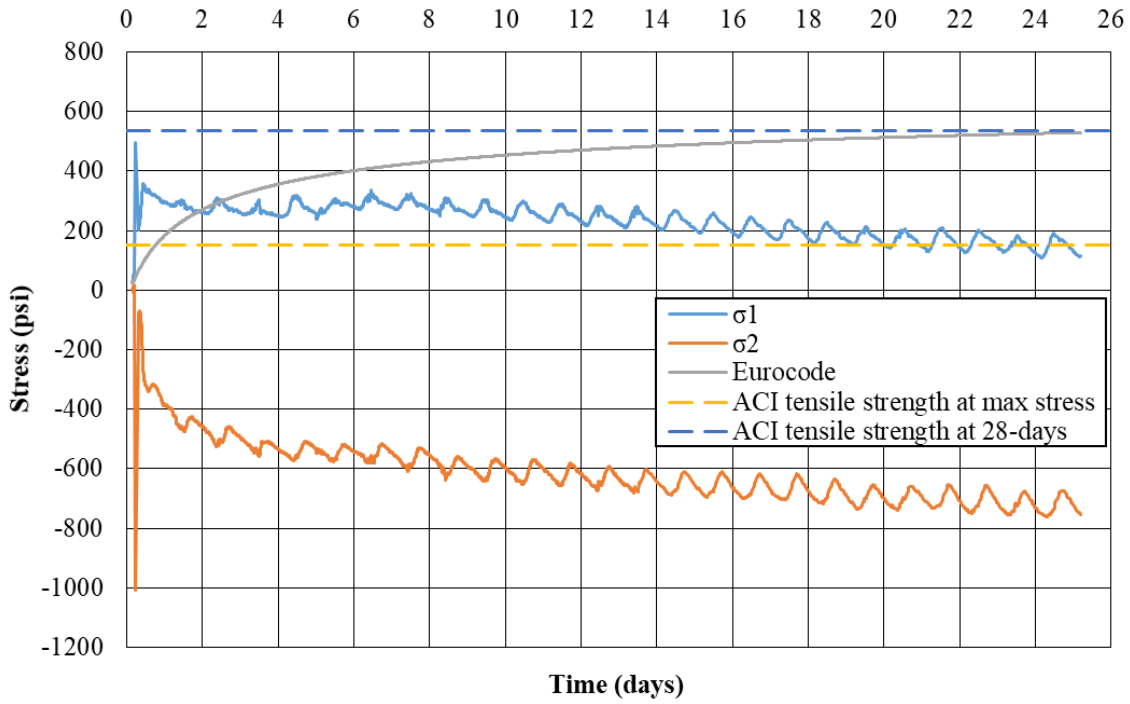

Figure 59. Principal stresses recorded in rosette 22, 23, 24 at bent 2.

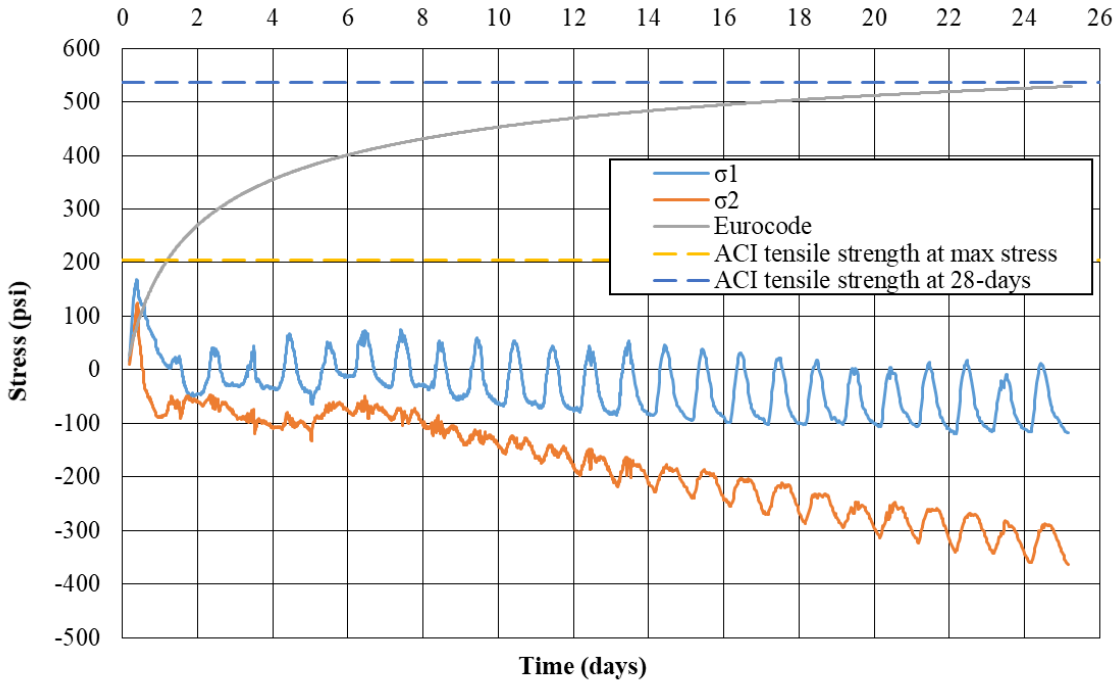

Figure 60. Principal stresses recorded in rosette 25, 26, 27 at bent 2.

CHAPTER VI

CONCLUSIONS AND RECOMMENDATIONS

6.1 Conclusions and recommendations

The laboratory and field results confirm that concrete mechanical properties vary greatly at early ages. Due to this variation, concrete strength capacity varies and stresses developed at a given time could compromise the concrete. Many engineers consider bridge deck cracking to be construction process related (improper construction practices and curing methods) and not design driven but and the end of the day, both will contribute to concrete cracking.

The Eurocode equations for concrete mechanical property development over time could be used to improve the finite element modeling for bridges and give more accurate values for the stress analysis. Mechanical property approximations derived this way will depend on the 28-day compressive strength. Laboratory test results showed a compressive strength that ranged from approximately 4,500 psi – 6, 000 psi for samples taken from different trucks. ARDOT's sampling resulted in an average of 6,400 psi for compressive strength at 28-days. Laboratory results might have been affected by storing conditions on site. Inconsistency in compressive strength at later ages compared to the specified strength can be a concern at the time of modeling when choosing an appropriate and representative value for $\mathbf{f'_c}$. Results from the laboratory testing reported in this document will help in the calibration of the finite element model to be performed in ABAQUS. The Eurocode equations would be recommended to use for the MOE and compressive strength development for bridge 030428 modeling. As for the tensile strength, ACI values showed to be a better representation of the tensile strengths behavior.

Field results confirmed that the highest strains usually occurred in the first 24 hours after casting the concrete. However, peak compressive stresses were seen at the end of the 25 day

monitoring period mostly. From the rosette results, stresses varied upon location and direction (0°, 45° and 90°). The tensile stresses developed in the concrete deck did surpass the concrete tensile strength according to the Eurocode and ACI approximate tensile strengths. These locations could be prone to experience some level of cracking. It is likely that many bridges cast around the state experience stresses at early ages that exceed the tension strength of the concrete. The compressive stresses kept increasing after 14 days meaning modulus of elasticity is still being changing at that time.

One month after the bridge deck was constructed no cracking has been observed in the surface by ARDOT personnel. The bridge deck inspection will continue indefinitely. Placing wet burlap after casting; reducing the cementitious content; improving early-age and long-term curing methods; reducing maximum compressive strength limits; limiting the maximum slump; controlling the concrete's temperature; and minimizing finishing operations are strongly recommended remedies to perform for reducing early age cracking [30].

Geokon 4200L VWSGs are recommended for monitoring of early age strains especially in plastic concrete. The 4200 VWSG sensors used in this project gave occasionally erroneous values when the concrete had a low modulus (semi-liquid state). Also, the sensor configuration could be improved for future bridge instrumentation depending on the purpose of the monitoring. A 3-dimensional tri-axial configuration could be useful to study how much concrete expanded and contracted vertically. Strain rosettes were useful to know principal longitudinal and transverse stresses developed in the concrete deck.

CHAPTER VII

REFERENCES

7.1 References

[1] F. Gara, G. Leoni and L. Dezi, "Slab Cracking Control in Contiuous Steel-Concrete Bridge Decks," *Journal of Bridge Engineering* , vol. 18, no. 12, pp. 1319-1327, 2013.

[2] M. Issa, "Investigation of Cracking in Concrete Bridge Decks at Early Ages," *Journal of Bridge Engineering,* vol. 4, no. 2, pp. 116-124, 1999.

[3] Minnesota Department of Transportation, "Transportation Research Synthesis - Bridge Deck Cracking," Minnesota Department of Transportation, St. Paul, MN, 2011.

[4] T. Hopper, A. Manafpour, A. Radlińska, G. Warn, F. Rajabipour, D. Morian and S. Jahangirnejad, "Bridge Deck Cracking: Effects on In-Service Performance, Prevention, and Remediation," The Pennsylvania Department of Transportation Bureau of Planning and Research, Harrisburg, 2015.

[5] C. L. Freyermuth, P. Klieger, D. C. Stark and H. N. Wenke, "Durability of concrete bridge decks - A cooperative study," Transportation Research Board, 1970.

[6] P. D. Cady, R. E. Carrier, T. Bkar and J. C. Theisen, "Final report on durability of bridge deck concrete: Part 3: Condition of 249 four yearl old bridge decks," University Park, PA, 1971.

[7] W. McKeel, "Evaluation of deck durability on continuous beam highway bridges," Charlottesville, VA, 1985.

[8] G. E. Ramey, A. R. Wolff and R. L. Wright, "Structural Design Actions to Mitigate Bridge Deck Cracking," American Society of Civil Engineers (ASCE), 1997.

[9] G. E. Ramey and R. and Wright, "Assessing and enhancing the durability/longevity performances of highway bridges," Auburn, Alabama, 1994.

[10] G. E. Ramey, R. Wright and A. Wolff, "Structural Design Actions to Mitigate Bridge Deck Cracking," *Practice Periodical On Structural Design and Construction,* vol. 2, no. 3, pp. 118-124, 1997.

[11] R. Hadidi and M. A. Saadeghvaziri, "Tranverse Cracking of Concrete Bridge Decks: State-of-the-Art," *Journal of Bridge Engineering,* vol. 10, no. 5, pp. 503-510, 2005.

[12] A. Manafpour, T. Hopper, F. Rajabipour, A. Radliska, G. P. Warn, P. Shokouhi, D. Morian and S. Jahangirnejad, "Field Investigation of In-Service Perfomance of Concrete

Bridge Decks in Pennsylvania," *Journal of the Transportation Research Board,* pp. 1-7, 2016.

[13] W. M. Hale, S. W. Peyton, C. L. Sanders and E. E. John, "Bridge deck cracking: A field study on concrete placement, curing, and performance," *Construction and Building Materials,* pp. 70-76, 2012.

[14] D. Su, H. Nassif and Y. Xia, "Optimization of Deck Constructuion Staging for Multiple-Span Continuous Steel Girder Bridge," *Journal of Performance of Construction Facilities,* vol. 32, no. 1, 2018.

[15] S. Kosmatka and M. Wilson, Design and Control of Concrete Mixtures. 15th Ed., Skokie, Illinois: Portland Cement Association, 2011.

[16] M. S. DalSoglio, "Investigation of Bridge Decks," Montana Department of Transportation, Northbrook, Illinois, 2017.

[17] P. J. Monteiro and P. Metha Kumar, "Thermal Shrinkage," in *Concrete: Microstructure, Properties and Materials*, Two Penn PLaza, NY, Prentice-Hall, Inc., 1986, pp. 108-117.

[18] Z. Group, "Civil + Structural Engineer," Zweig Group, 14 February 2014. [Online]. Available: https://csengineermag.com/article/addressing-drying-shrinkage-in-concrete/. [Accessed 1 January 2019].

[19] K. Carper, "Structural failures during construction," *American Society of Civil Engineers (ASCE),* vol. 1, no. 3, pp. 132-144, 1987.

[20] Minnesota Department of Transportation, "Transportation Research Systhesis: Bridge Deck Cracking," TRS 1105, St. Paul, 2011.

[21] P. Krauss and E. Rogalla, "Transverse cracking in newly constructed bridge decks," Transportation Research Board, Washington, D.C., 1996.

[22] H. Aktan, G. Fu, W. Dekelbab and U. Attanayaka, "Investigate Causes and Develop Methods to Minimize Early-Age Deck Cracking on Michigan Bridge Deck," Michigan Department of Transportation, Detroit, Michigan, 2003.

[23] Mapchart, "Mapchart," [Online]. Available: https://mapchart.net/. [Accessed 8 12 2018].

[24] Indiana Department of Transportation, "Indiana Department of Transportation," 2018. [Online]. Available: https://www.in.gov/dot/div/contracts/standards/book/index.html. [Accessed 1 15 2019].

[25] Louisiana Department of Transportation, "Louisiana Department of Transportation," 3 12 2018. [Online]. Available:

http://wwwsp.dotd.la.gov/Inside_LaDOTD/Divisions/Engineering/Standard_Specifications/Pages/Standard%20Specifications.aspx. [Accessed 15 1 2019].

[26] Virginia Department of Transportation, "Virginia Department of Transportation," 2016. [Online]. Available: http://www.virginiadot.org/business/resources/const/VDOT_2016_RB_Specs.pdf. [Accessed 15 1 2019].

[27] ASTM International, "Standard Test Method for Length Change of Hardened Hydraulic-Cement Mortar and Concrete," ASTM, West Conshohocken, PA, 2017.

[28] ASTM International, "Standard Specification for Lightweight Aggregates for Structural Concrete," ASTM, West Conshohocken, PA, 2017.

[29] Federal Highway Administration, "U.S. Department of Transporation," 04 12 2018. [Online]. Available: https://www.fhwa.dot.gov/bridge/nbi/no10/mat16.cfm#a. [Accessed 12 18 2018].

[30] D. Darwin, R. Khajehdehi, A. Alhmood, M. Feng, J. Lafikes, Ibrahim, Eman and M. O'Reilly, "Construction of Crack-Free Brdige Decks: Final Report," Structural Engineering and Materials, Lawrence, Kansas, 2016.

[31] Ohio Department of Transportation, "Ohio Department of Transportation," [Online]. Available: http://www.dot.state.oh.us/Divisions/ConstructionMgt/OnlineDocs/Pages/2019-Online-Spec-Book.aspx. [Accessed 18 07 2019].

[32] CEN, *Eurocode 4: Design of Composite Steel and Concrete Structures- Part 1-1: General Rules and Rules of Buildings,* Brussels: European Comittee for Standarization, 2004.

[33] American Concrete Institute, "Concrete Design Properties," in *Building Code Requirements for Structural Concrete and Commentary*, Farmington Hills, MI, American Concrete Institute (ACI), 2014, pp. 315-316.

[34] ASTM International, *Standard Test Method for Compressive Strength of Cylindrical Concrete Specimens,* West Conshohocken, PA: ASTM International, 2018.

[35] ASTM International, *Standard Test Method for Splitting Tensile Strength of Cylindrical Concrete Specimens,* West Conshohocken, PA: ASTM International, 2017.

[36] ASTM International , *Standard Test Method for Static Modulus of Elasticity and Poisson's Ratio of Concrete in Compression,* West Conshohocken, PA: ASTM International , 2014.

[37] Geokon Inc., "Geokon," Geokon Inc., 2019. [Online]. Available: https://www.geokon.com/8002-16. [Accessed 25 09 2019].

[38] A. C. Ugural and S. K. Fenster, Advanced Mechanics of Materials and Applied Elasticity, New Jersey: Pearson Education, Inc. , 2012.

[39] C. French, L. Eppers, Q. Le and J. F. Hajjar, "Trasverse Cracking in Concrete Bridge Decks," *Transportation Research Record: Journal of the Transportation Research Board*, vol. 1688, no. 1, pp. 21-29, 1999.

[40] P. D. Krauss and E. A. Rogalla, "NCHRP Report 380 - Transverse Cracking in Newly Constructed Bridge Decks," Transportation Research Board, Northbrook, IL, 1996.

[41] Arkansas Department of Transportation, "ARDOT Arkansas Department of Transportation," 2014. [Online]. Available: https://www.arkansashighways.com/standard_specifications.aspx. [Accessed 30 09 2019].

CHAPTER VIII

APPENDIX

8.1 Appendices

Appendix A. Eurocode's strength and deformation characteristics for concrete

Table 3.1 Strength and deformation characteristics for concrete

Strength classes for concrete															Analytical relation / Explanation
f_{ck} (MPa)	12	16	20	25	30	35	40	45	50	55	60	70	80	90	
$f_{ck,cube}$ (MPa)	15	20	25	30	37	45	50	55	60	67	75	85	95	105	2.8
f_{cm} (MPa)	20	24	28	33	38	43	48	53	58	63	68	78	88	98	$f_{cm} = f_{ck}+8$(MPa)
f_{ctm} (MPa)	1,6	1,9	2,2	2,6	2,9	3,2	3,5	3,8	4,1	4,2	4,4	4,6	4,8	5,0	$f_{ctm}=0,30\times f_{ck}^{(2/3)} \leq$C50/60 $f_{ctm}=2,12\cdot\ln(1+(f_{cm}/10))$ > C50/60
$f_{ctk,\ 0.05}$ (MPa)	1,1	1,3	1,5	1,8	2,0	2,2	2,5	2,7	2,9	3,0	3,1	3,2	3,4	3,5	$f_{ctk;0.05} = 0,7\times f_{ctm}$ 5% fractile
$f_{ctk,0.95}$ (MPa)	2,0	2,5	2,9	3,3	3,8	4,2	4,6	4,9	5,3	5,5	5,7	6,0	6,3	6,6	$f_{ctk;0.95} = 1,3\times f_{ctm}$ 95% fractile
E_{cm} (GPa)	27	29	30	31	33	34	35	36	37	38	39	41	42	44	$E_{cm} = 22[(f_{cm})/10]^{0,3}$ (f_{cm} in MPa)
ε_{c1} (‰)	1,8	1,9	2,0	2,1	2,2	2,25	2,3	2,4	2,45	2,5	2,6	2,7	2,8	2,8	see Figure 3.2 $\varepsilon_{c1}(^0/_{00}) = 0,7 f_{cm}^{0,31} \leq 2,8$
ε_{cu1} (‰)	3,5									3,2	3,0	2,8	2,8	2,8	see Figure 3.2 for $f_{ck} \geq 50$ Mpa $\varepsilon_{cu1}(^0/_{00})=2,8+27[(98-f_{cm})/100]^4$
ε_{c2} (‰)	2,0									2,2	2,3	2,4	2, 5	2,6	see Figure 3.3 for $f_{ck} \geq 50$ Mpa $\varepsilon_{c2}(^0/_{00})=2,0+0,085(f_{ck}-50)^{0,53}$
ε_{cu2} (‰)	3,5									3,1	2,9	2,7	2,6	2,6	see Figure 3.3 for $f_{ck} \geq 50$ Mpa $\varepsilon_{cu2}(^0/_{00})=2,6+35[(90-f_{ck})/100]^4$
n	2,0									1,75	1,6	1,45	1,4	1,4	for $f_{ck} \geq 50$ Mpa $n=1,4+23,4[(90- f_{ck})/100]^4$
ε_{c3} (‰)	1,75									1,8	1,9	2,0	2,2	2,3	see Figure 3.4 for $f_{ck} \geq 50$ Mpa $\varepsilon_{c3}(^0/_{00})=1,75+0,55[(f_{ck}-50)/40]$
ε_{cu3} (‰)	3,5									3,1	2,9	2,7	2,6	2,6	see Figure 3.4 for $f_{ck} \geq 50$ Mpa $\varepsilon_{cu3}(^0/_{00})=2,6+35[(90-f_{ck})/100]^4$

29

BS EN 1992-1-1:2004
EN 1992-1-1:2004 (E)

Appendix B. Weather conditions report on bridge 030428

Current As Of: 9/30/2019 12:58:41 PM

BURKE CREEK & COSSATOT RELIEF STRS. & APPRS. (S)
Job No. 030428
F. A. P. No. NHPP-0066(28)
Sevier County
August 22, 2019 to August 22, 2019
This is a working day contract.

Thursday **August 22** **327 / 200+2** **Date Authorized:** 8/26/2019 **Authorized By:** Jason L. Efird
Time Charged: Contractor able to employ 60% of normal forces and equipment.

DWR Created By: Austin D. Mote **Date Authorized:** 8/26/2019
Weather: AM: Clear PM: Clear High: 95 Low: 73
Working Conditions: Good.
Engineering Activities: Office work and inspection.
Daily Staff:

Austin Mote	J.R. Mills
Buck Keys	Joe Thompson
Travis Black	William Ryan

Roadway Work:
None.
Structure Work:
James Construction placed class SAE concrete for stage 2 bridge deck from station 117+46 to station 119+39. James Construction placed Sinak Liuthium cure from station 117+46 to station 119+39. James Construction started spraying Sinak at 10:05 and finish
ed at 11:27.

General Notes:
Weather conditions during stage 2 bridge deck are as follows.

Start of pour 3:58 AM- Humidity 85.7, Temp 75.6, Dew point 71.1, Wet bulb 70.4

45 yards at 4:45 AM - Humidity 86.2, Temp 77.5, Dew point 70.4, Wet bulb 70.4

90 yards at 5:37 AM - Hum
idity 85.5, Temp 74.1, Dew point 69.1 Wet bulb 70.4

135 yards at 6:28 AM - Humidity 81.5, Temp 76.9, Dew point 71.1, Wet bulb 73.6

180 yards at 7:20 AM - Humidity 79.2, Temp 78.7, Dew point 71.1, Wet bulb 73.3

225 yards at 8:07 AM - Humidity 76.
5, Temp 81.1, Dew point 72.5, Wet bulb 74.6

270 yards at 8:52 AM - Humidity 70.1, Temp 85.2, Dew point 73.2, Wet bulb 78.1

The joints were saw cut at 4:00 PM.

NTB Associates were on site setting survey monuments.

Mickey with Forterra and two

Appendix C. Numerical results for mechanical properties samples from bridge 030428

Samples @ 3:50 AM					
Testing Date	Age (days)	Compressive Strength Results **[psi, lbf]**		MOE **[psi]**	Poissons
8/23/2019	1	2681	33691	3,105,387	-0.16
8/25/2019	3	5041	63351	3521937	
8/29/2019	7	4946	62154	3586099	-0.05
9/5/2019	14	5723	71924	4035864	
9/19/2019	28	6174	77588	3206045	-0.15

Samples @ 6:00 AM					
Testing Date	Age (days)	Compressive Strength Results **[psi, lbf]**		MOE **[psi]**	Poissons
8/23/2019	1	3144	39513	2,907,747	-0.05
8/25/2019	3	4994	62758	3156576	-0.14
8/29/2019	7	5178	65068	3154254	-0.15
9/5/2019	14	5417	68075	3165509	-0.16
9/19/2019	28	5418	68088	3136626	-0.11

Samples @ 7:45 AM					
Testing Date	Age (days)	Compressive Strength Results **[psi, lbf]**		MOE **[psi]**	Poissons
8/23/2019	1	2954	37123	2,593,308	-0.12
8/25/2019	3	4079	51259	2849858	-0.13
8/29/2019	7	3979	50005	3194237	-0.15
9/19/2019	28	4640	58312	2979729	-0.12